

The Multi-Blade project

Boron-10-based detector for reflectometry instruments

Francesco Piscitelli



Detector Group

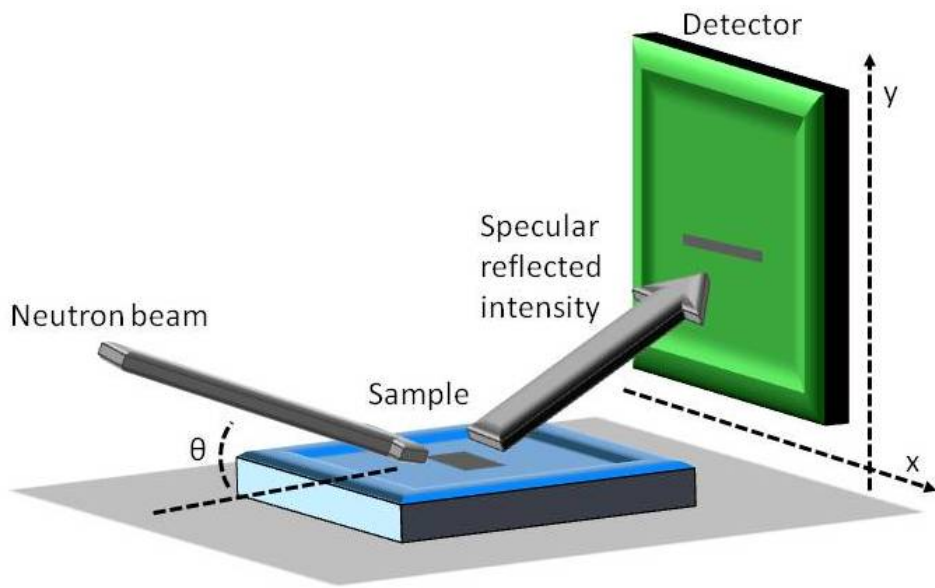
NSS seminar

2016/01/19

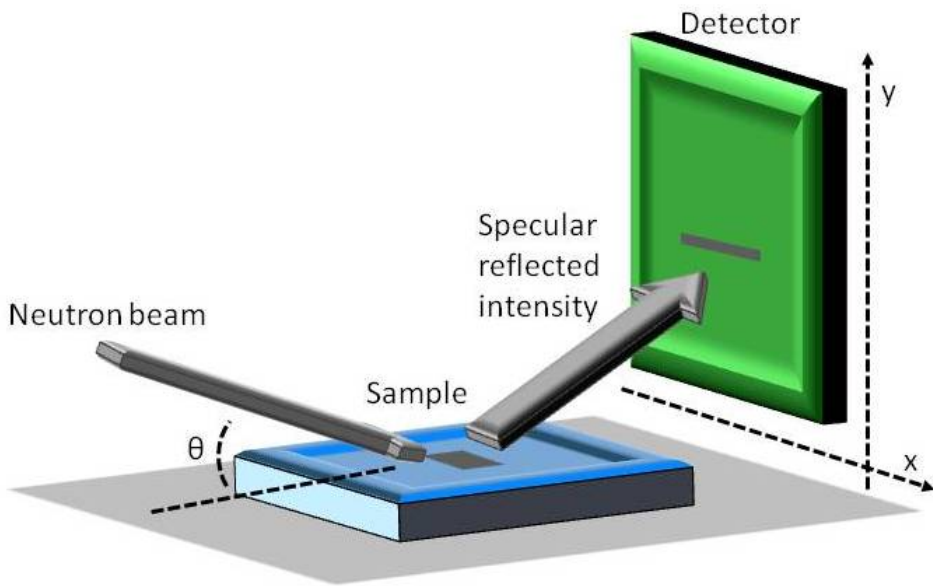
Outline

- Reflectometry
- Reflectometry at ESS: FREIA and ESTIA
- The Multi-Blade detector
- Forthcoming plans

Reflectometry: an introduction

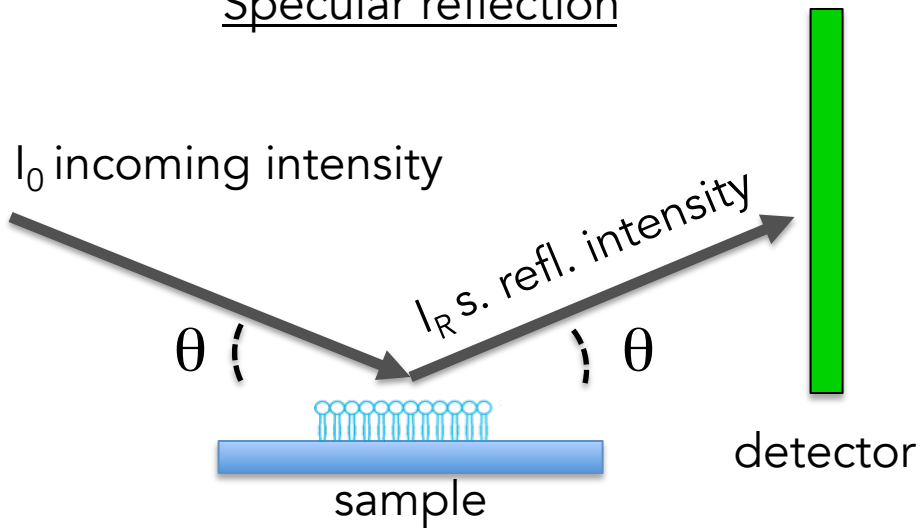


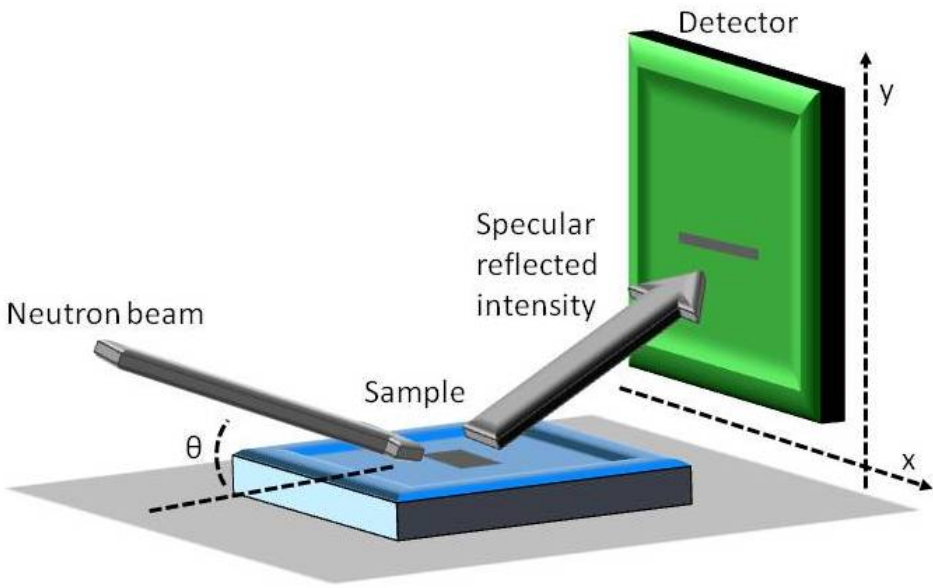
Reflectometry is a technique to study
SURFACES AND INTERFACES



Reflectometry is a technique to study
SURFACES AND INTERFACES

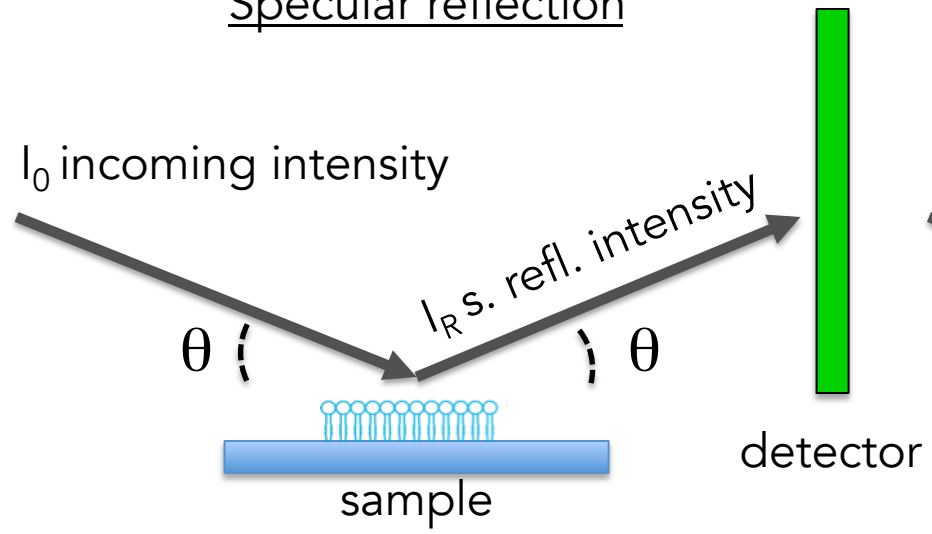
Specular reflection



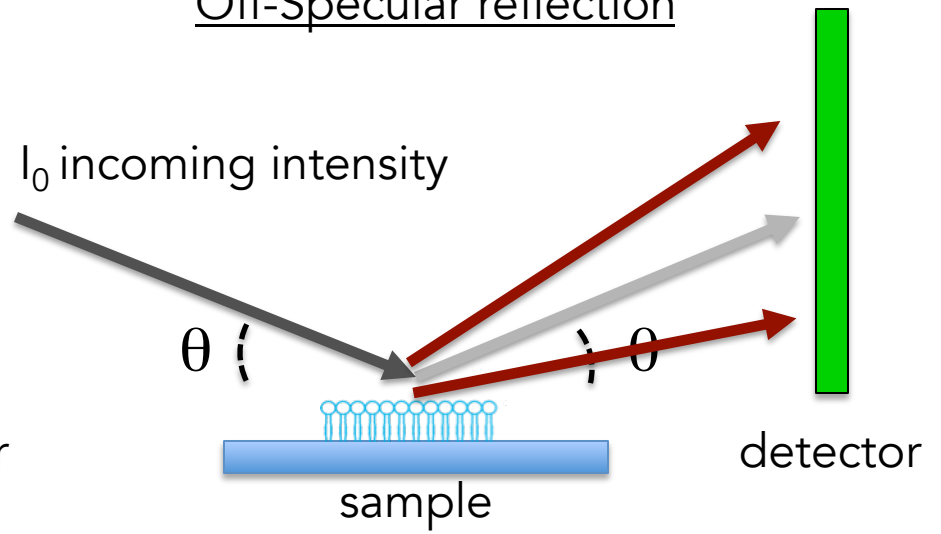


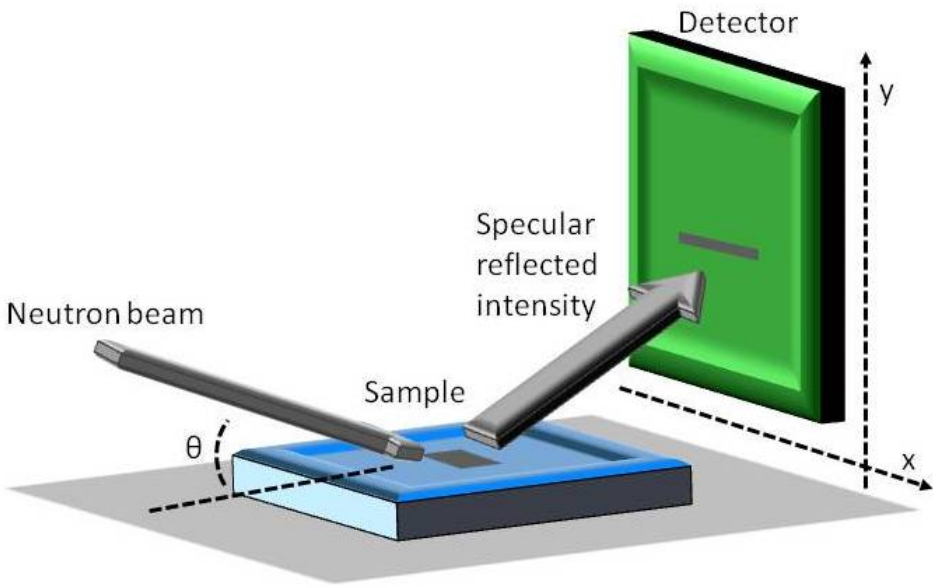
Reflectometry is a technique to study SURFACES AND INTERFACES

Specular reflection



Off-Specular reflection

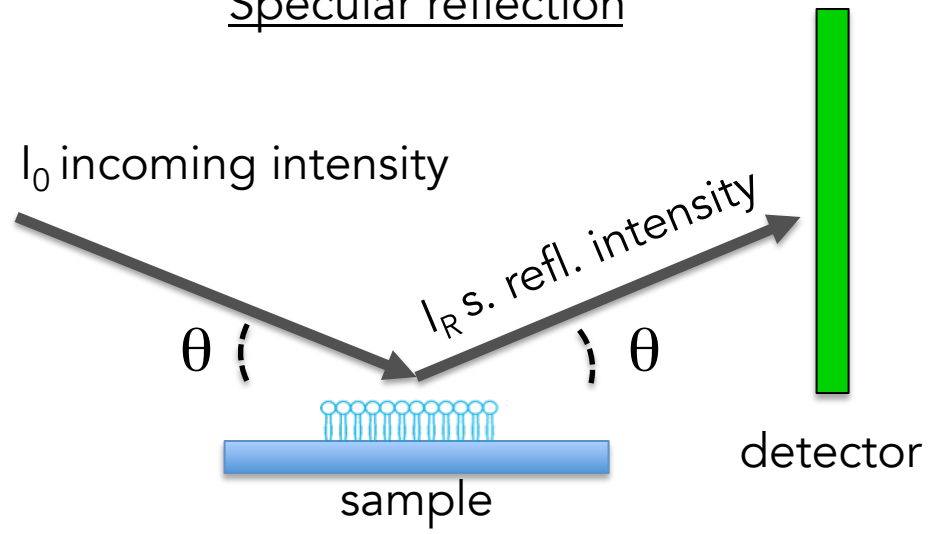


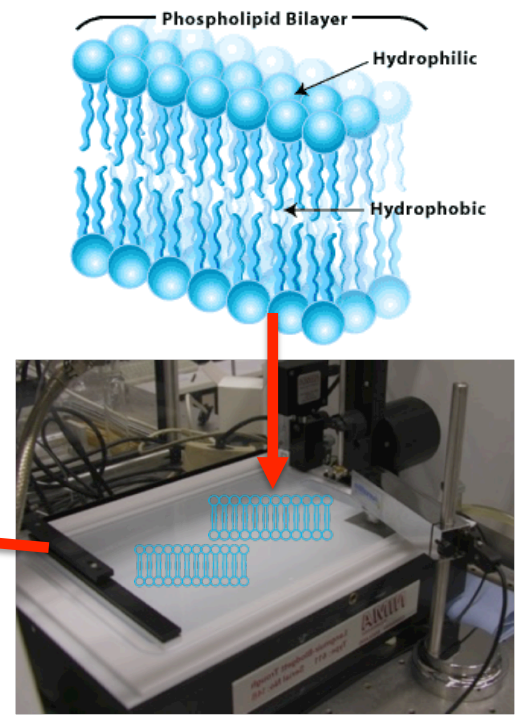
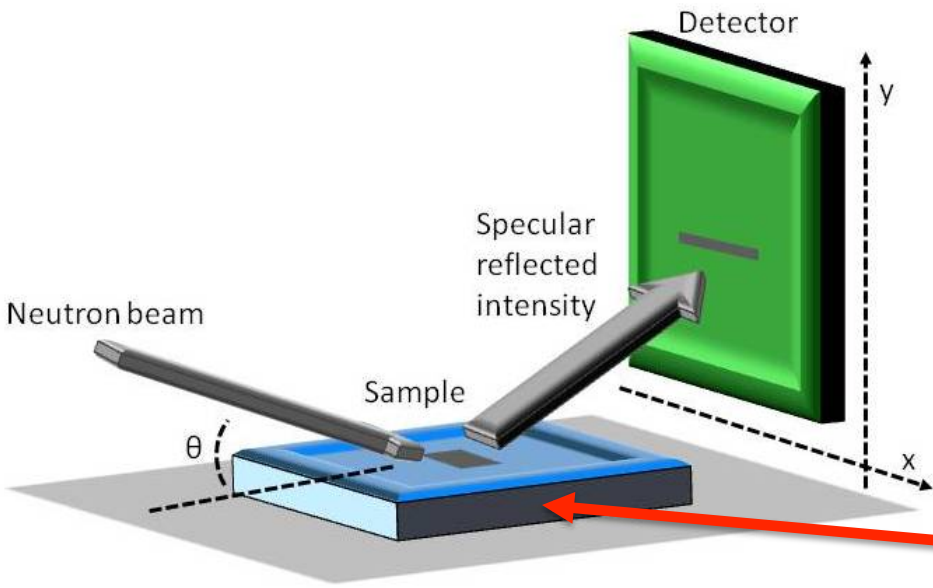


Reflectometry is a technique to study SURFACES AND INTERFACES

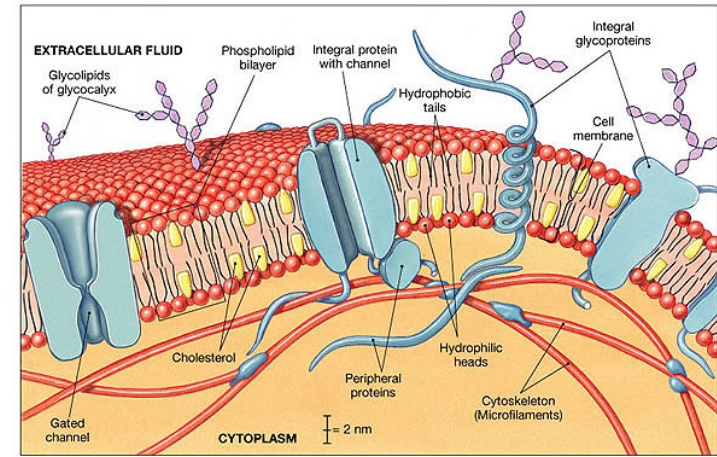
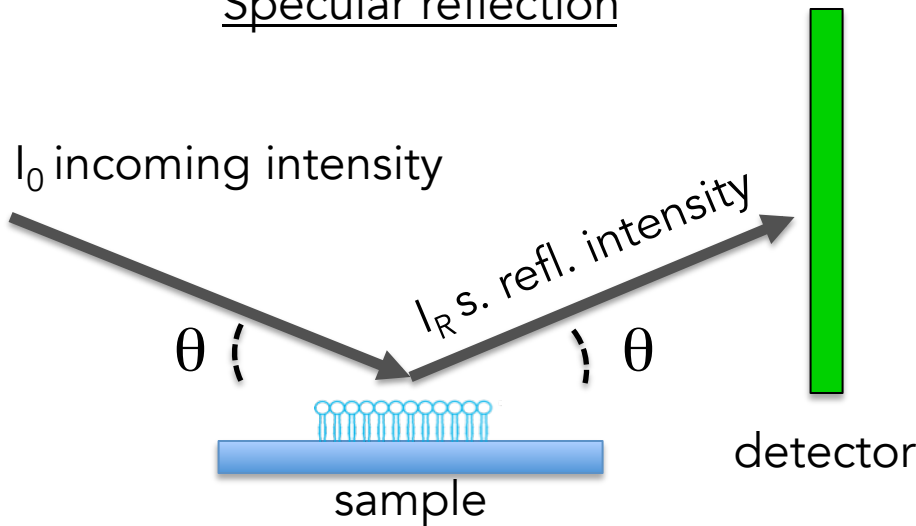


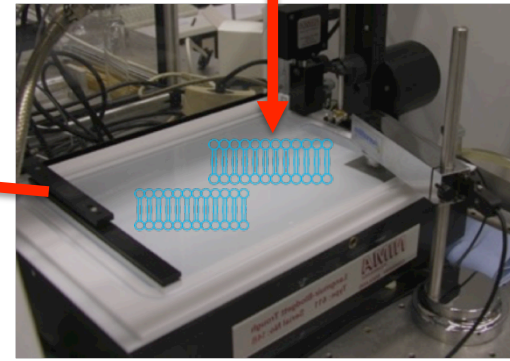
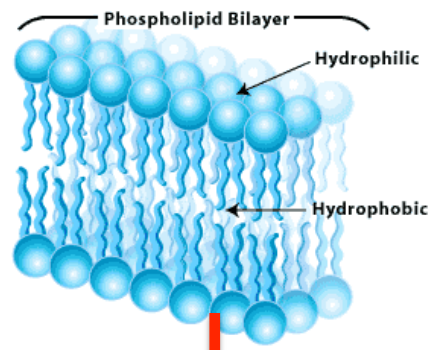
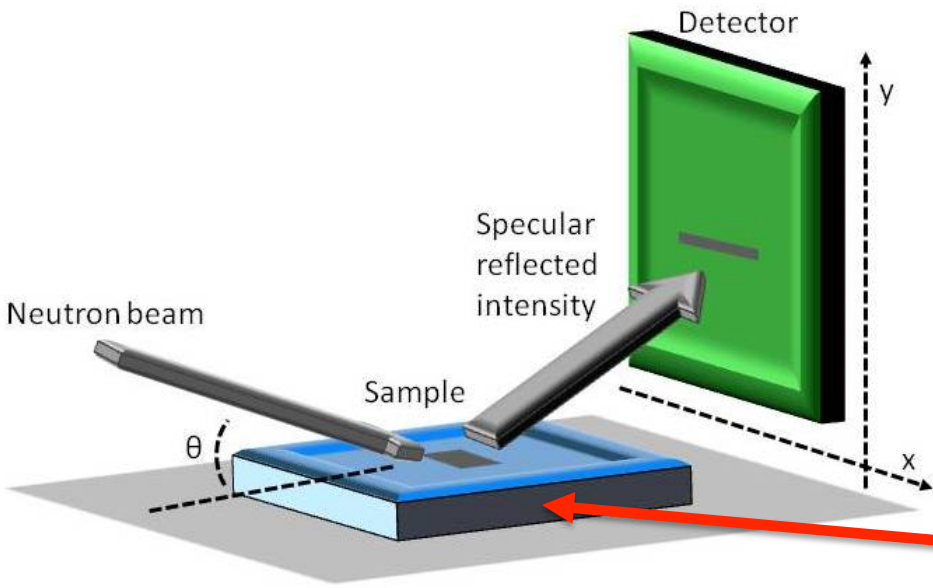
Specular reflection





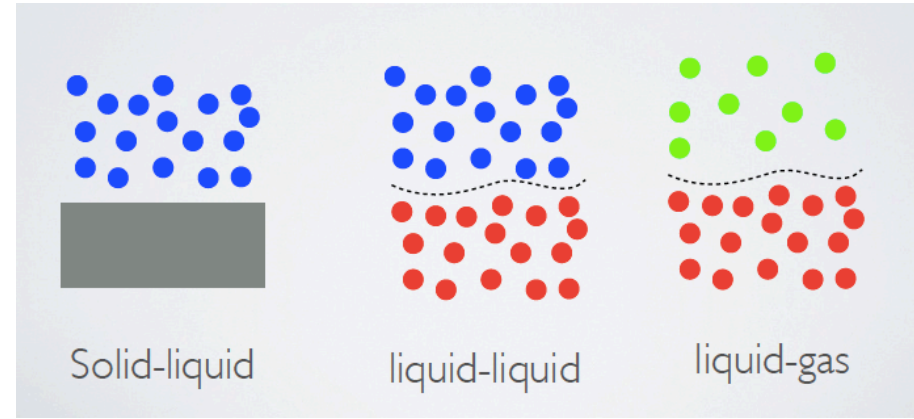
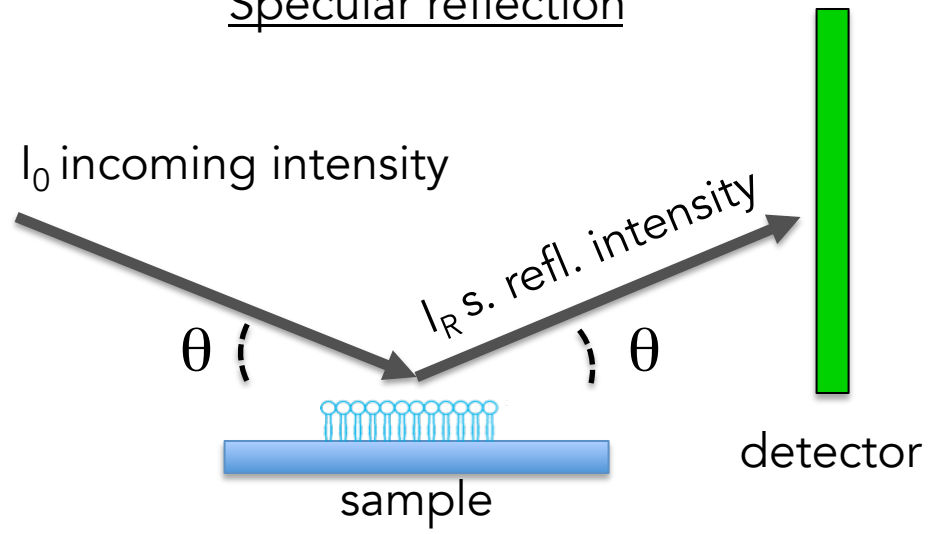
Specular reflection



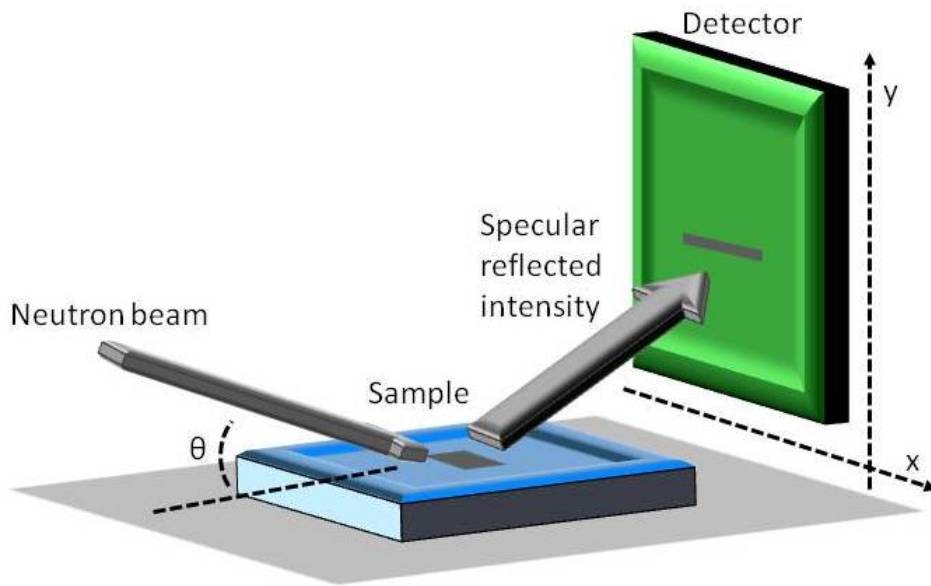


Langmuir-Blodgett trough

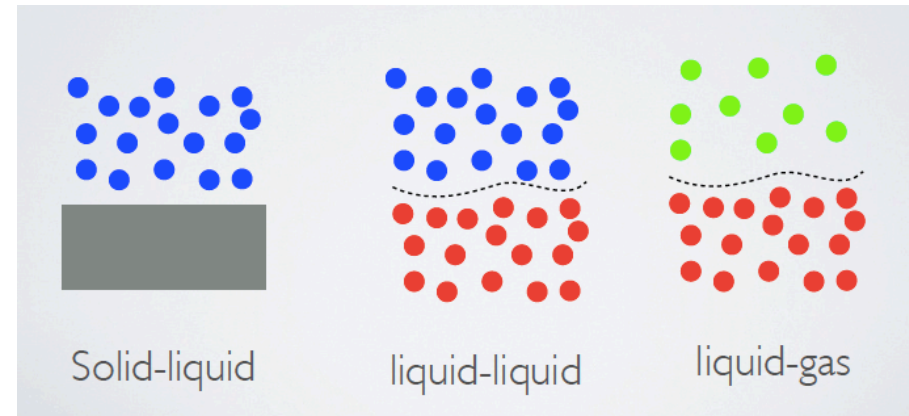
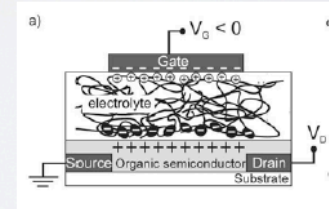
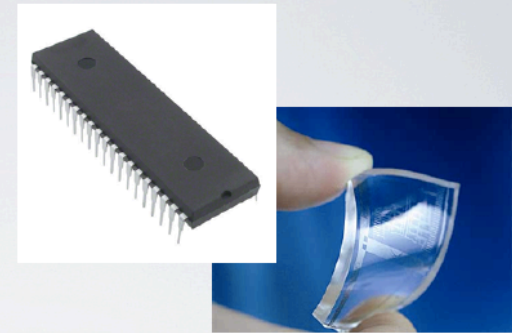
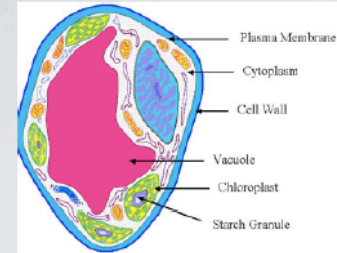
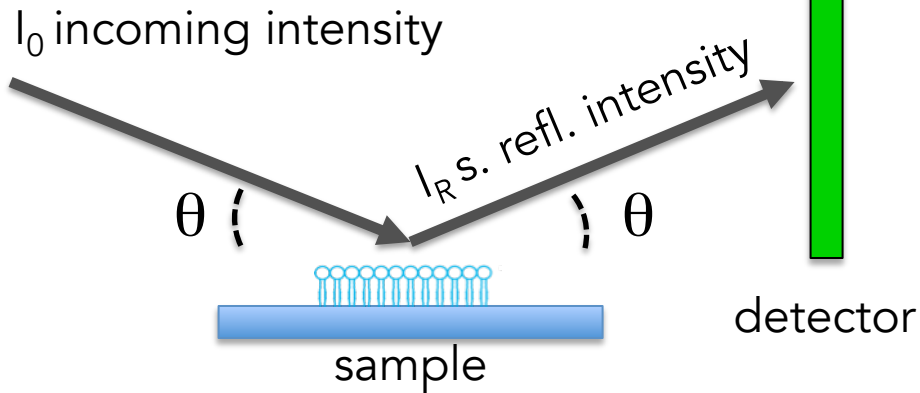
Specular reflection

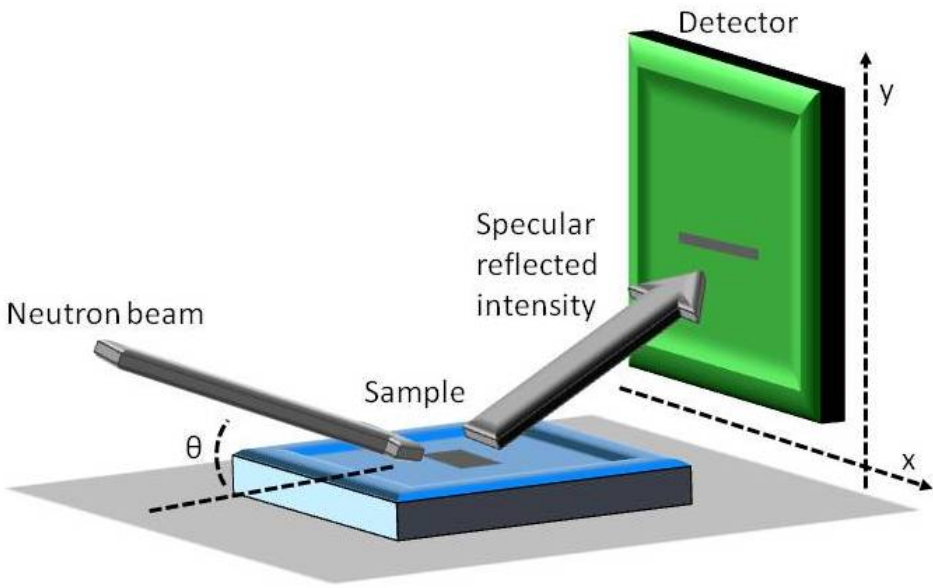


Reflectometry is a technique to study SURFACES AND INTERFACES



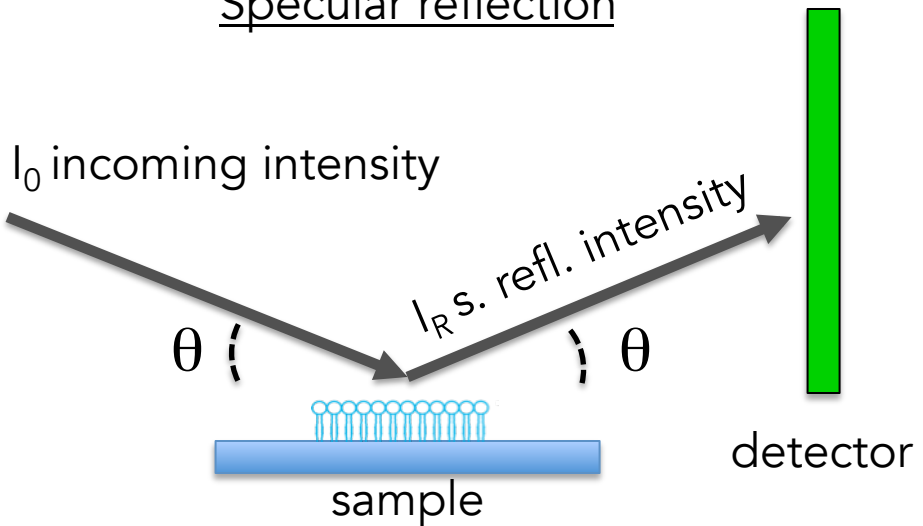
Specular reflection





To measure the reflected neutrons as a function of q

Specular reflection

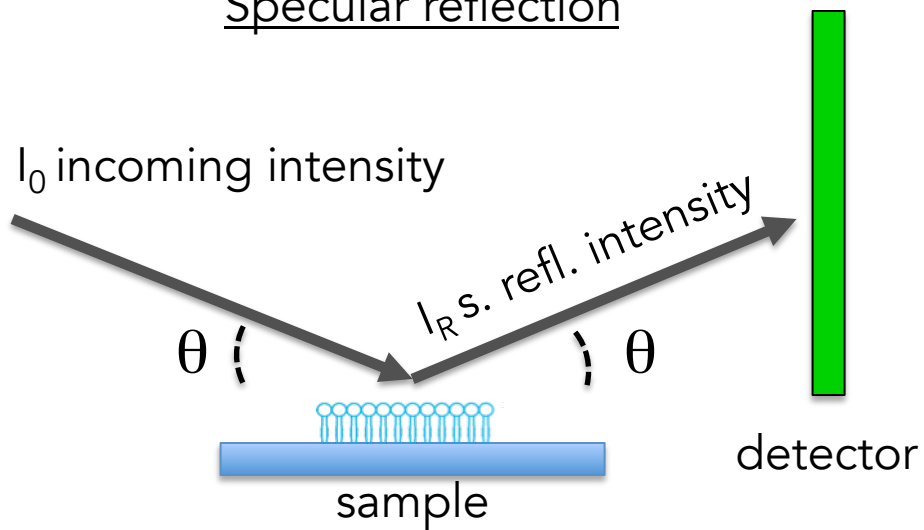


Neutron wavelength

$$q = (4\pi/\lambda) \sin(\theta)$$

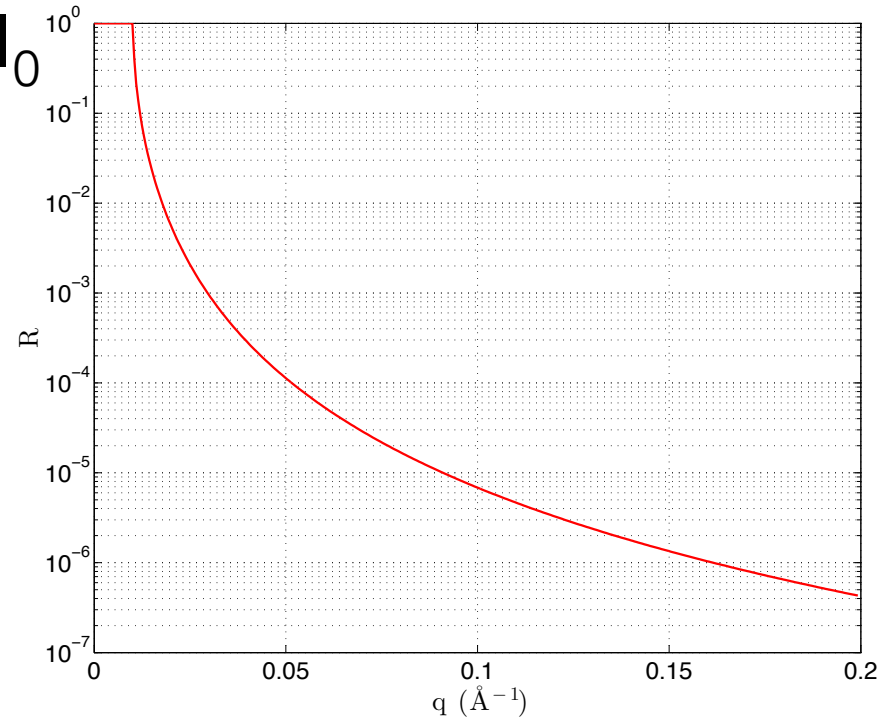
Incidence angle

Specular reflection



$$q = (4\pi/\lambda) \sin(\theta)$$

$$R = I_R / I_0$$



Specular reflection

I_0 incoming intensity

I_R s. refl. intensity

θ

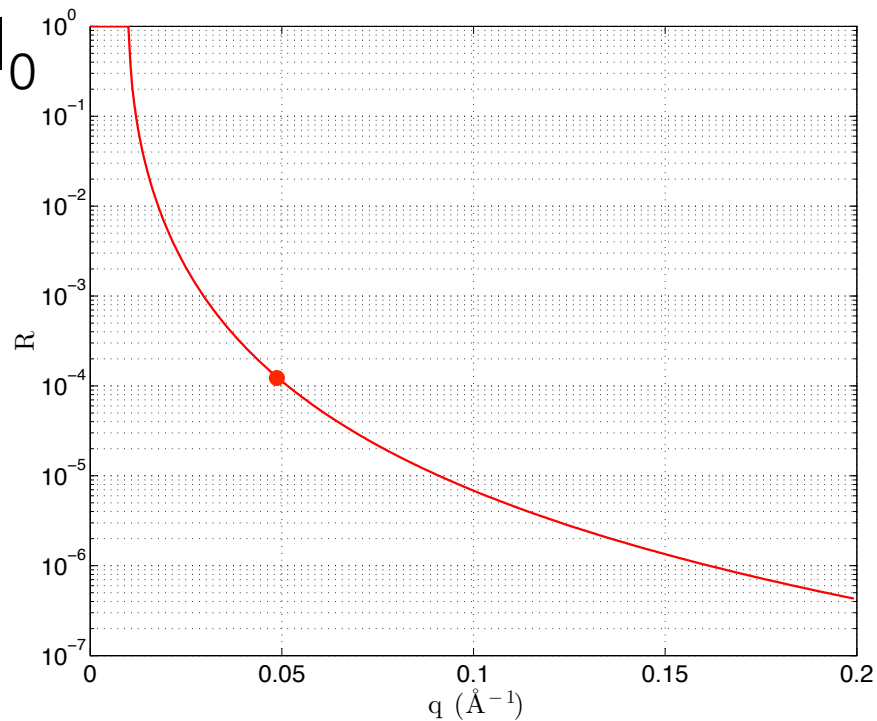
θ

detector

$$q = (4\pi/\lambda) \sin(\theta)$$

Substrate ∞

$$R = I_R / I_0$$



Specular reflection

I_0 incoming intensity

I_R s. refl. intensity

λ

θ

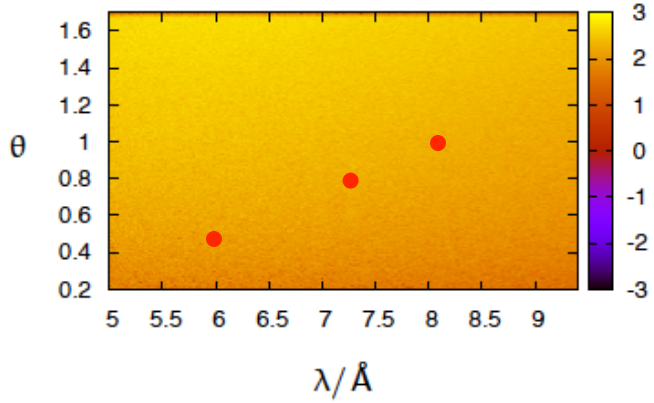
θ

detector

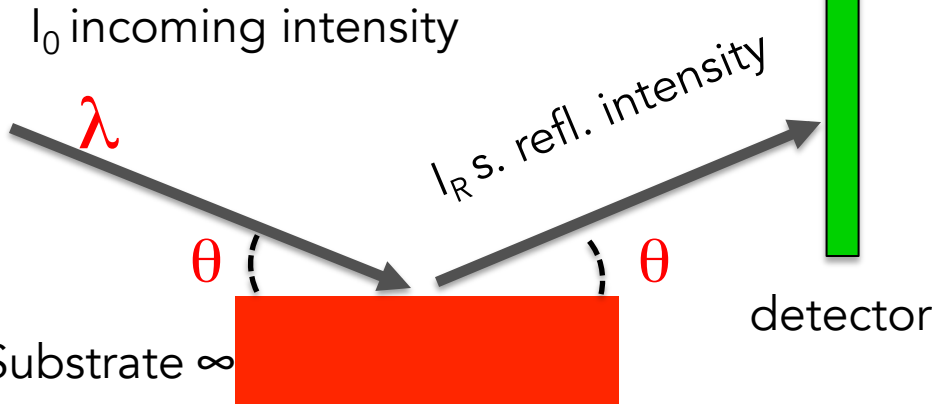
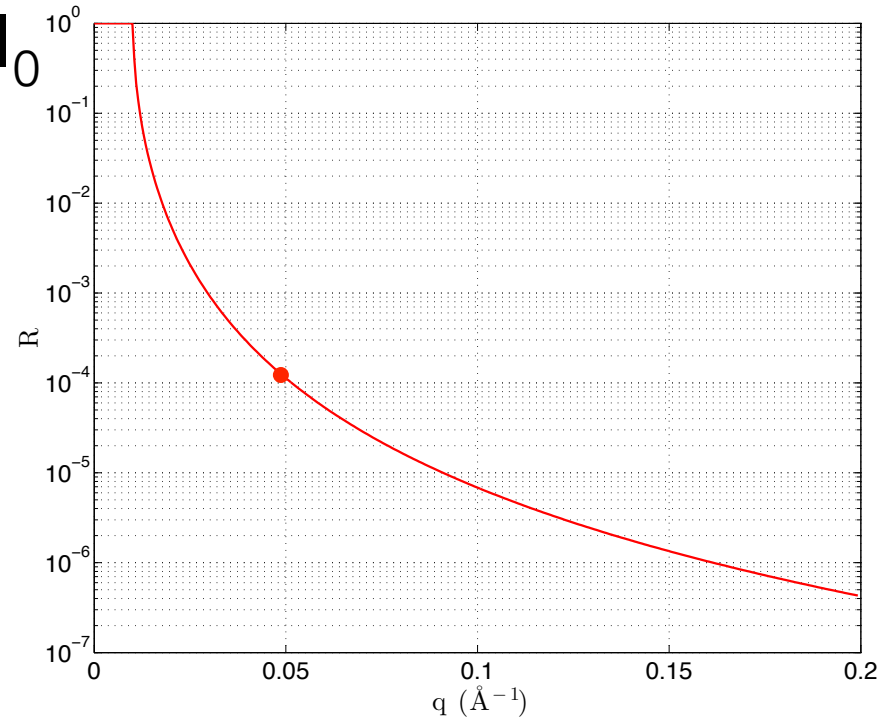
Substrate ∞

$$q = (4\pi/\lambda) \sin(\theta)$$

$$R = I_R / I_0$$

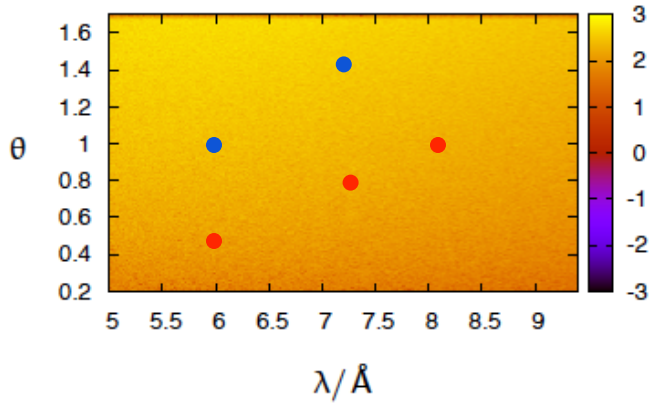


Specular reflection

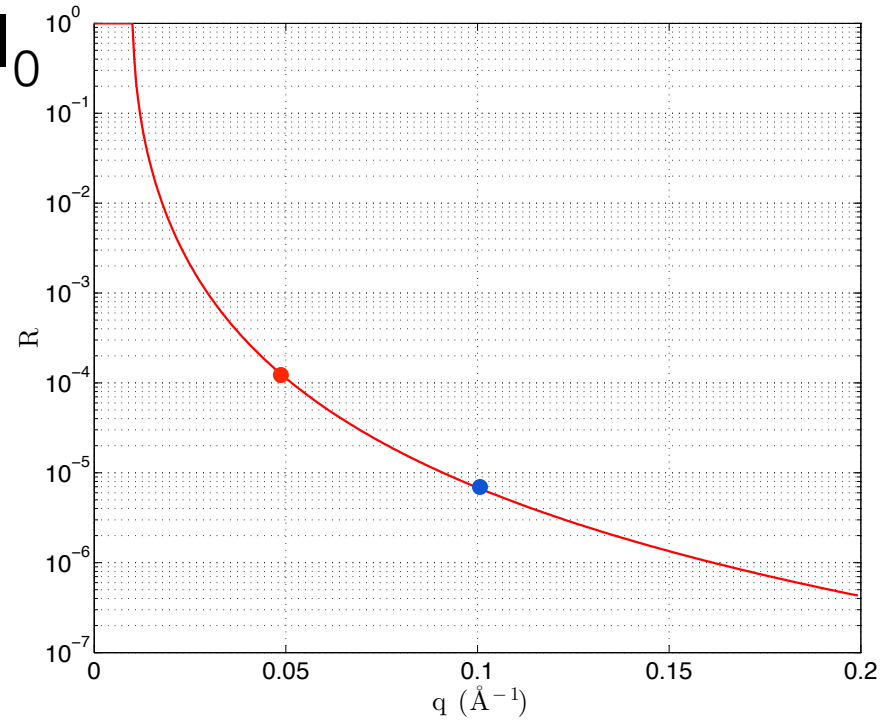


$$q = (4\pi/\lambda) \sin(\theta)$$

$$R = I_R / I_0$$



Specular reflection



I_0 incoming intensity

I_R s. refl. intensity

$$q = (4\pi/\lambda) \sin(\theta)$$

λ

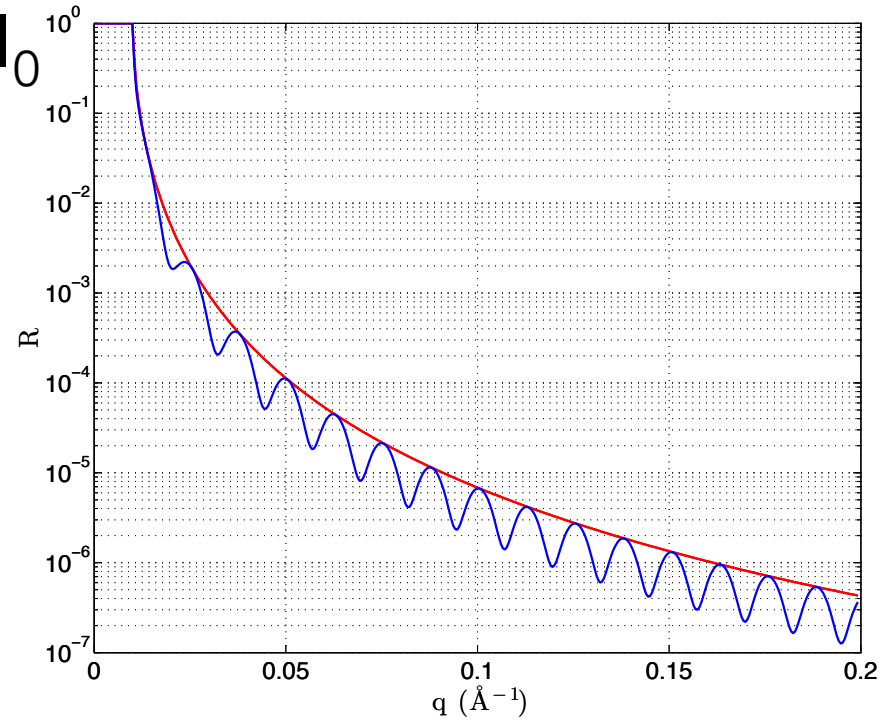
θ

θ

detector

Substrate ∞

$$R = I_R / I_0$$



Specular reflection

I_0 incoming intensity

I_R s. refl. intensity

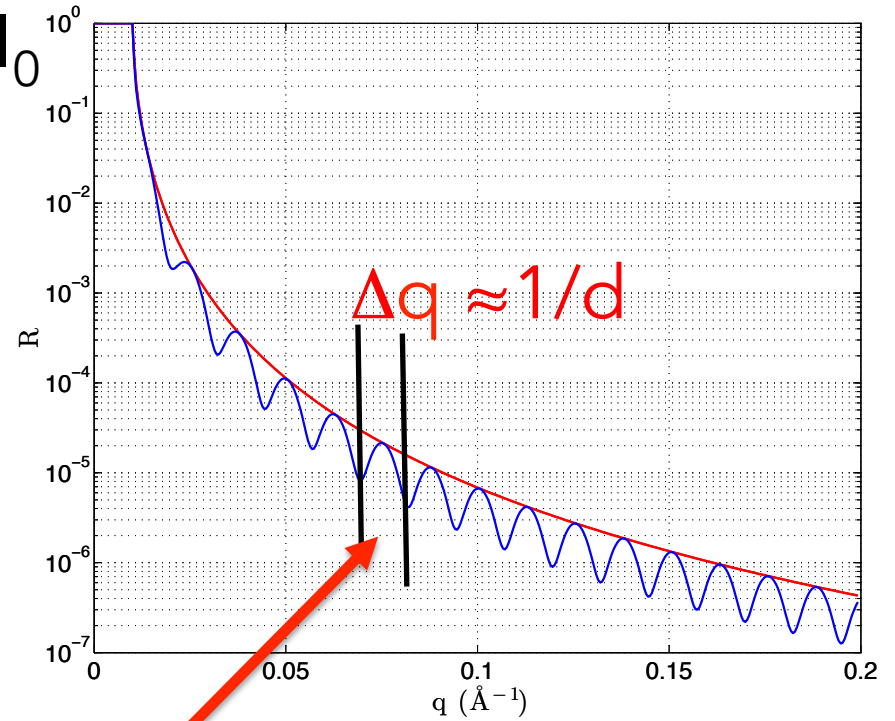
Sample 5nm

Substrate ∞

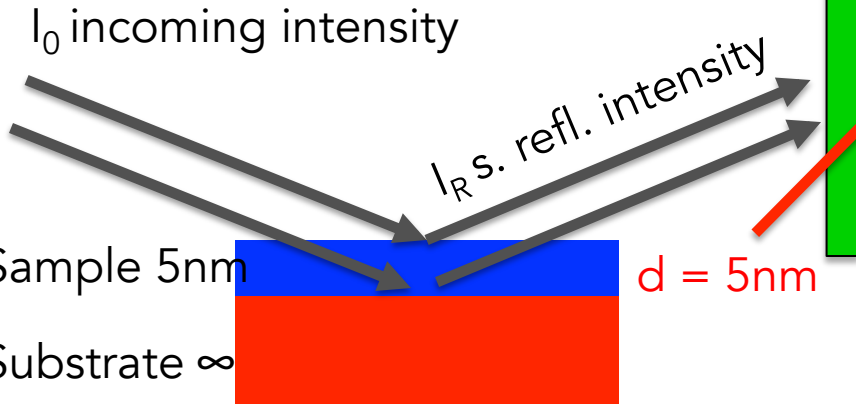
detector

$$q = (4\pi/\lambda) \sin(\theta)$$

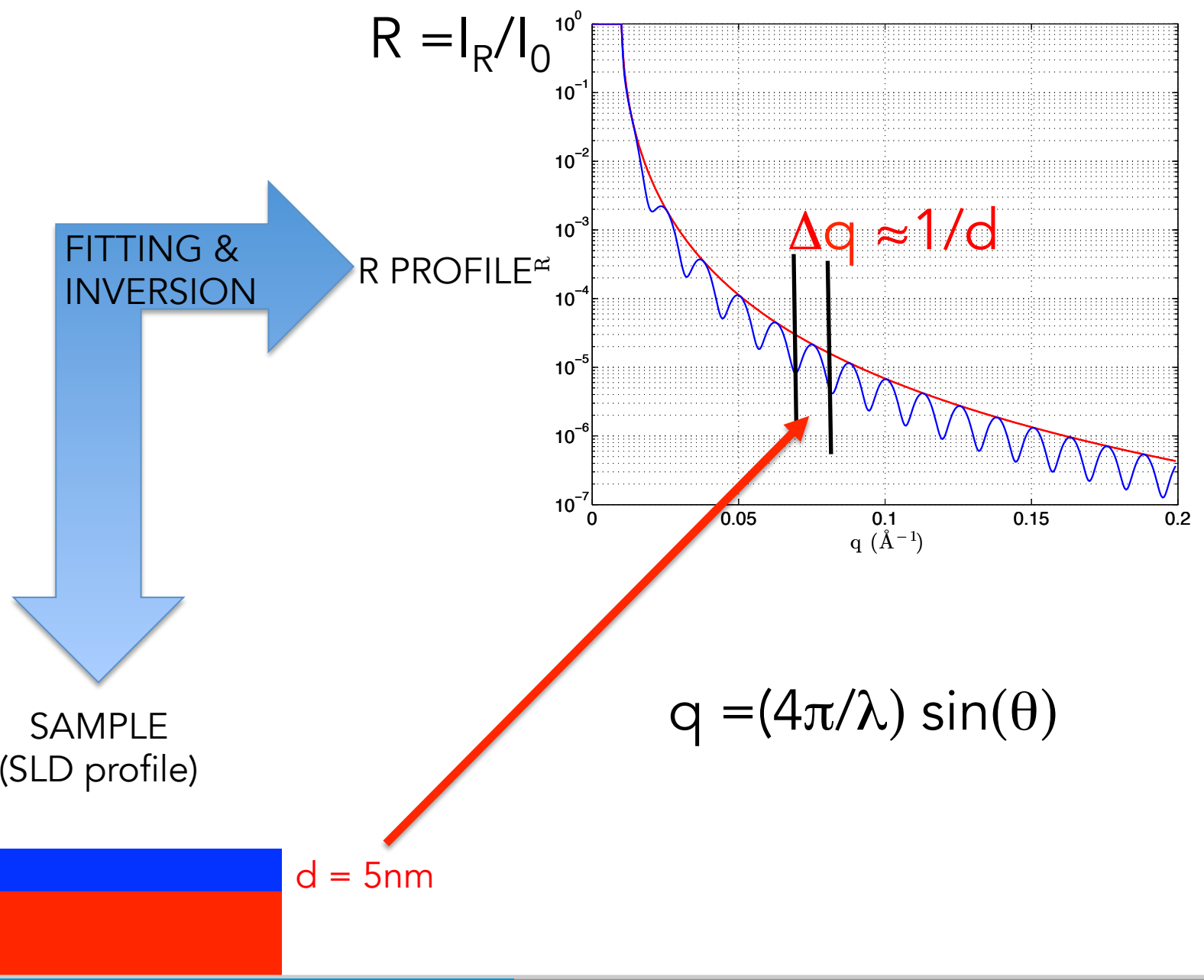
$$R = I_R / I_0$$



Specular reflection



$$q = (4\pi/\lambda) \sin(\theta)$$



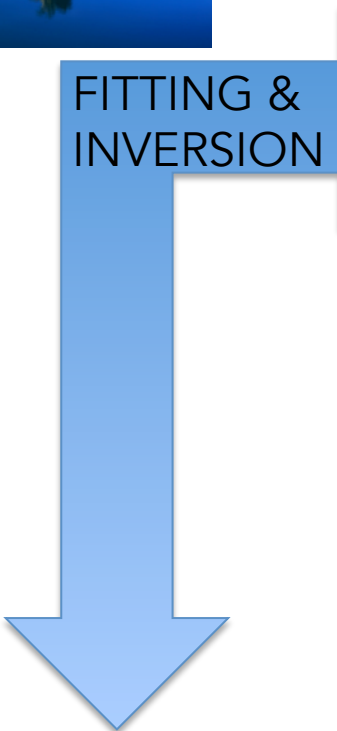
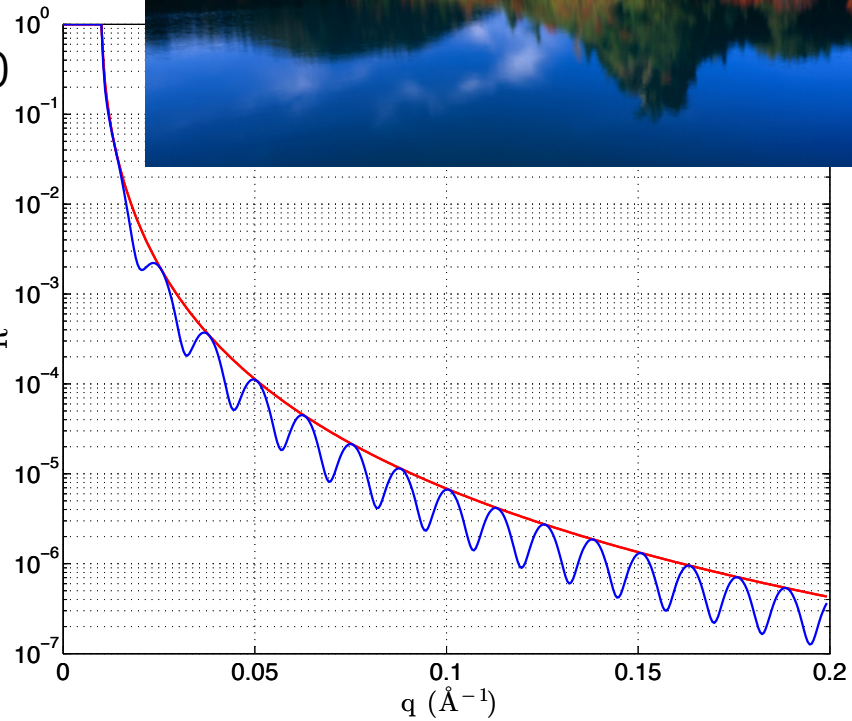


$$R = I_R / I_0$$



FITTING &
INVERSION

R PROFILE R



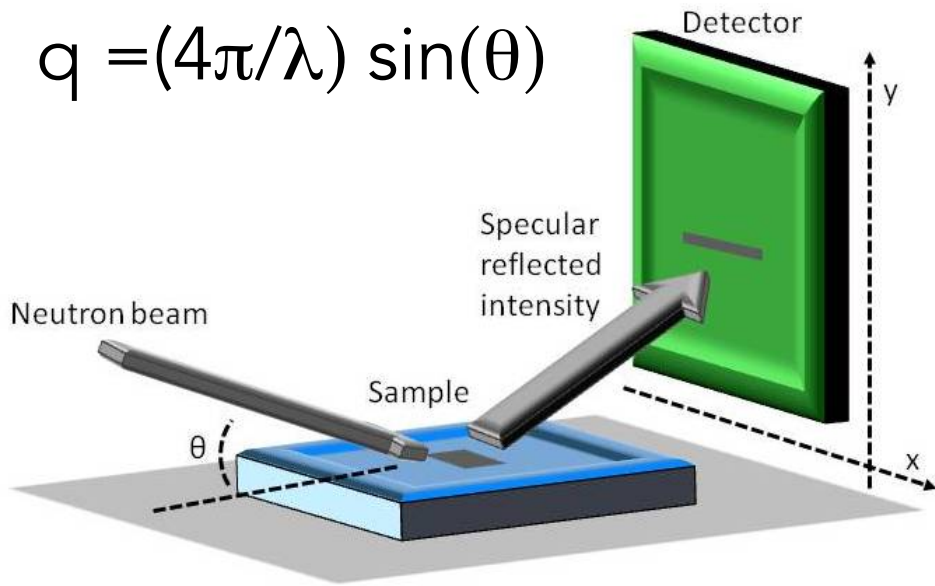
SAMPLE
(SLD profile)

Sample 5nm

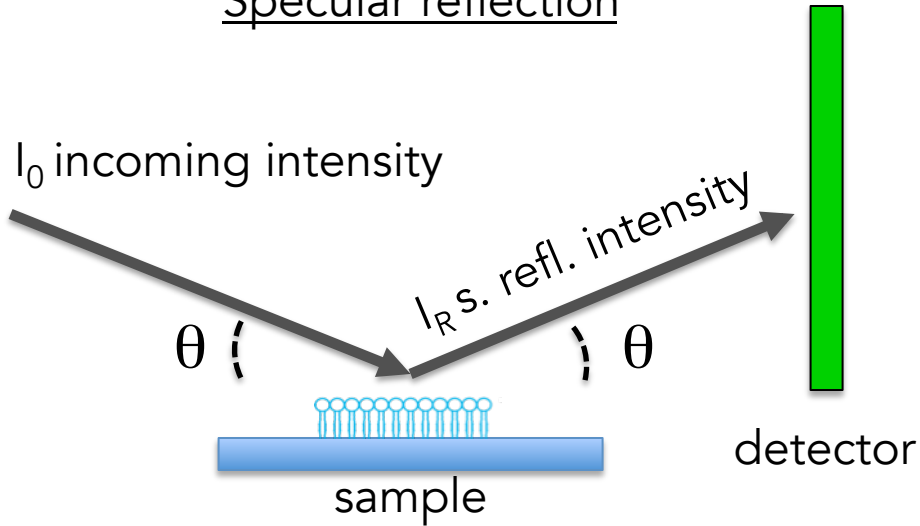
Substrate ∞



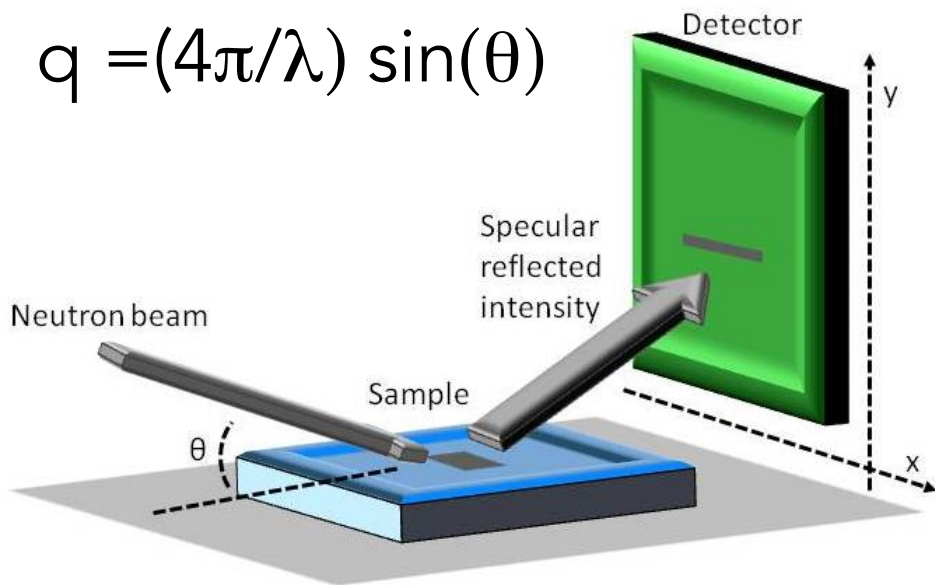
$$q = (4\pi/\lambda) \sin(\theta)$$



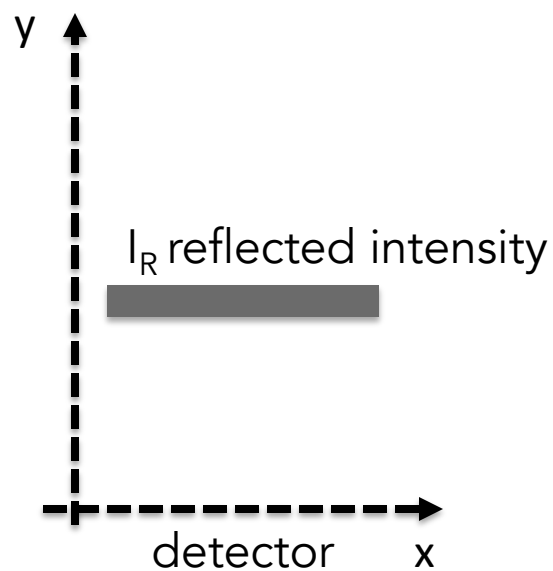
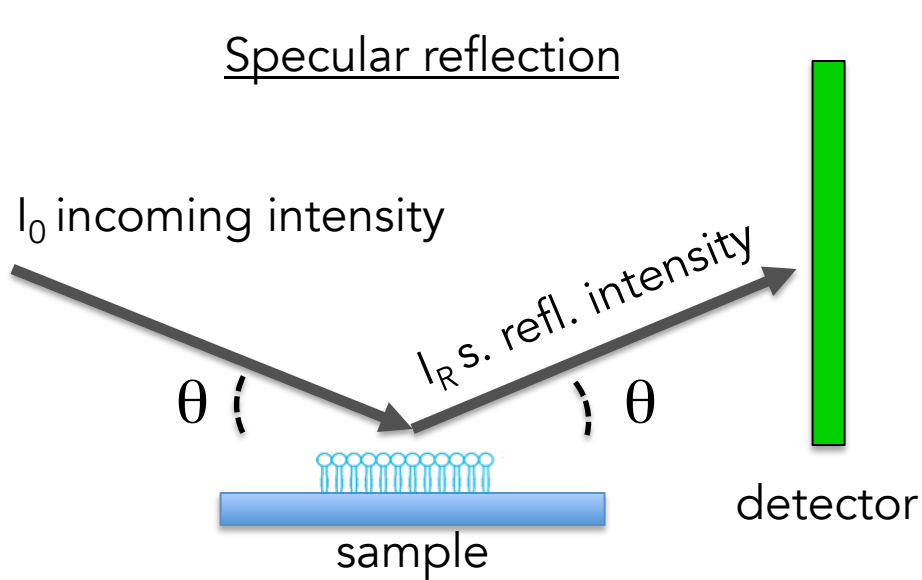
Specular reflection



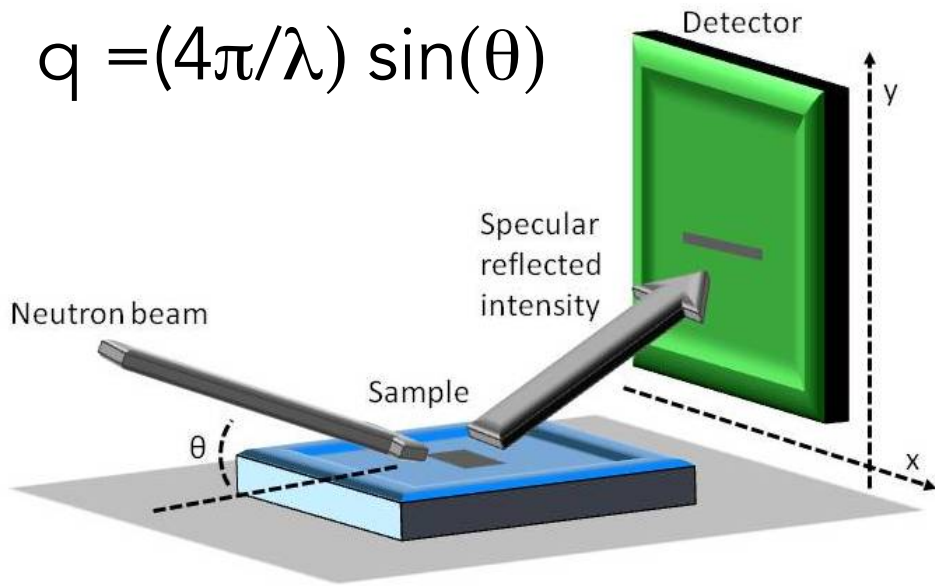
$$q = (4\pi/\lambda) \sin(\theta)$$



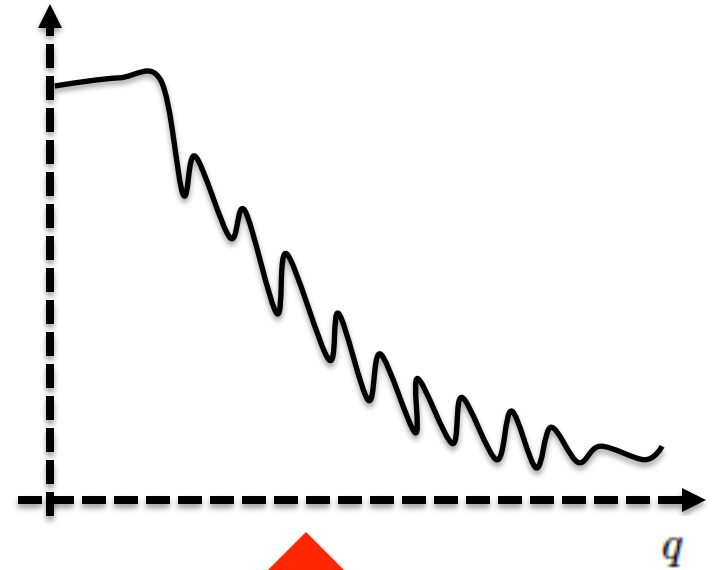
Specular reflection



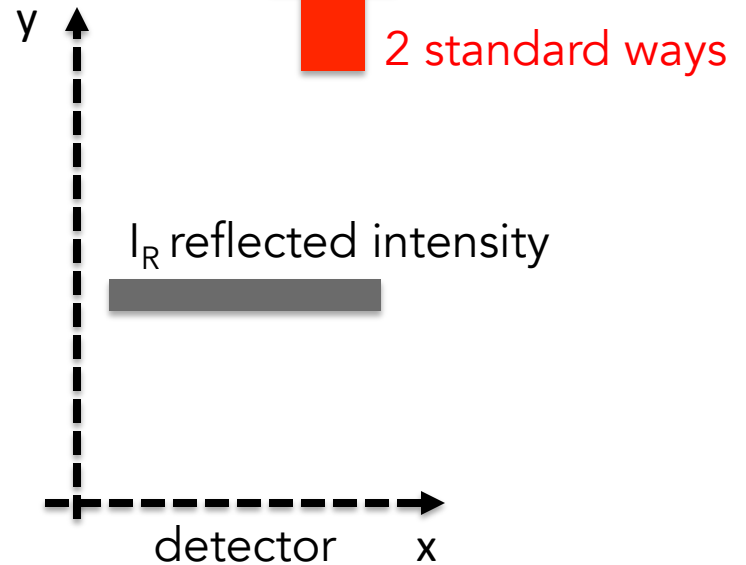
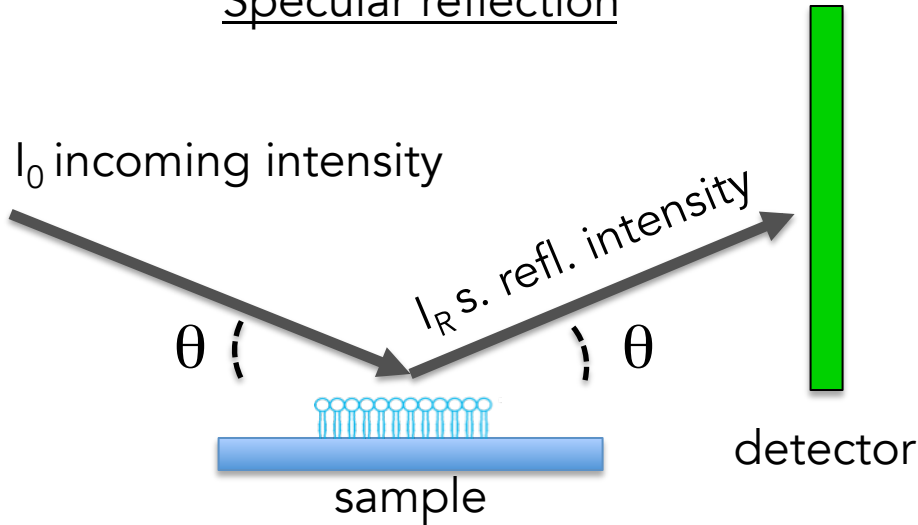
$$q = (4\pi/\lambda) \sin(\theta)$$



$$\text{Log } R = I_R/I_0$$

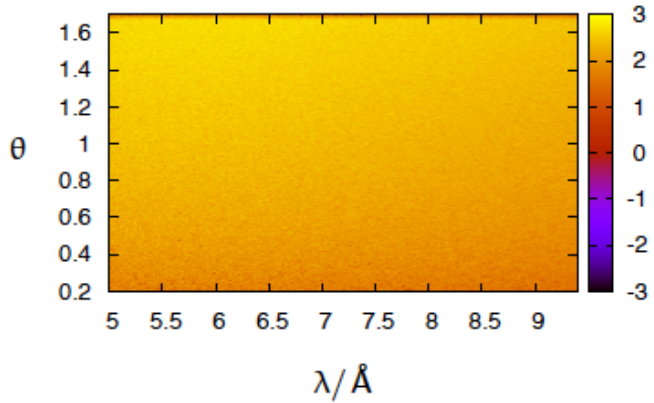


Specular reflection

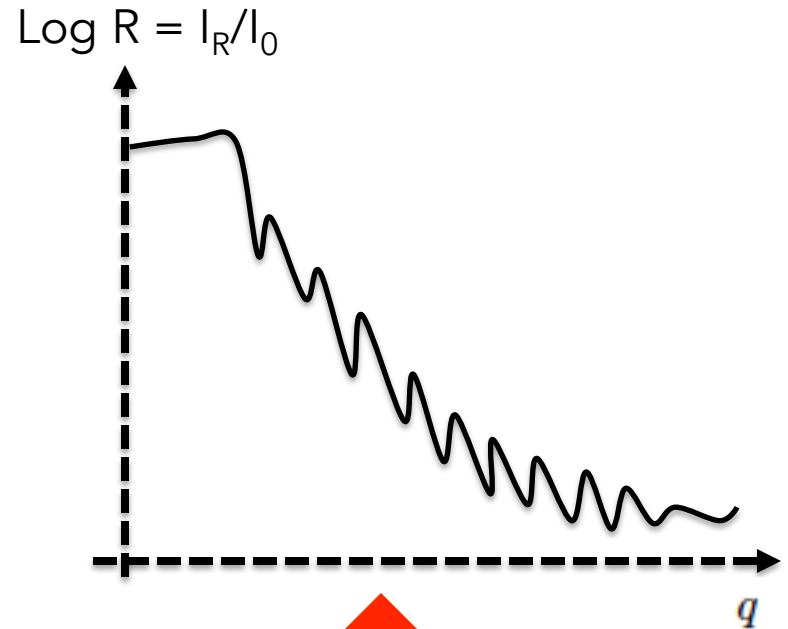
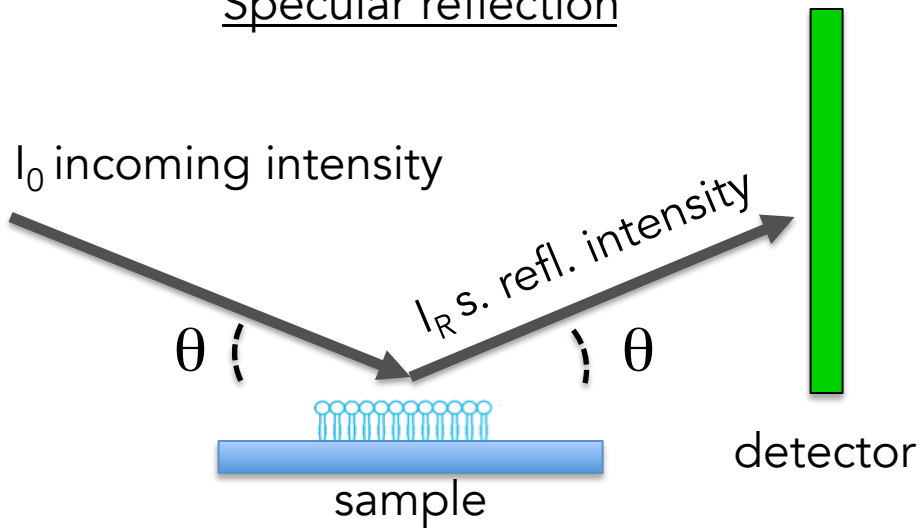


$$q = (4\pi/\lambda) \sin(\theta)$$

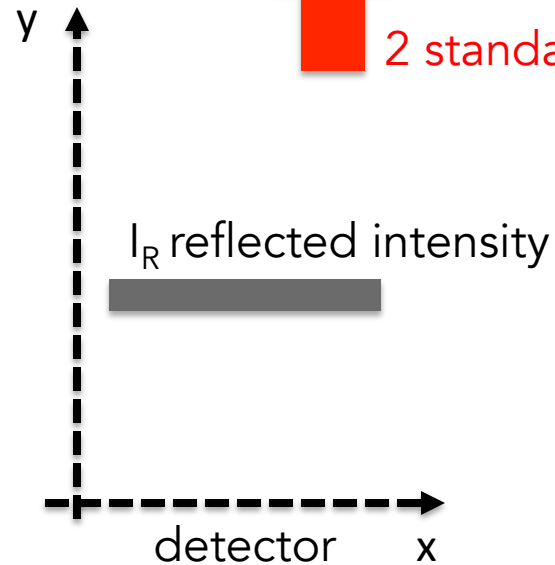
1. ToF (λ scan, θ fixed)
2. Monochromatic (λ fixed, θ scan)



Specular reflection

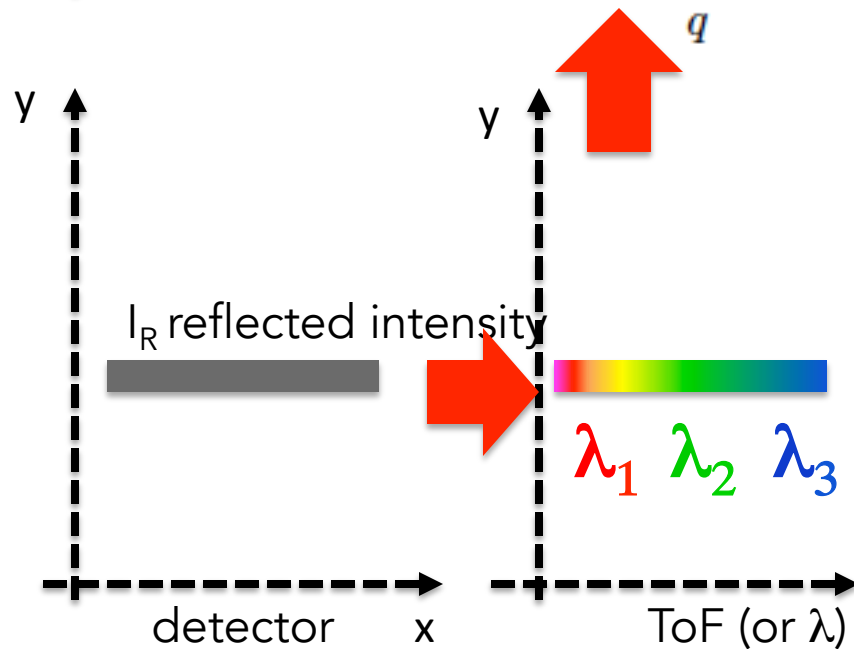
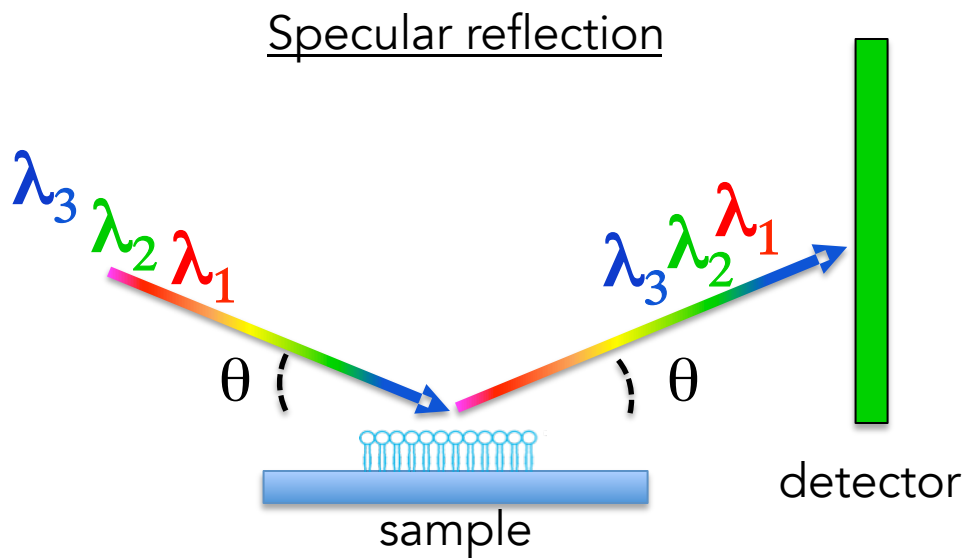
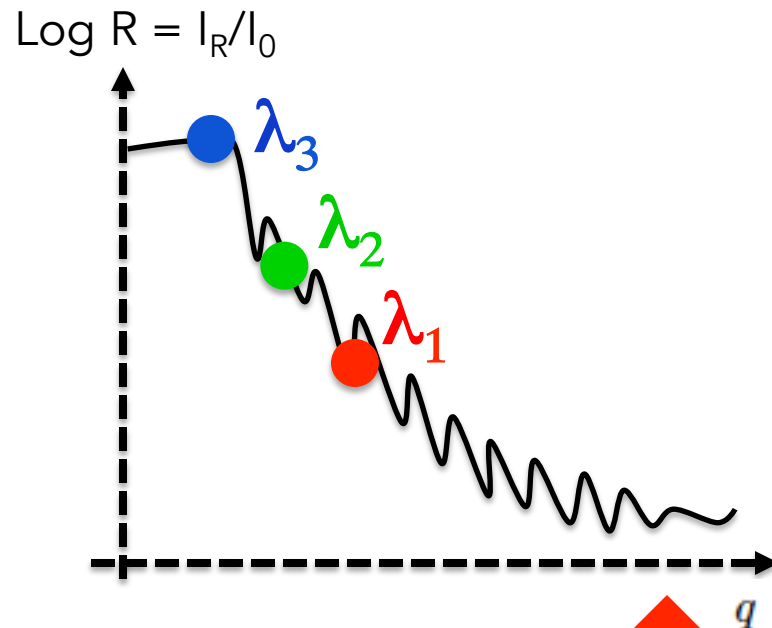
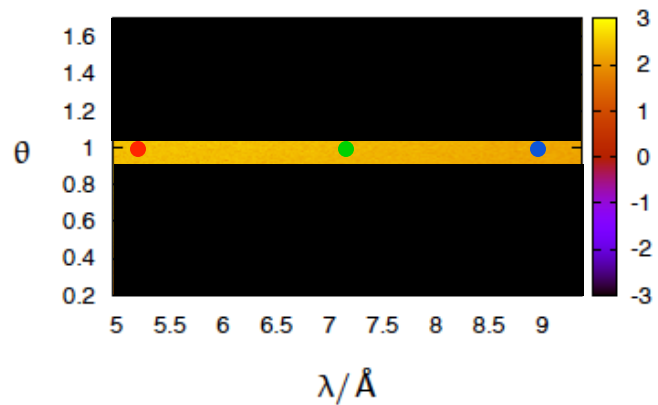


2 standard ways



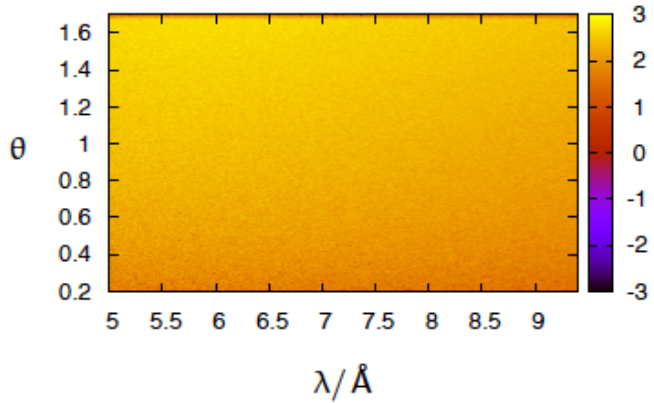
$$q = (4\pi/\lambda) \sin(\theta)$$

1. ToF (λ scan, θ fixed)
2. Monochromatic (λ fixed, θ scan)

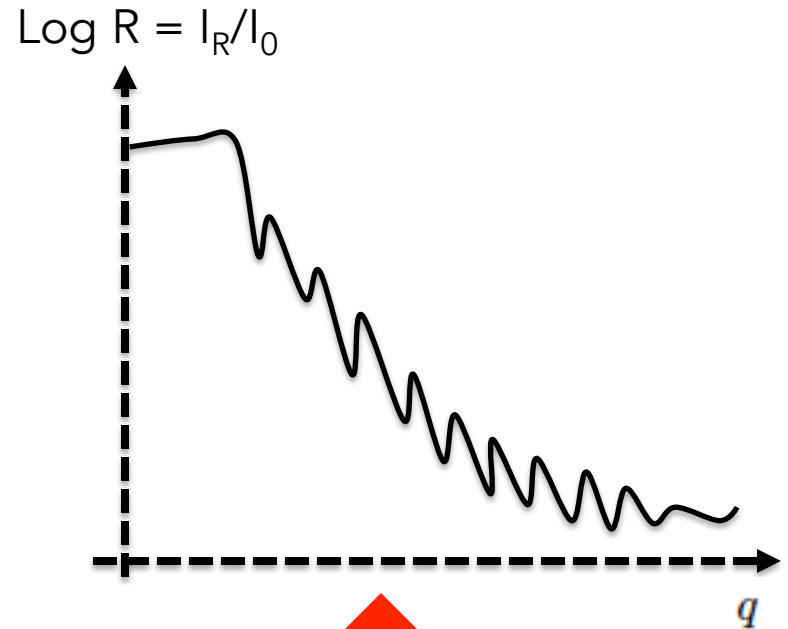
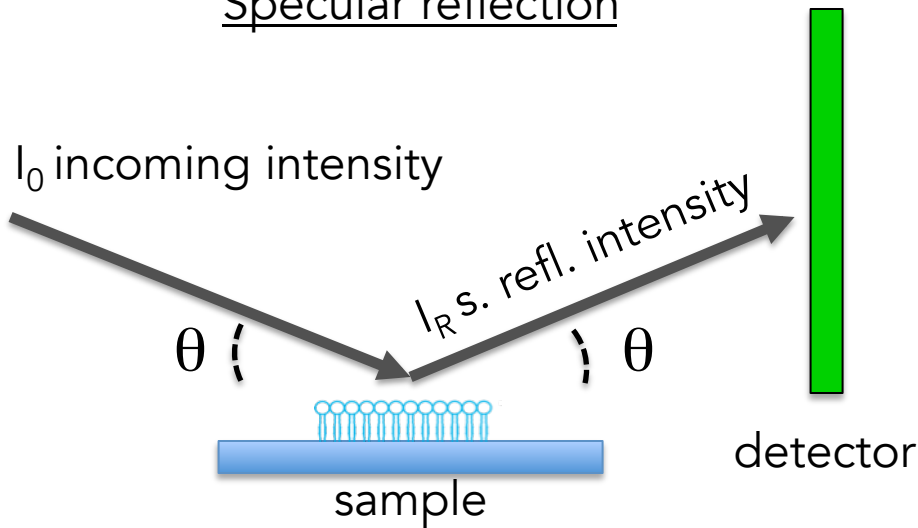


$$q = (4\pi/\lambda) \sin(\theta)$$

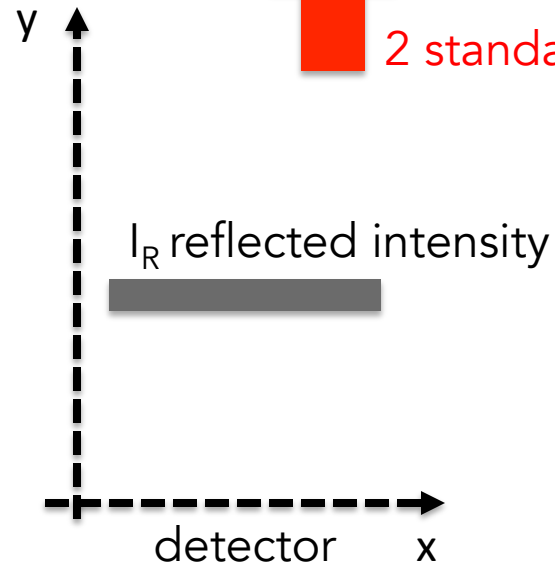
1. ToF (λ scan, θ fixed)
2. Monochromatic (λ fixed, θ scan)



Specular reflection

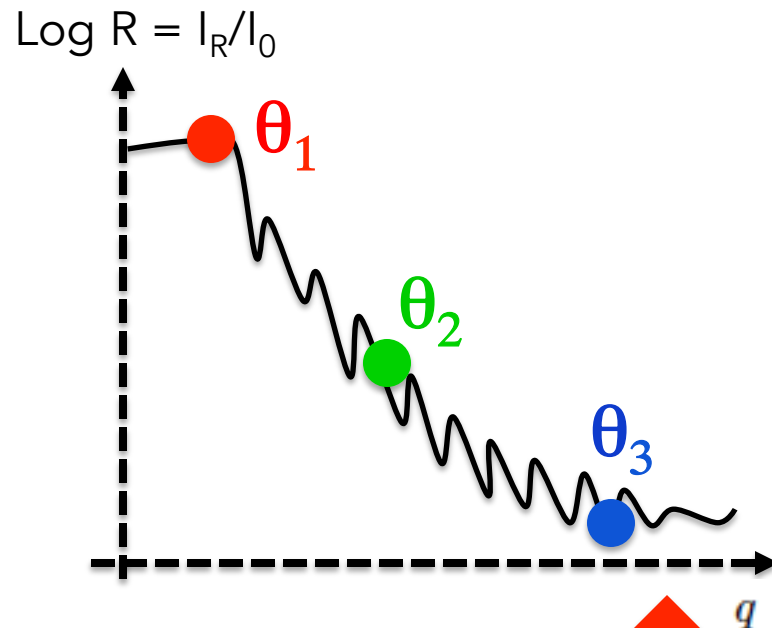
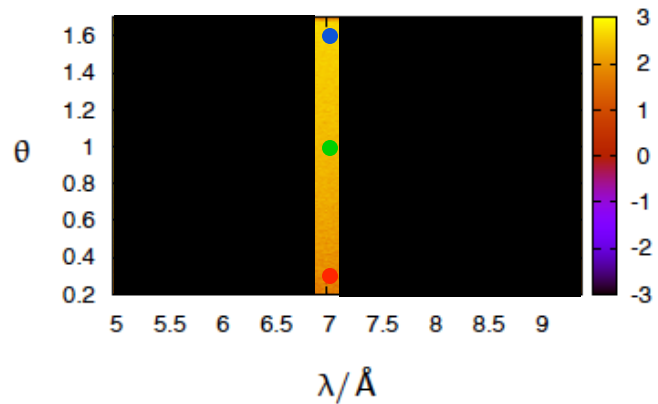


2 standard ways

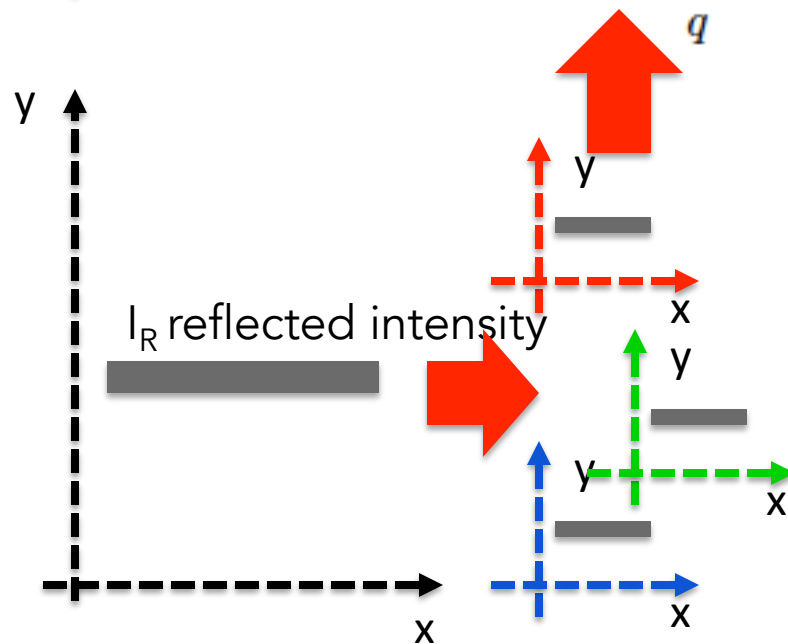
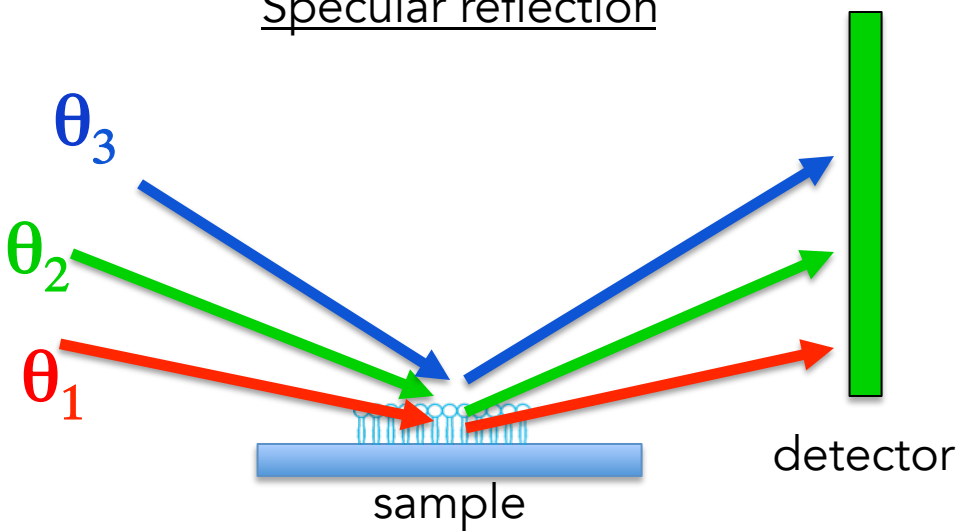


$$q = (4\pi/\lambda) \sin(\theta)$$

1. ToF (λ scan, θ fixed)
2. **Monochromatic** (λ fixed, θ scan)



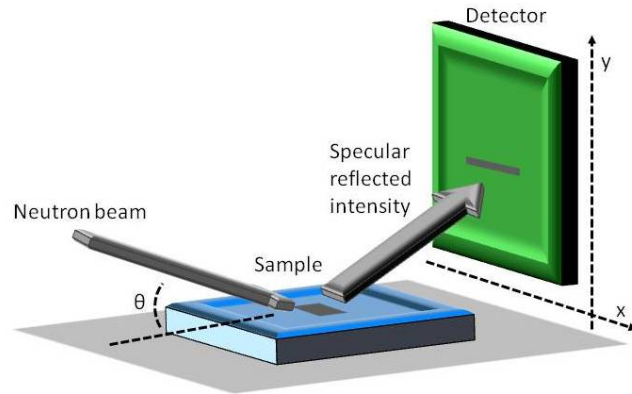
Specular reflection



Reflectometry at ESS: FREIA and ESTIA

Reflectometry at ESS: FREIA and ESTIA

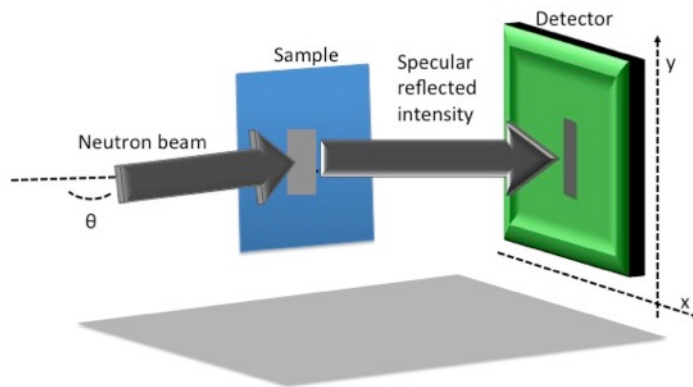
FREIA



Horizontal Reflectometer (FREIA)

Suitable for liquids
(limited angular range)

Estia



Vertical Reflectometer (ESTIA)

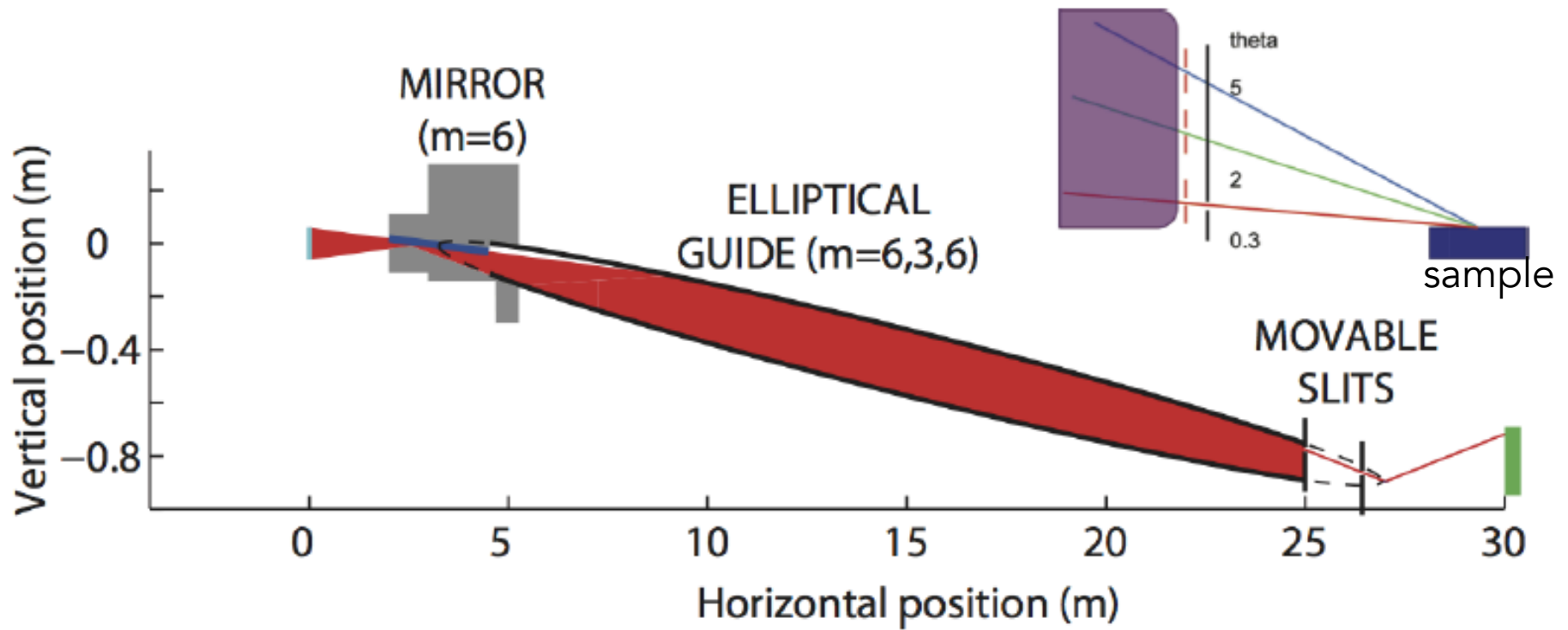
Not suitable for liquids
More versatile
(wide angle range)

Freia, (Frejya, Freyia, Frøya, Frøjya, and Freja) in Old Norse the "Lady", one of the Vanir gods, rules over the heavenly afterlife field Fólkvangr and there receives half of those that die in battle.

FREIA – a reflectometer for kinetics and liquid surfaces

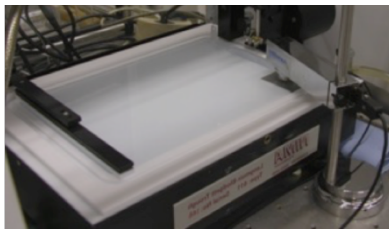
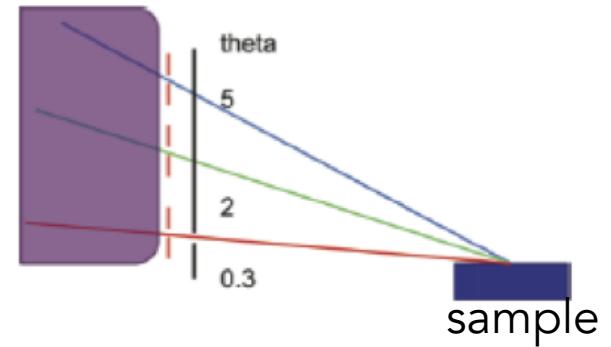
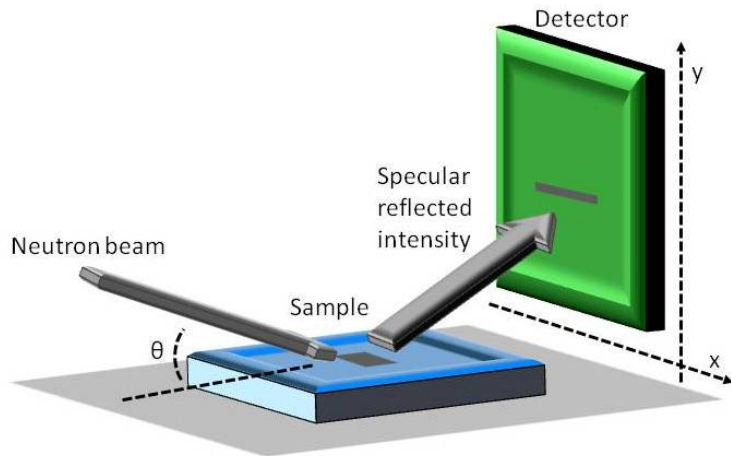


FREIA



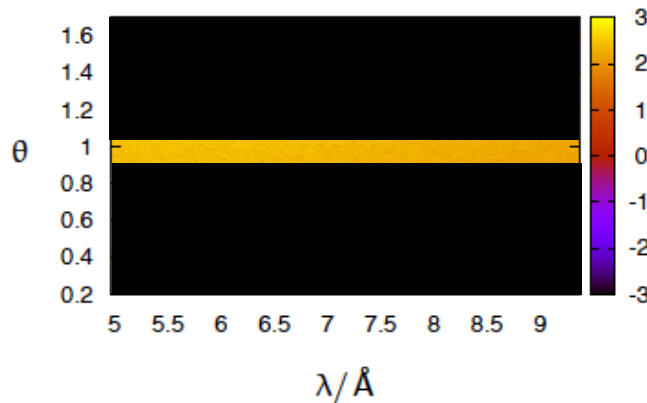
FREIA

$$q = (4\pi/\lambda) \sin(\theta)$$

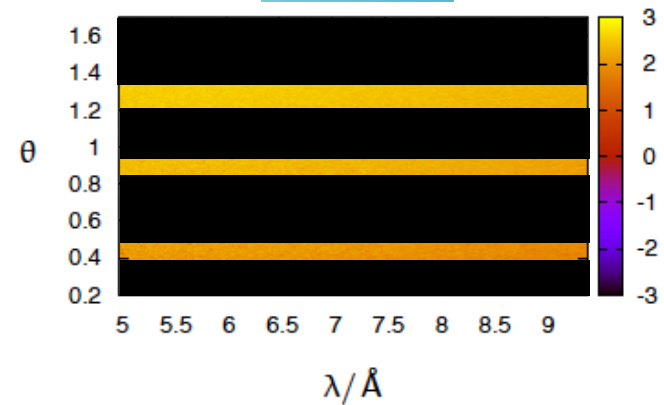


Langmuir-Blodgett trough

Conventional ToF refl.



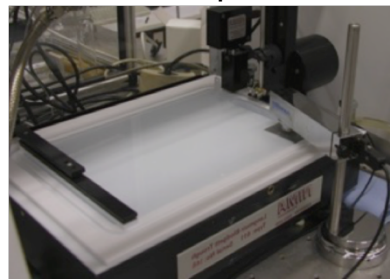
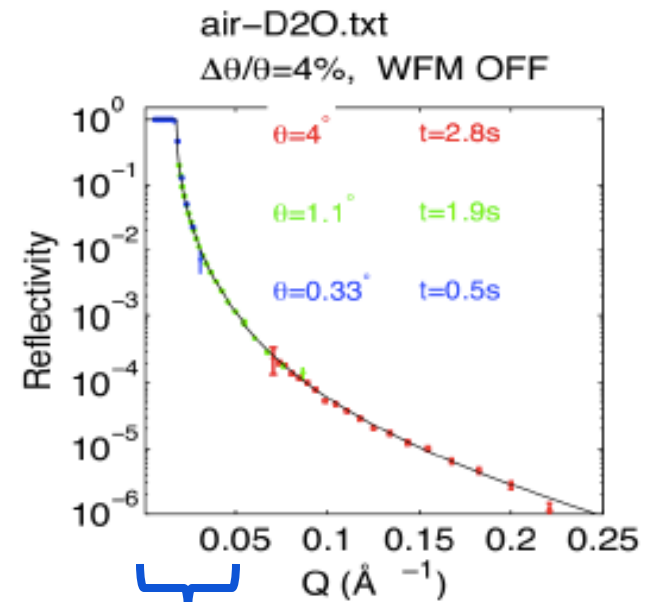
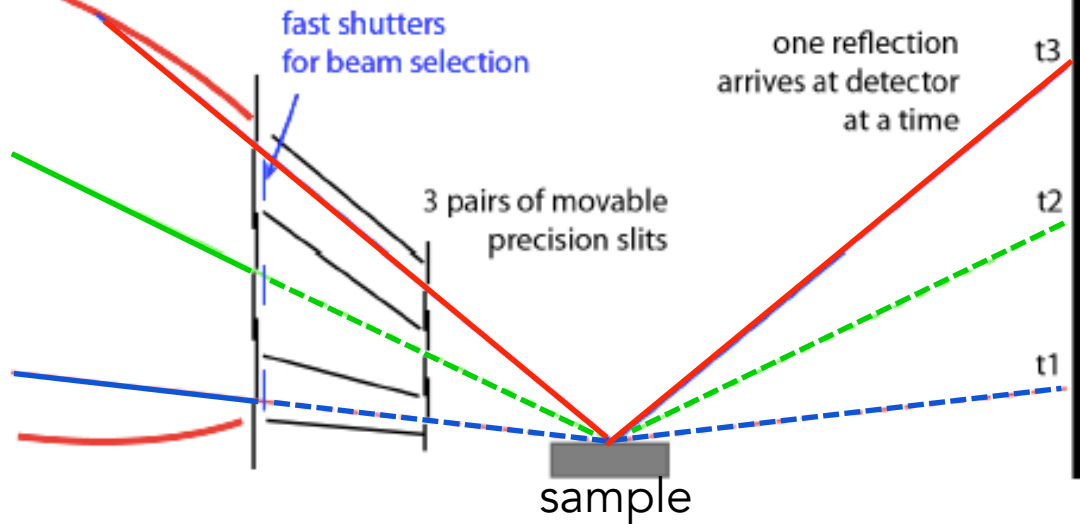
FREIA



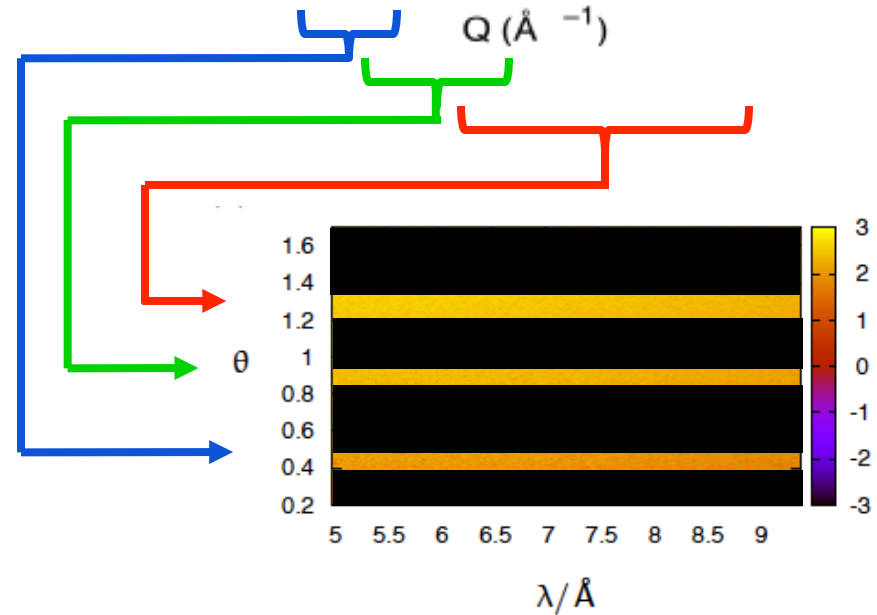
FREIA

$$q = (4\pi/\lambda) \sin(\theta)$$

3 ranges in q measured at once without moving the sample

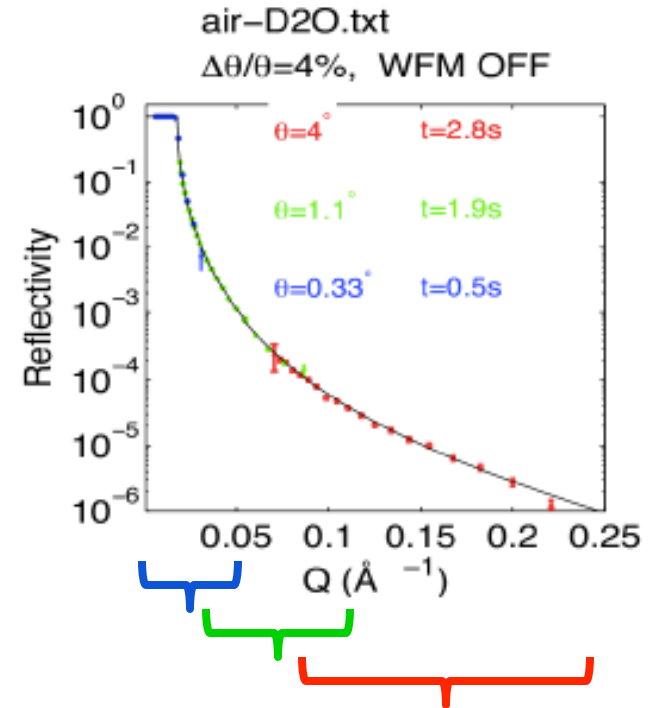
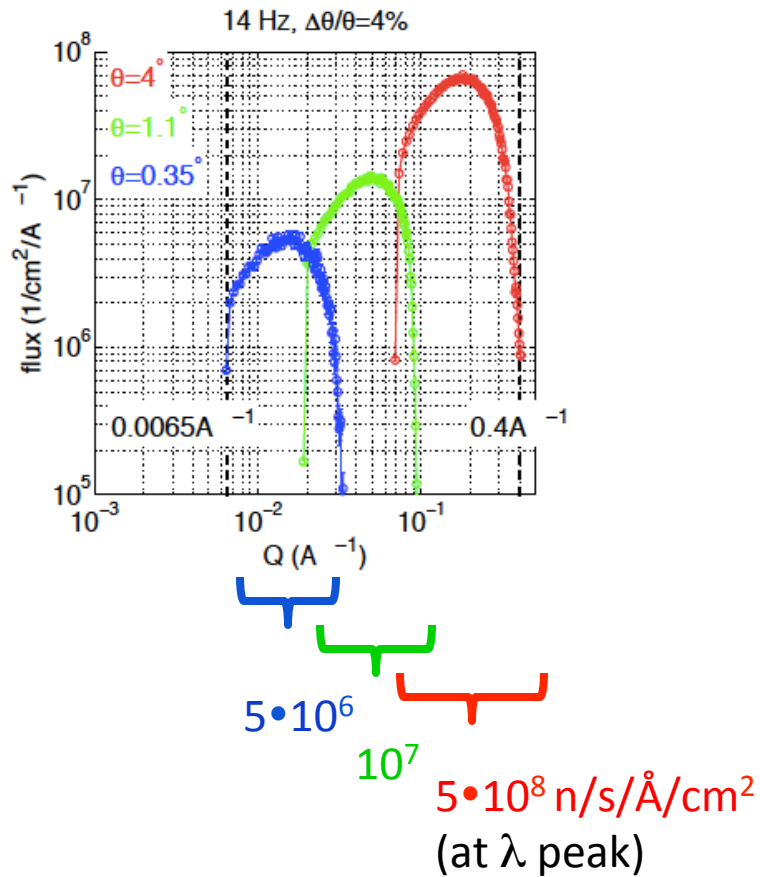


Langmuir-Blodgett trough

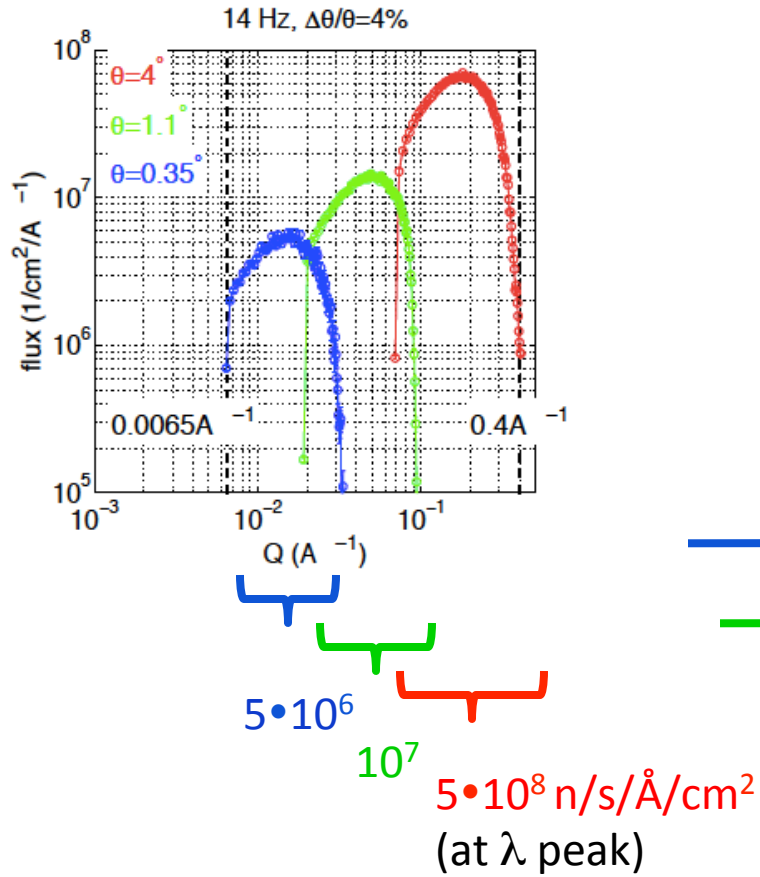


$$q = (4\pi/\lambda) \sin(\theta)$$

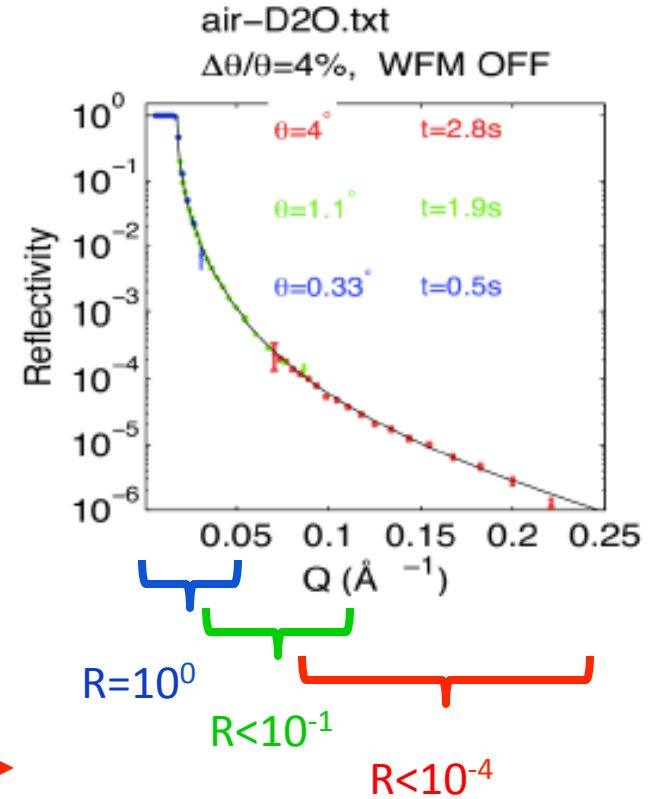
Flux at sample



Flux at sample

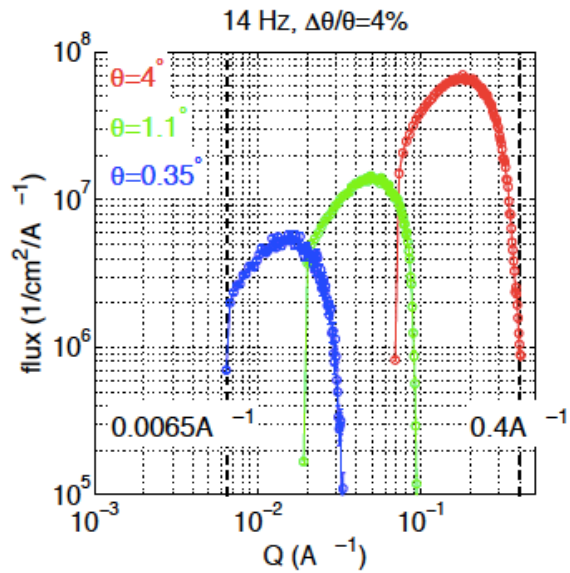


$$q = (4\pi/\lambda) \sin(\theta)$$



$$q = (4\pi/\lambda) \sin(\theta)$$

Flux at sample



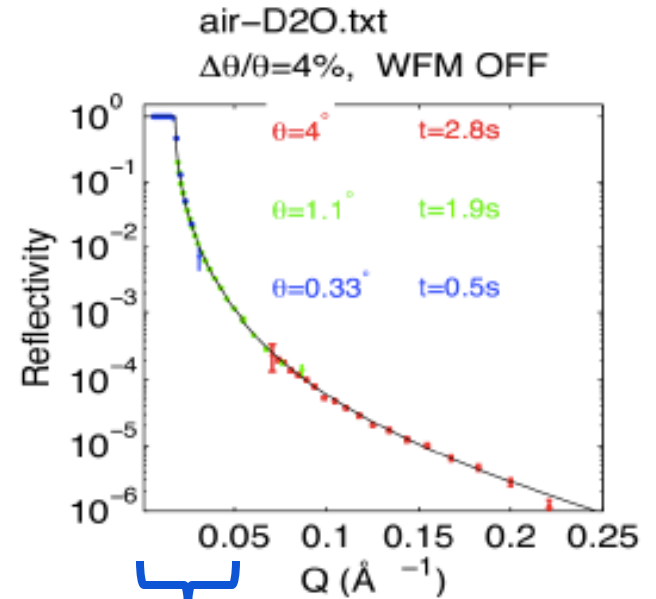
$5 \cdot 10^6$

10^7

$5 \cdot 10^8 \text{ n/s/\AA/cm}^2$
 (at λ peak)



Flux at detector



$R=10^0$

$R < 10^{-1}$

$R < 10^{-4}$

$< 10^4 \text{ n/s/\AA/mm}^2$

$< 10^2 \text{ n/s/\AA/mm}^2$

$10^0 \cdot 5 \cdot 10^6 =$

$5 \cdot 10^6 \text{ n/s/\AA/cm}^2 =$

$= 5 \cdot 10^4 \text{ n/s/\AA/mm}^2$

The state of the art

Instrument	Facility	techn.	area ($mm \times mm$)	spatial res. ($mm \times mm$)	efficiency	global rate (s^{-1})	local rate ($s^{-1}mm^{-2}$)
FIGARO [9]	ILL	3He	512×256	$\sim 2 \times 7.5$	$\sim 63\% @ 2.5\text{\AA}$ $\sim 90\% @ 10\text{\AA}$ $\sim 80\% @ 30\text{\AA}$	$3 \cdot 10^7$	230
SuperADAM [11]	ILL	3He	300×300	2.8×2.8	$76\% @ 4.4\text{\AA}$	$2 \cdot 10^5$	-
REFSANS [12]	FRM2	3He	500×500	$\sim 2 \times 2$	$58\% @ 10\text{\AA}$ $\geq 50\% \in [5, 18]\text{\AA}$	$2.2 \cdot 10^5$	300
INTER [13]	ISIS	$^3He, ^6Li$	200×200	$\sim 1 \times 1$	-	-	-
POLREF [14, 15]	ISIS	3He	200×200	$\leq 1 \times 1$	-	-	-
BIOREF [16]	HZB	3He	300×300	2×3	$\sim 60\% @ 10\text{\AA}$	$2 \cdot 10^5$	300
LR	SNS	3He	200×200	1.3×1.3	-	-	-
MR	SNS	3He	210×180	1.5×1.5	-	-	-
Platypus [17]	OPAL	3He	500×250	1.2×1.2	$\sim 60\% @ 10\text{\AA}$	$2 \cdot 10^5$	300
SOFIA [18, 19]	J-PARC	3He	128×128	2×2	-	-	300
		6Li	256×256	4×4	-	-	300

The state of the art

Instrument	Facility	techn.	area (mm × mm)	spatial res. (mm × mm)	efficiency	global rate (s ⁻¹)	local rate (s ⁻¹ mm ⁻²)
FIGARO [9]	ILL	³ He	512 × 256	~ 2 × 7.5	~ 63% @ 2.5Å ~ 90% @ 10Å ~ 80% @ 30Å	3 · 10 ⁷	230
SuperADAM [11]	ILL	³ He	300 × 300	2.8 × 2.8	76% @ 4.4Å	2 · 10 ⁵	-
REFSANS [12]	FRM2	³ He	500 × 500	~ 2 × 2	58% @ 10Å ≥ 50% ∈ [5, 18]Å	2.2 · 10 ⁵	300
INTER [13]	ISIS	³ He, ⁶ Li	200 × 200	~ 1 × 1	-	-	-
POLREF [14, 15]	ISIS	³ He	200 × 200	≤ 1 × 1	-	-	-
BIOREF [16]	HZB	³ He	300 × 300	2 × 3	~ 60% @ 10Å	2 · 10 ⁵	300
LR	SNS	³ He	200 × 200	1.3 × 1.3	-	-	-
MR	SNS	³ He	210 × 180	1.5 × 1.5	-	-	-
Platypus [17]	OPAL	³ He	500 × 250	1.2 × 1.2	~ 60% @ 10Å	2 · 10 ⁵	300
SOFIA [18, 19]	J-PARC	³ He	128 × 128	2 × 2	-	-	300
		⁶ Li	256 × 256	4 × 4	-	-	300

FREIA

Max rate on detector (at peak)	10 ⁵ n/s/Å/mm ²
Max global rate	12 MHz (1.2x100mm ² footprint*) 12 MHz (detector area*)
Wavelength range	2.5 – 12 Å (optional up to 25Å)
Efficiency	>60% (above 4Å)
Max detector size	500x500mm ²
Spatial resolution	4mm x 1mm
Sample-Detector distance	Not fixed (mostly 3m)
Window scattering	<10 ⁻⁴

x300

Flux at detector

The state of the art

Instrument	Facility	techn.	area (mm × mm)	spatial res. (mm × mm)	efficiency	global rate (s ⁻¹)	local rate (s ⁻¹ mm ⁻²)
FIGARO [9]	ILL	³ He	512 × 256	~ 2 × 7.5	~ 63% @ 2.5Å ~ 90% @ 10Å ~ 80% @ 30Å	3 · 10 ⁷	230
SuperADAM [11]	ILL	³ He	300 × 300	2.8 × 2.8	76% @ 4.4Å	2 · 10 ⁵	-
REFSANS [12]	FRM2	³ He	500 × 500	~ 2 × 2	58% @ 10Å ≥ 50% ∈ [5, 18]Å	2.2 · 10 ⁵	300
INTER [13]	ISIS	³ He, ⁶ Li	200 × 200	~ 1 × 1	-	-	-
POLREF [14, 15]	ISIS	³ He	200 × 200	≤ 1 × 1	-	-	-
BIOREF [16]	HZB	³ He	300 × 300	2 × 3	~ 60% @ 10Å	2 · 10 ⁵	300
LR	SNS	³ He	200 × 200	1.3 × 1.3	-	-	-
MR	SNS	³ He	210 × 180	1.5 × 1.5	-	-	-
Platypus [17]	OPAL	³ He	500 × 250	1.2 × 1.2	~ 60% @ 10Å	2 · 10 ⁵	300
SOFIA [18, 19]	J-PARC	³ He ⁶ Li	128 × 128 256 × 256	2 × 2 4 × 4	- -	- -	300 300

FREIA

Max rate on detector (at peak)	10 ⁵ n/s/Å/mm ²
Max global rate	12 MHz (1.2x100mm ² footprint*) 12 MHz (detector area*)
Wavelength range	2.5 – 12 Å (optional up to 25Å)
Efficiency	>60% (above 4Å)
Max detector size	500x500mm ²
Spatial resolution	4mm x 1mm
Sample-Detector distance	Not fixed (mostly 3m)
Window scattering	<10 ⁻⁴

x300

Flux at detector



Swiss-Danish ESS
Instrumentation consortium

Jochen Stahn
Marité Cardenas
Ursula B. Hansen

ESS SAC Meeting
21.05.2014, Lund

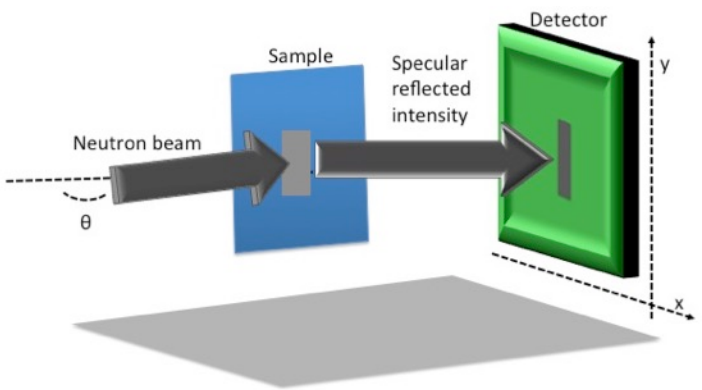
Estia

a

focusing reflectometer for small samples

based on the

Selene guide concept

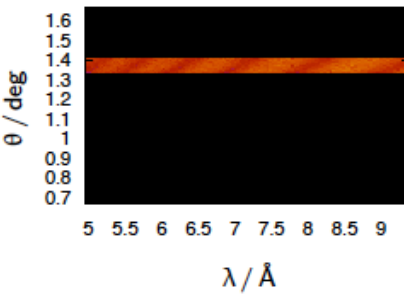
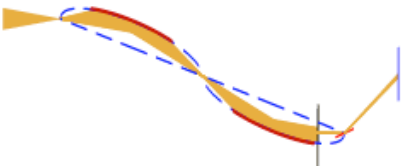


Vertical ToF Reflectometer

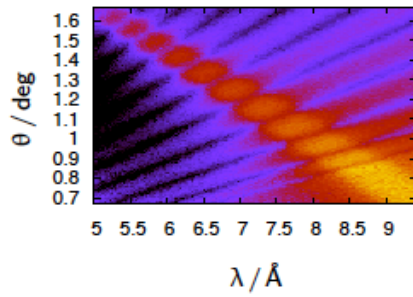
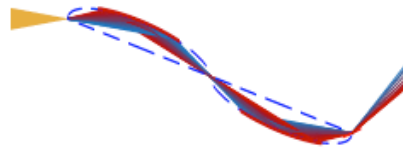
$$q = (4\pi/\lambda) \sin(\theta)$$

It can work in 3 different modes:

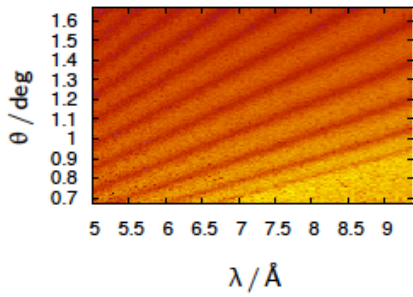
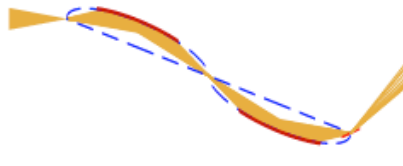
almost conventional reflectivity [→2.8.1]



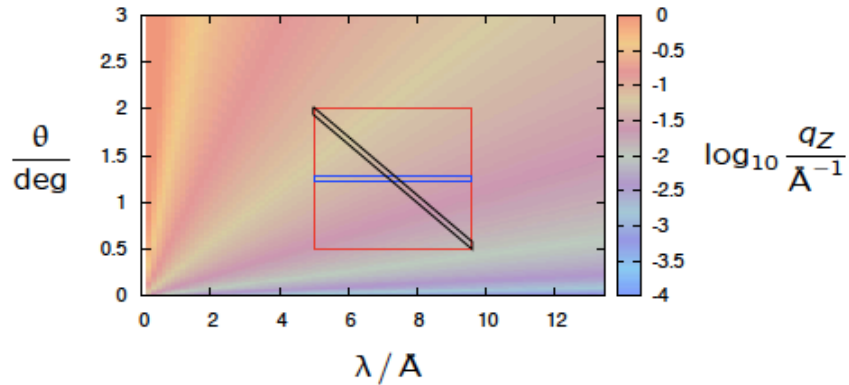
λ - θ -encoding [→2.8.2]



high-intensity specular reflectivity [→2.8.3]



operation modes



almost conventional reflectivity

= TOF

- o defined foot-print
- o off-specular reflectivity

lambda-theta-encoding

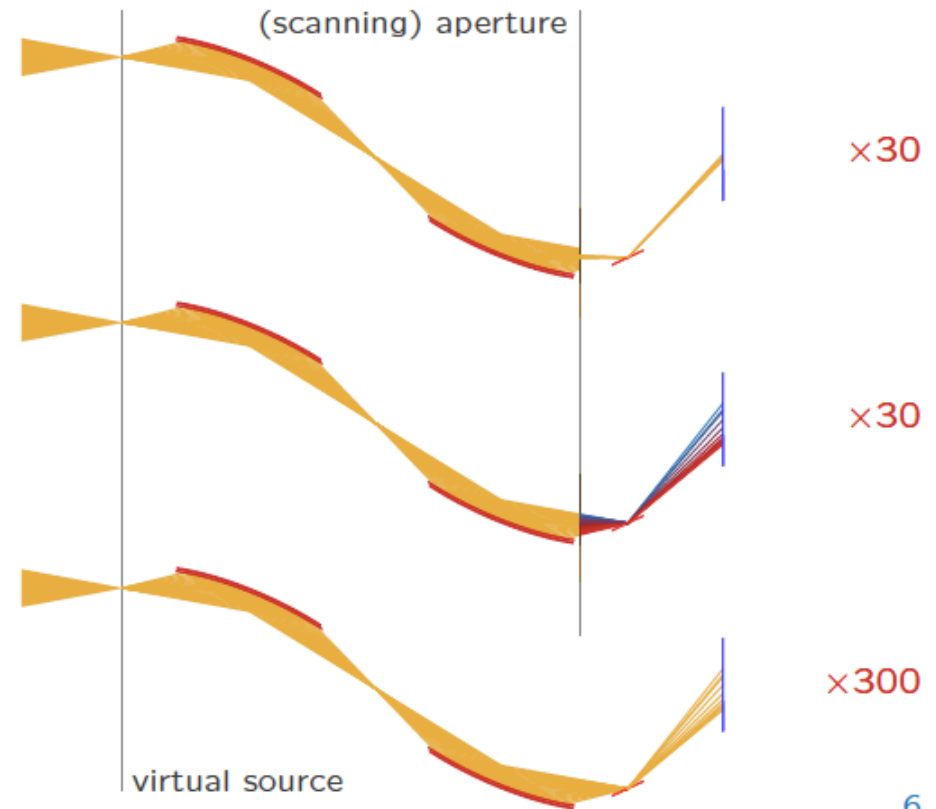
= TOF(θ)

- o wider q_z -range
- o constant $\Delta q/q$

high-intensity specular reflectivity

= TOF \times θ -dispersive

- o split-second t -resolution
- o screening of parameter space



Conventional Reflectivity mode

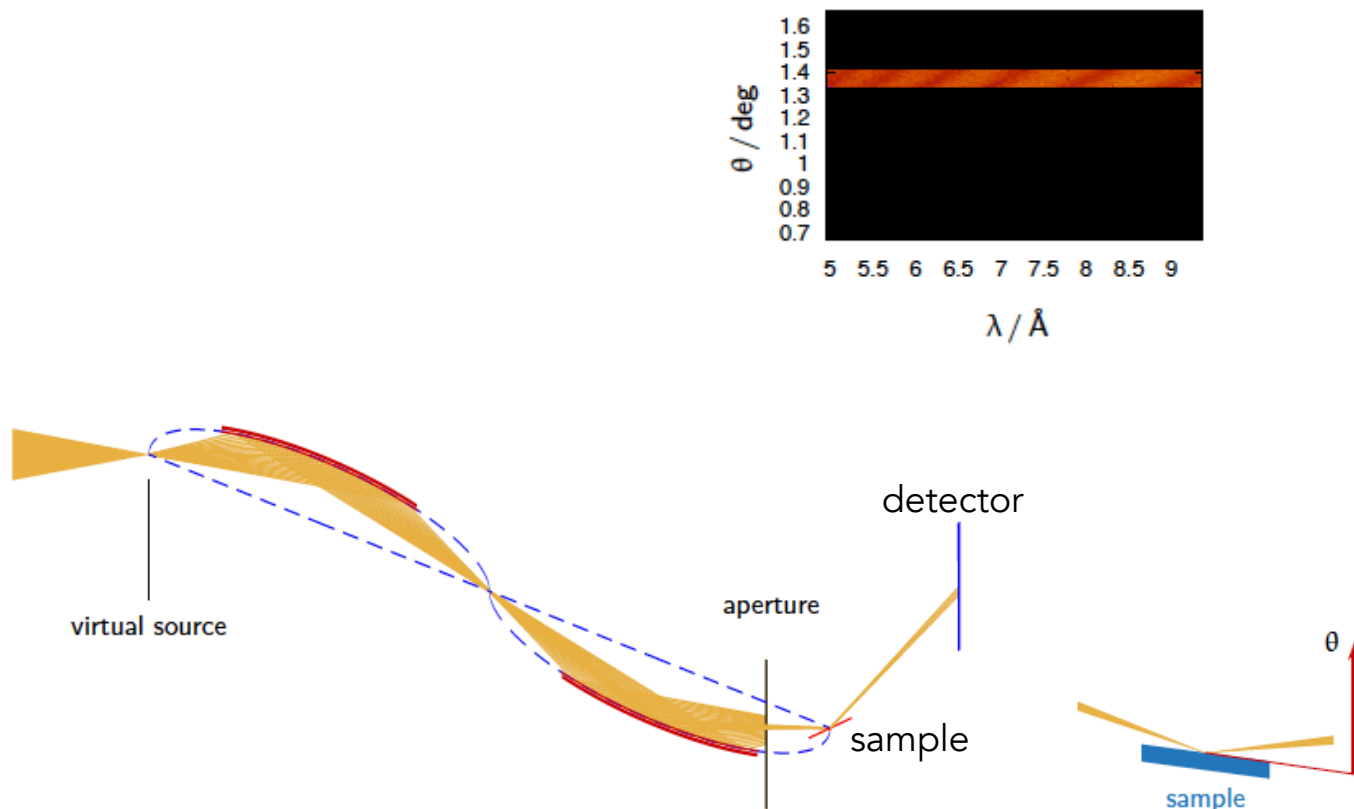


Figure 10.1: Sketch to illustrate the operation scheme: the beam (gold) is transported with the full divergence and without chopping to the end of the guide system. There an aperture (black) defines $\Delta\theta$, and its position together with the sample orientation ω also the angle of incidence θ . The beam footprint on the sample is defined by size and orientation of the virtual source.

The flux at sample is spread on about $5 \times 1 \text{ cm}^2$ area maximum. On detector, due to divergence, will be same flux (below critical edge $R=1$) on $2 \text{ mm} \times 6 \text{ cm}$ area; then about $10^5 \text{ n/s/\AA/mm}^2$ (at peak).

λ - θ encoding

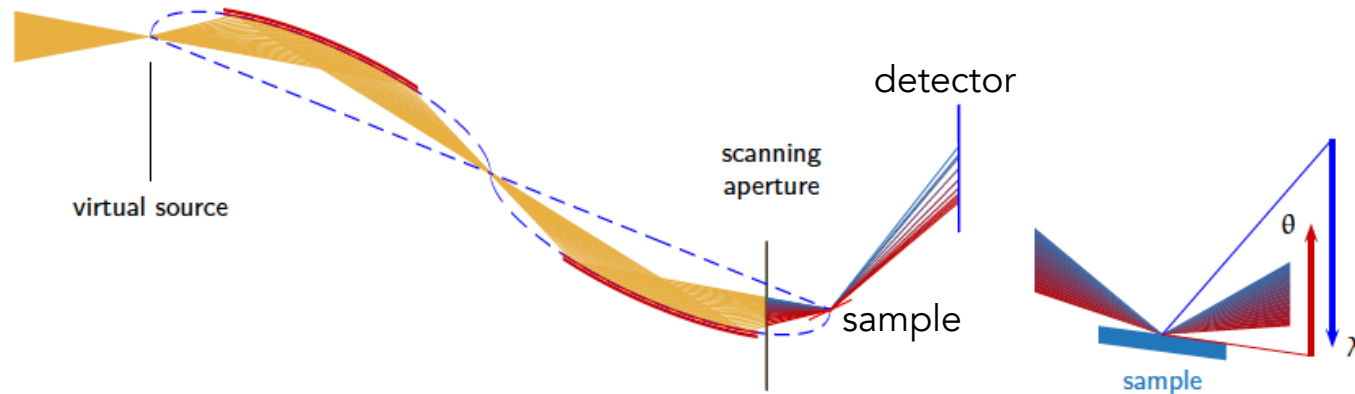
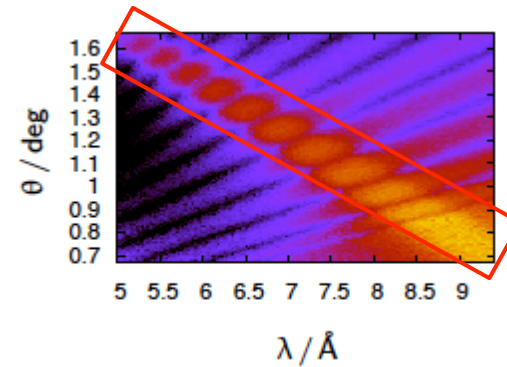


Figure 10.2: Sketch to illustrate the operation scheme: the beam (gold) is transported with the full divergence and without chopping to the end of the guide system. As in the conventional mode [→10.2], a slit (black) defines $\Delta\theta$ and together with the sample orientation ω also the angle of incidence θ . But the opening and position change during the passing of each pulse. This way high θ can be related to low λ and vice versa.

The flux is spread on a wider detector surface with respect to the conventional reflectometry mode. Spatial resolution (0.5mm) is needed to resolve the different theta.

High intensity mode

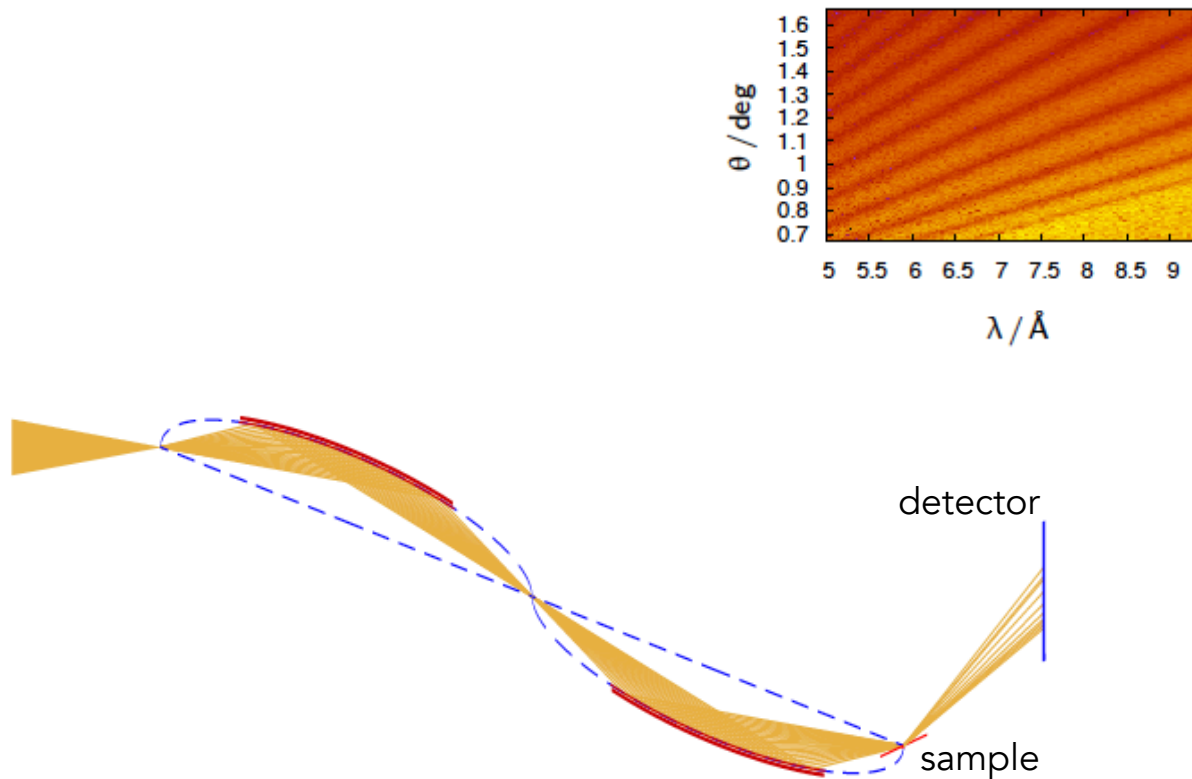


Figure 10.7: Sketch to illustrate the high-intensity specular reflectivity operation mode.

The flux is spread on a wider detector surface with respect to the conventional reflectometry mode. Spatial resolution (0.5mm) is needed to resolve the different theta.

In the high-intensity mode about $105 \times 105 \text{ mm}^2$ area of the detector is illuminated with 10^8 n/s , i.e. 10^4 n/s/mm^2 (at peak).
The final optimal detector size is $40 \times 25 \text{ cm}^2$.

The state of the art

Instrument	Facility	techn.	area (mm × mm)	spatial res. (mm × mm)	efficiency	global rate (s ⁻¹)	local rate (s ⁻¹ mm ⁻²)
FIGARO [9]	ILL	³ He	512 × 256	~ 2 × 7.5	~ 63% @ 2.5Å ~ 90% @ 10Å ~ 80% @ 30Å	3 · 10 ⁷	230
SuperADAM [11]	ILL	³ He	300 × 300	2.8 × 2.8	76% @ 4.4Å	2 · 10 ⁵	-
REFSANS [12]	FRM2	³ He	500 × 500	~ 2 × 2	58% @ 10Å ≥ 50% ∈ [5, 18]Å	2.2 · 10 ⁵	300
INTER [13]	ISIS	³ He, ⁶ Li	200 × 200	~ 1 × 1	-	-	-
POLREF [14, 15]	ISIS	³ He	200 × 200	≤ 1 × 1	-	-	-
BIOREF [16]	HZB	³ He	300 × 300	2 × 3	~ 60% @ 10Å	2 · 10 ⁵	300
LR	SNS	³ He	200 × 200	1.3 × 1.3	-	-	-
MR	SNS	³ He	210 × 180	1.5 × 1.5	-	-	-
Platypus [17]	OPAL	³ He	500 × 250	1.2 × 1.2	~ 60% @ 10Å	2 · 10 ⁵	300
SOFIA [18, 19]	J-PARC	³ He	128 × 128	2 × 2	-	-	300
		⁶ Li	256 × 256	4 × 4	-	-	300

The state of the art

Instrument	Facility	techn.	area (mm × mm)	spatial res. (mm × mm)	efficiency	global rate (s ⁻¹)	local rate (s ⁻¹ mm ⁻²)
FIGARO [9]	ILL	³ He	512 × 256	~ 2 × 7.5	~ 63% @ 2.5Å ~ 90% @ 10Å ~ 80% @ 30Å	3 · 10 ⁷	230
SuperADAM [11]	ILL	³ He	300 × 300	2.8 × 2.8	76% @ 4.4Å	2 · 10 ⁵	-
REFSANS [12]	FRM2	³ He	500 × 500	~ 2 × 2	58% @ 10Å ≥ 50% ∈ [5, 18]Å	2.2 · 10 ⁵	300
INTER [13]	ISIS	³ He, ⁶ Li	200 × 200	~ 1 × 1	-	-	-
POLREF [14, 15]	ISIS	³ He	200 × 200	≤ 1 × 1	-	-	-
BIOREF [16]	HZB	³ He	300 × 300	2 × 3	~ 60% @ 10Å	2 · 10 ⁵	300
LR	SNS	³ He	200 × 200	1.3 × 1.3	-	-	-
MR	SNS	³ He	210 × 180	1.5 × 1.5	-	-	-
Platypus [17]	OPAL	³ He	500 × 250	1.2 × 1.2	~ 60% @ 10Å	2 · 10 ⁵	300
SOFIA [18, 19]	J-PARC	³ He	128 × 128	2 × 2	-	-	300
		⁶ Li	256 × 256	4 × 4	-	-	300

Estia

Max rate on detector (at peak)	<ul style="list-style-type: none"> Conventional refl. 10⁵ n/s/Å/mm² High intensity mode 10⁴ n/s/Å/mm²
Max global rate	<ul style="list-style-type: none"> Conventional refl. 12MHz (2x60mm² footprint or on whole detect. area) High intensity mode 100MHz ** (105x105mm² footprint or on whole detect. area)
Wavelength range	4 – 12 Å
Efficiency	>60% (above 4Å)
Max detector size	300x500mm ²
Spatial resolution	4mm x 0.5mm
Sample-Detector distance	Fixed ~4m



Flux at detector

The state of the art

Instrument	Facility	techn.	area (mm × mm)	spatial res. (mm × mm)	efficiency	global rate (s ⁻¹)	local rate (s ⁻¹ mm ⁻²)
FIGARO [9]	ILL	³ He	512 × 256	~ 2 × 7.5	~ 63% @ 2.5Å ~ 90% @ 10Å ~ 80% @ 30Å	3 · 10 ⁷	230
SuperADAM [11]	ILL	³ He	300 × 300	2.8 × 2.8	76% @ 4.4Å	2 · 10 ⁵	-
REFSANS [12]	FRM2	³ He	500 × 500	~ 2 × 2	58% @ 10Å ≥ 50% ∈ [5, 18]Å	2.2 · 10 ⁵	300
INTER [13]	ISIS	³ He, ⁶ Li	200 × 200	~ 1 × 1	-	-	-
POLREF [14, 15]	ISIS	³ He	200 × 200	≤ 1 × 1	-	-	-
BIOREF [16]	HZB	³ He	300 × 300	2 × 3	~ 60% @ 10Å	2 · 10 ⁵	300
LR	SNS	³ He	200 × 200	1.3 × 1.3	-	-	-
MR	SNS	³ He	210 × 180	1.5 × 1.5	-	-	-
Platypus [17]	OPAL	³ He	500 × 250	1.2 × 1.2	~ 60% @ 10Å	2 · 10 ⁵	300
SOFIA [18, 19]	J-PARC	³ He ⁶ Li	128 × 128 256 × 256	2 × 2 4 × 4	- -	- -	300 300

Estia

Max rate on detector (at peak)	<ul style="list-style-type: none"> Conventional refl. 10⁵ n/s/Å/mm² High intensity mode 10⁴ n/s/Å/mm²
Max global rate	<ul style="list-style-type: none"> Conventional refl. 12MHz (2x60mm² footprint or on whole detect. area) High intensity mode 100MHz ** (105x105mm² footprint or on whole detect. area)
Wavelength range	4 – 12 Å
Efficiency	>60% (above 4Å)
Max detector size	300x500mm ²
Spatial resolution	4mm x 0.5mm
Sample-Detector distance	Fixed ~4m

x300

Flux at detector

The state of the art

Instrument	Facility	techn.	area (mm × mm)	spatial res. (mm × mm)	efficiency	global rate (s ⁻¹)	local rate (s ⁻¹ mm ⁻²)
FIGARO [9]	ILL	³ He	512 × 256	~ 2 × 7.5	~ 63% @ 2.5Å ~ 90% @ 10Å ~ 80% @ 30Å	3 · 10 ⁷	230
SuperADAM [11]	ILL	³ He	300 × 300	2.8 × 2.8	76% @ 4.4Å	2 · 10 ⁵	-
REFSANS [12]	FRM2	³ He	500 × 500	~ 2 × 2	58% @ 10Å ≥ 50% ∈ [5, 18]Å	2.2 · 10 ⁵	300
INTER [13]	ISIS	³ He, ⁶ Li	200 × 200	~ 1 × 1	-	-	-
POLREF [14, 15]	ISIS	³ He	200 × 200	≤ 1 × 1	-	-	-
BIOREF [16]	HZB	³ He	300 × 300	2 × 3	~ 60% @ 10Å	2 · 10 ⁵	300
LR	SNS	³ He	200 × 200	1.3 × 1.3	-	-	-
MR	SNS	³ He	210 × 180	1.5 × 1.5	-	-	-
Platypus [17]	OPAL	³ He	500 × 250	1.2 × 1.2	~ 60% @ 10Å	2 · 10 ⁵	300
SOFIA [18, 19]	J-PARC	³ He	128 × 128	2 × 2	-	-	300
		⁶ Li	256 × 256	4 × 4	-	-	300

The ESS requirements

	FREIA	Estia
Max local rate	10 ⁵ n/s/Å/mm ²	<ul style="list-style-type: none"> Conventional refl. 10⁵ n/s/Å/mm² High intensity mode 10⁴ n/s/Å/mm²
Spatial resolution	4mm x 1mm	4mm x 0.5mm

The Multi-Blade project

BrightnESS



LUND UNIVERSITY



Wigner Research Institute

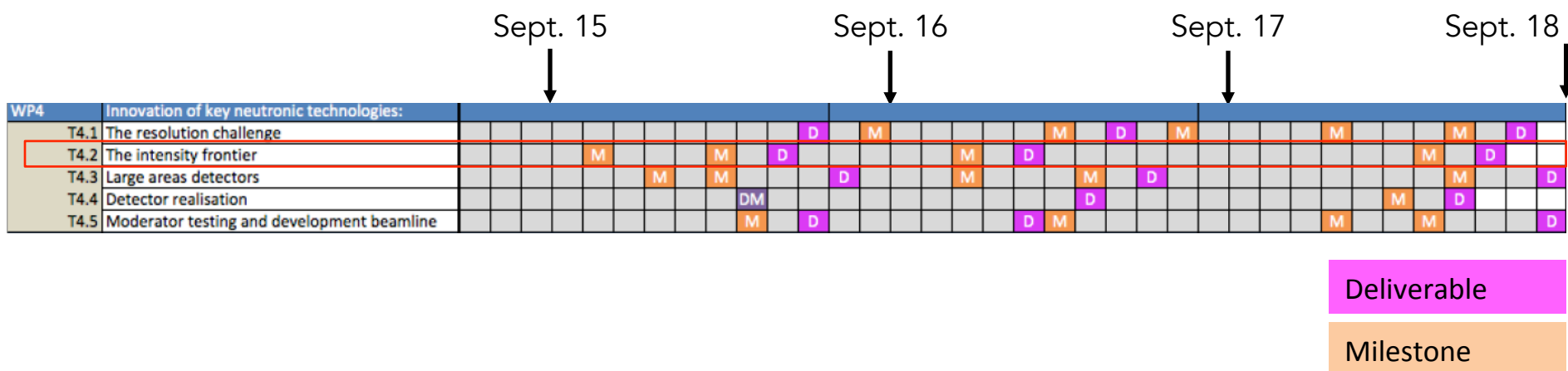


Budapest Neutron Centre

Task 4.2 Neutron Detectors – The Intensity Frontier

The key objective of WP4 is the technological evolution of neutron detectors in terms of resolution, intensity and dimensions.

3 years





ESS Detector Group
(Francesco Piscitelli)



Wigner Research Institute
(Dezső Varga and Eszter Dian)

BNC-Wigner is the largest organization in Hungary comprising 45 research group of various profile. BNC-Wigner has a long tradition in working with industrial companies; in 10y over 25 companies of various size and profile were involved in technology transfer related to neutron developments. BNC-Wigner will support with the detector development required in the intensity frontier task in WP4.



LUND UNIVERSITY
Division of Nuclear Physics
(Kevin Fissum)

LU has a long story of developing novel particle detectors for hostile particle accelerator. LU has completed the construction of the Source-Testing Facility for prototype commissioning. Their experience with developing and testing detectors will be crucial for the task in WP4.

The Multi-Blade project

concept introduced in 2005



Institut Laue-Langevin

proof of concept in 2012



Institut Laue-Langevin



University of Perugia

Jinst

PUBLISHED BY IOP PUBLISHING FOR SISSA MEDIALAB

RECEIVED: December 10, 2013

REVISED: February 6, 2014

ACCEPTED: February 13, 2014

PUBLISHED: March 12, 2014

Study of a high spatial resolution ^{10}B -based thermal neutron detector for application in neutron reflectometry: the Multi-Blade prototype

F. Piccitelli,^{a,b,1} J.G. Buffot,^a J.F. Clergeau,^a S. Cuccaro,^a B. Guérard,^a
A. Khaplanov,^{a,c} Q. La Manna,^a J.M. Rigal^b and P. Van Esch^a

^aInstitut Laue-Langevin (ILL),

6, Jules Horowitz, 38042, Grenoble, France

^bDepartment of Physics, University of Perugia,

Piazza Università 1, 06123 Perugia, Italy

^cEuropean Spallation Source,

P.O. Box 176, SE-22100 Lund, Sweden

E-mail: piccitelli@ill.fr

ABSTRACT: Although for large area detectors it is crucial to find an alternative to detect thermal neutrons because of the ^3He shortage, this is not the case for small area detectors. Neutron scattering science is still growing its instruments' power and the neutron flux a detector must tolerate is increasing. For small area detectors the main effort is to expand the detectors' performances.

At Institut Laue-Langevin (ILL) we developed the Multi-Blade detector which wants to increase the spatial resolution of ^3He -based detectors for high flux applications. We developed a high spatial resolution prototype suitable for neutron reflectometry instruments. It exploits solid ^{10}B -films employed in a proportional gas chamber. Two prototypes have been constructed at ILL and the results obtained on our monochromatic test beam line are presented here.

KEYWORDS: Neutron detectors (cold, thermal, fast neutrons); Gaseous detectors

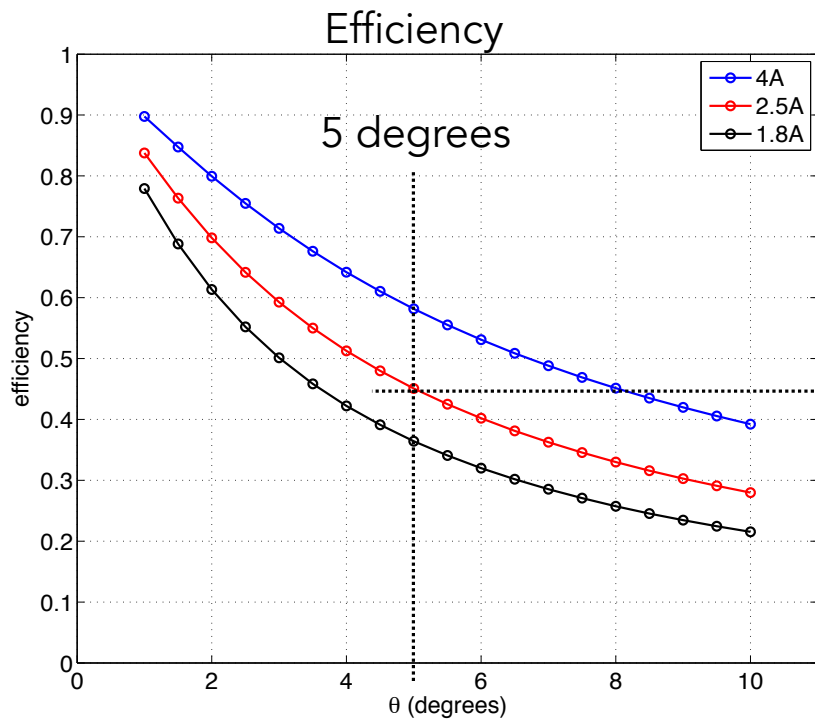
ARXIV EPRINT: [1312.2473](https://arxiv.org/abs/1312.2473)

¹Corresponding author.

© 2014 IOP Publishing Ltd and Sissa Medialab srl

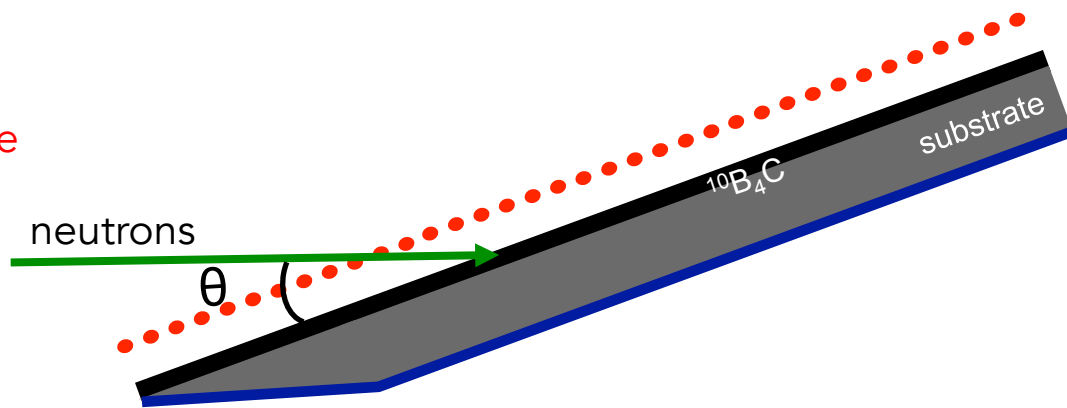
doi:10.1088/1748-0221/9/03/P03007

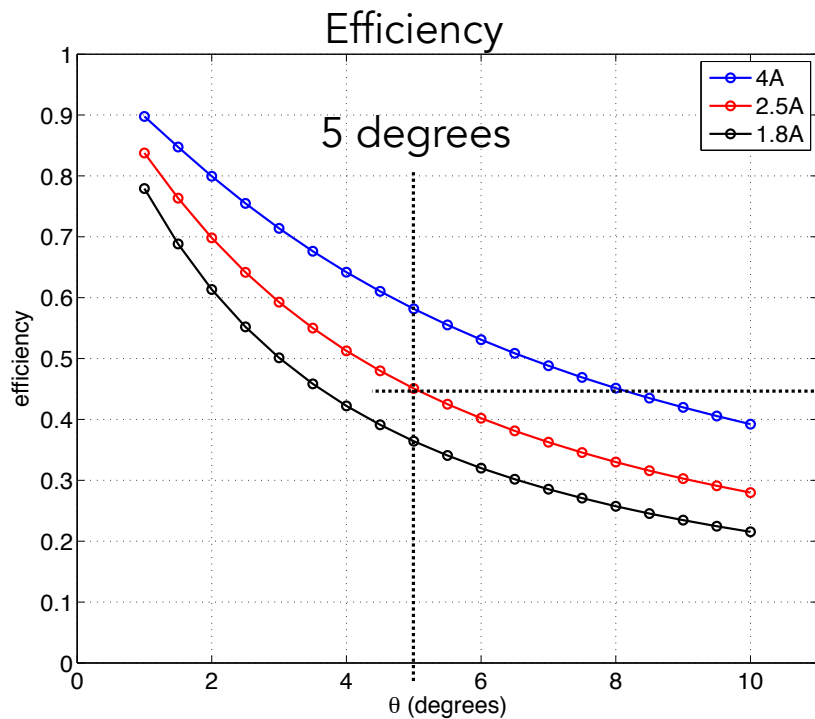
2014 JINST 9 P03007



Efficiency 45% at 2.5Å
 A single Boron layer inclined at 5 degrees

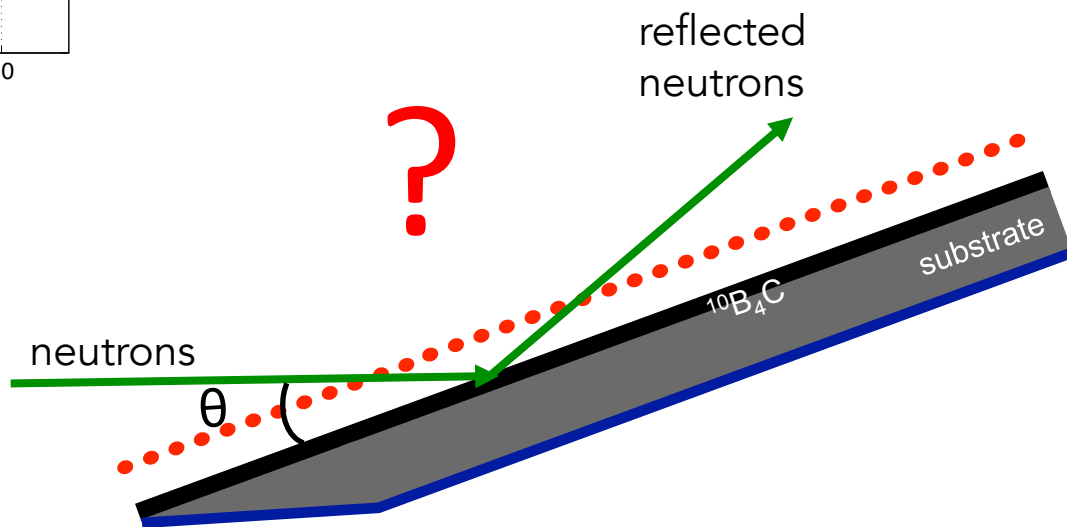
The intensity is spread over a wider surface
 (5 degrees = factor x10)



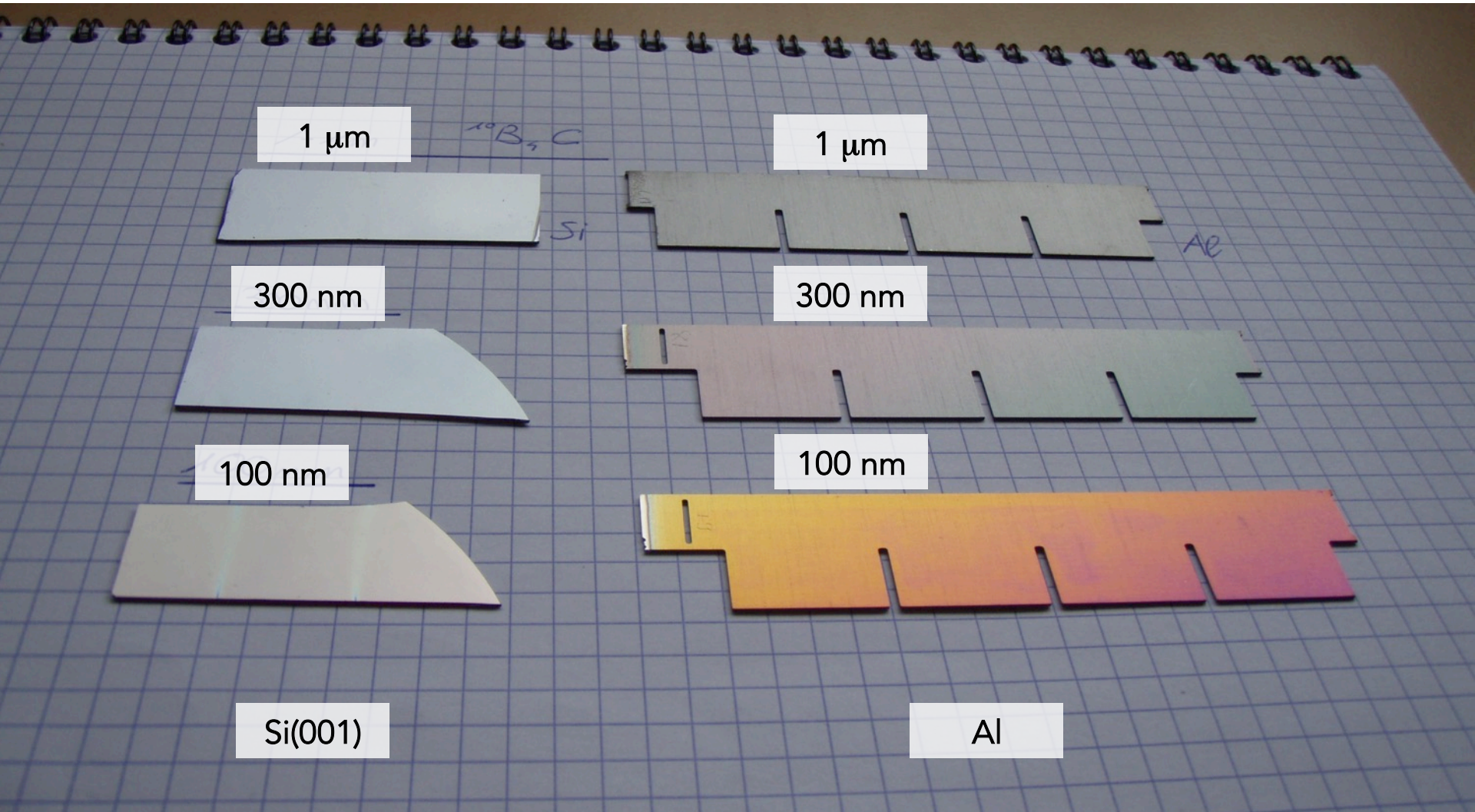


Reflection can reduce the efficiency

Efficiency 45% at 2.5Å
A single Boron layer inclined at 5 degrees



$^{10}\text{B}_4\text{C}$ Samples





Cite this article: Piscitelli F *et al.* 2016
Neutron reflectometry on highly absorbing
films and its application to $^{10}\text{B}_4\text{C}$ -based
neutron detectors. *Proc. R. Soc. A* 20150711.
<http://dx.doi.org/10.1098/rspa.2015.0711>

Received: 15 October 2015

Accepted: 22 December 2015

Subject Areas:
materials science

Keywords:
neutron-induced fluorescence, neutron
reflectometry, Boron-10, neutron detection

Author for correspondence:

F. Piscitelli

e-mail: francesco.piscitelli@ess.se

Electronic supplementary material is available
at <http://dx.doi.org/10.1098/rspa.2015.0711> or
via <http://rspa.royalsocietypublishing.org>.

THE ROYAL SOCIETY
PUBLISHING

Neutron reflectometry on highly absorbing films and its application to $^{10}\text{B}_4\text{C}$ -based neutron detectors

F. Piscitelli^{1,2,3}, A. Khaplanov^{1,2}, A. Devishvili⁴,
S. Schmidt^{1,5}, C. Höglund^{1,5}, J. Birch⁵,
A. J. C. Dennison^{2,6}, P. Gutfreund², R. Hall-Wilton^{1,7}
and P. Van Esch²

¹European Spallation Source ERIC, PO Box 176, Lund 22100, Sweden

²Institut Laue-Langevin (ILL), 71, Avenue des Martyrs, Grenoble
38042, France

³Department of Physics, University of Perugia, Piazza Università 1,
Perugia 06123, Italy

⁴Ruhr-Universität Bochum, Bochum 44780, Germany

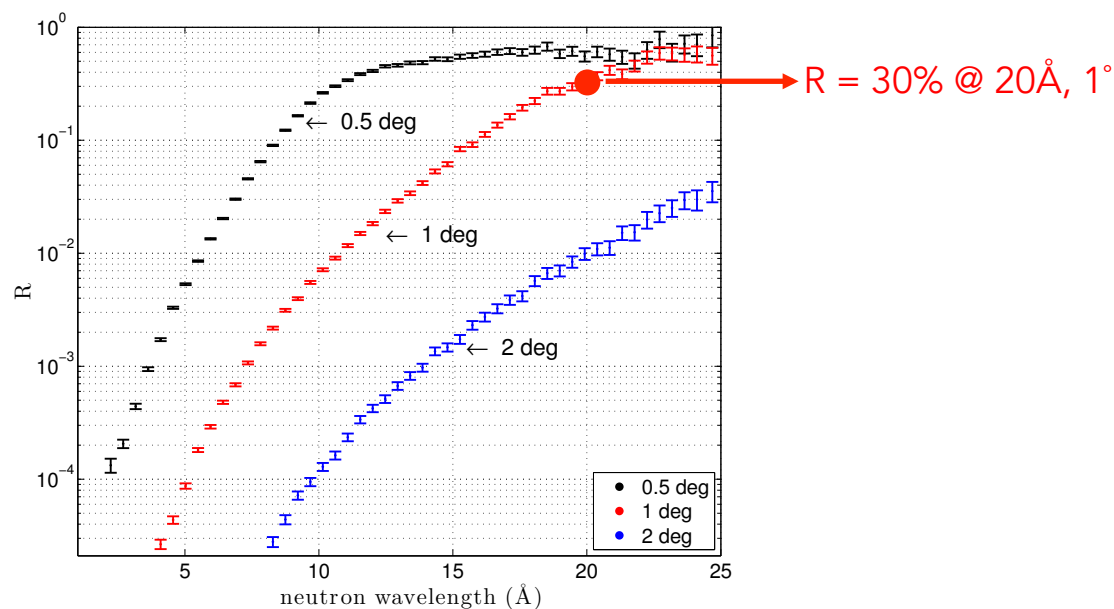
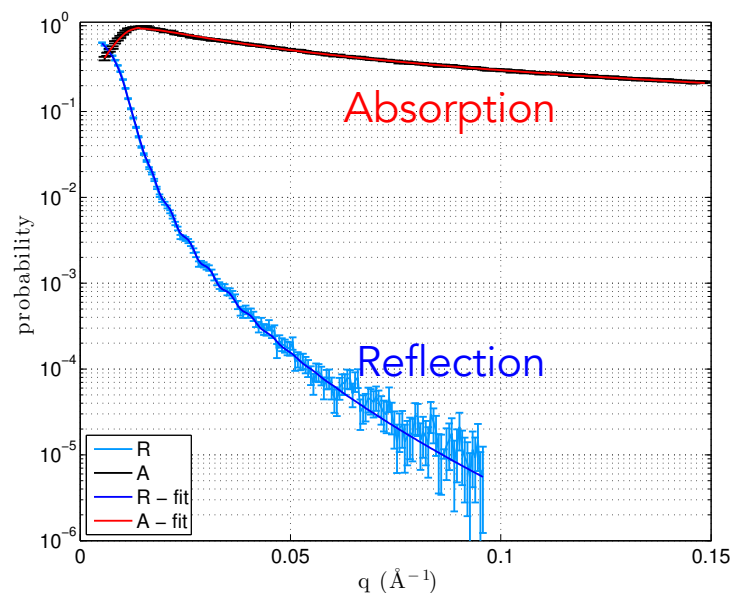
⁵Thin Film Physics Division, Linköping University, Linköping 58183,
Sweden

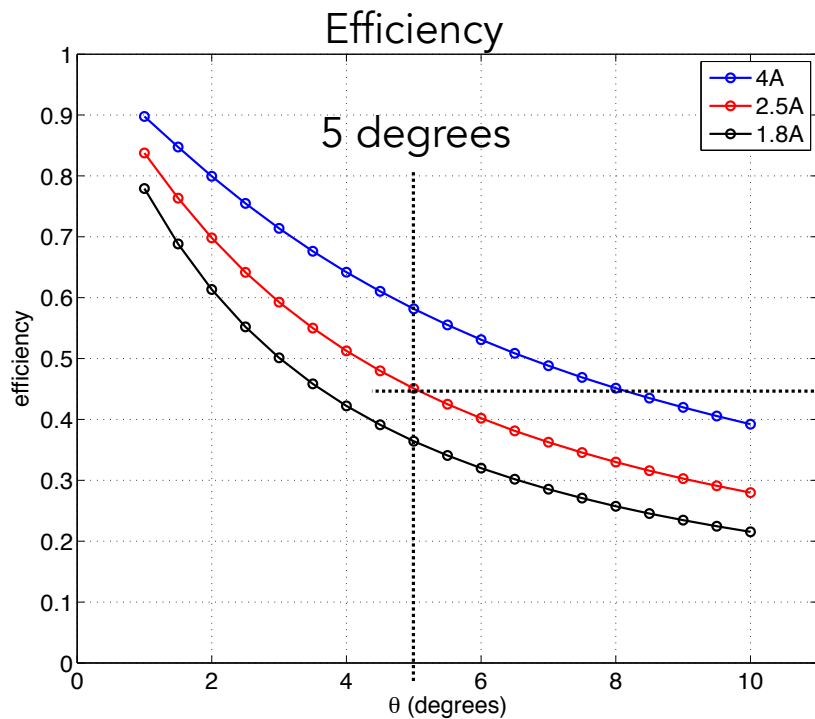
⁶Department of Physics and Astronomy, Uppsala University, BP 516,
Uppsala 75120, Sweden

⁷Mid-Sweden University, Sundsvall 85170, Sweden

Neutron reflectometry is a powerful tool used for studies of surfaces and interfaces. The absorption in the typical studied materials is neglected and this technique is limited only to the reflectivity measurement. For strongly absorbing nuclei, the absorption can be directly measured by using the neutron-induced fluorescence technique which exploits the prompt particle emission of absorbing isotopes. This technique is emerging from soft matter and biology where highly absorbing nuclei, in very small quantities, are used as a label for buried layers. Nowadays, the importance of absorbing layers is rapidly increasing, partially because of their application in neutron detection; a field that has become more active also due to the ^3He -shortage. We extend the neutron-induced fluorescence technique to the study of layers of highly absorbing materials; in

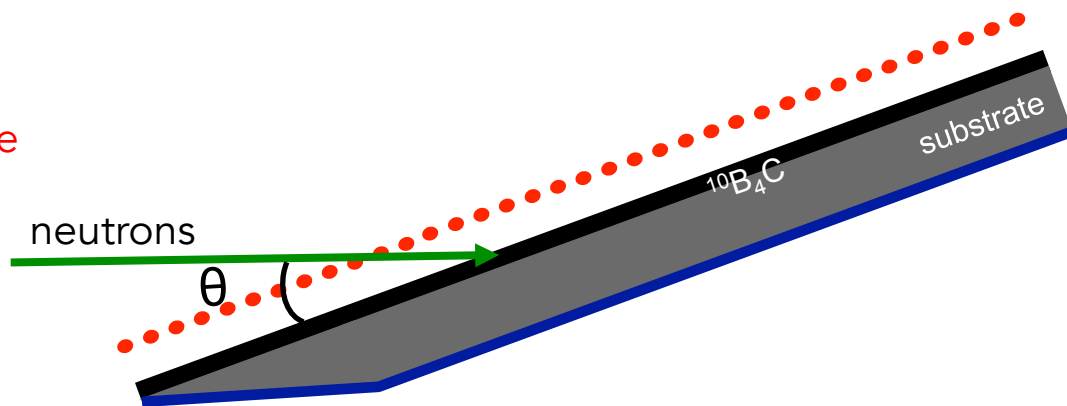
© 2016 The Authors. Published by the Royal Society under the terms of the Creative Commons Attribution License <http://creativecommons.org/licenses/by/4.0/>, which permits unrestricted use, provided the original author and source are credited.

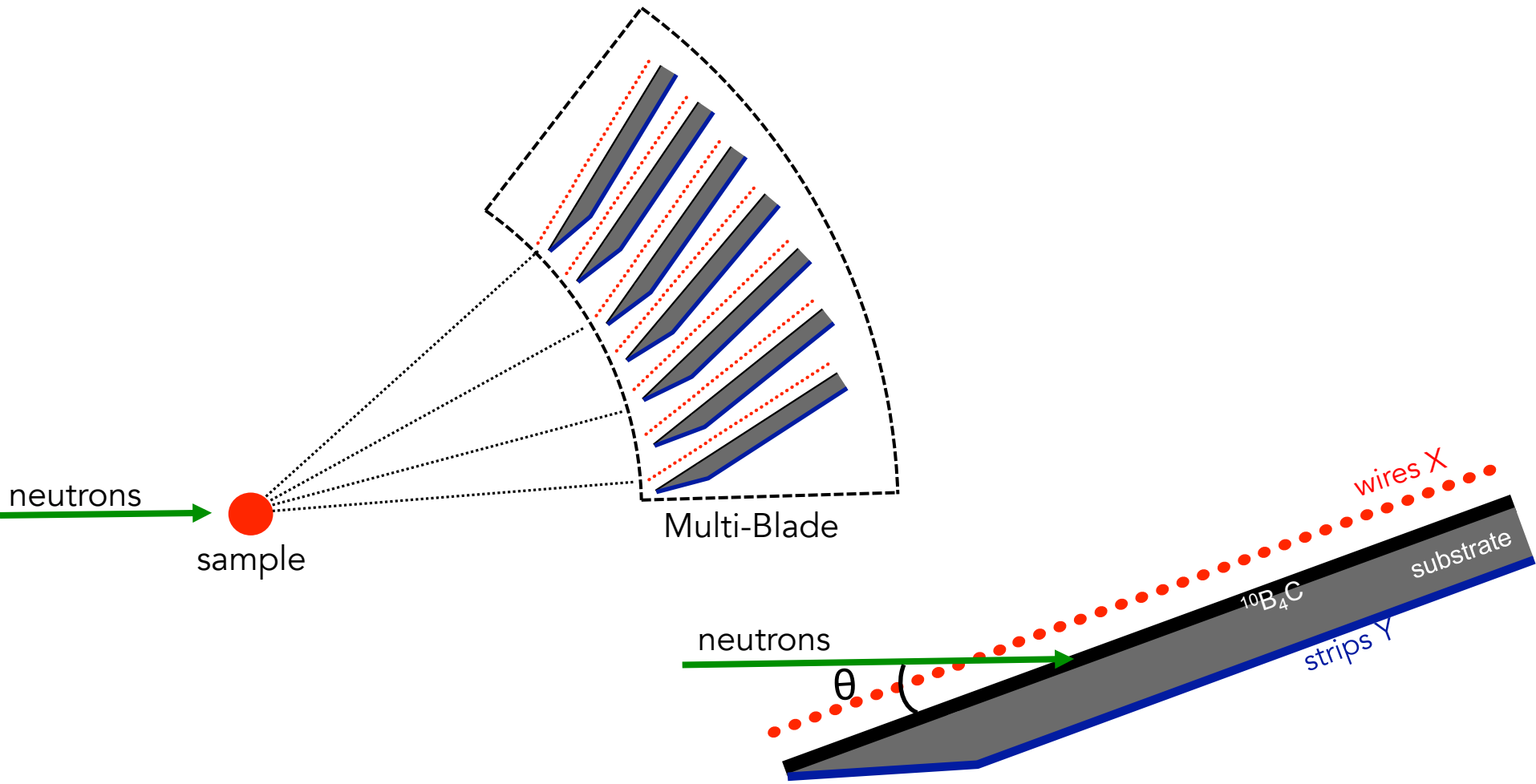




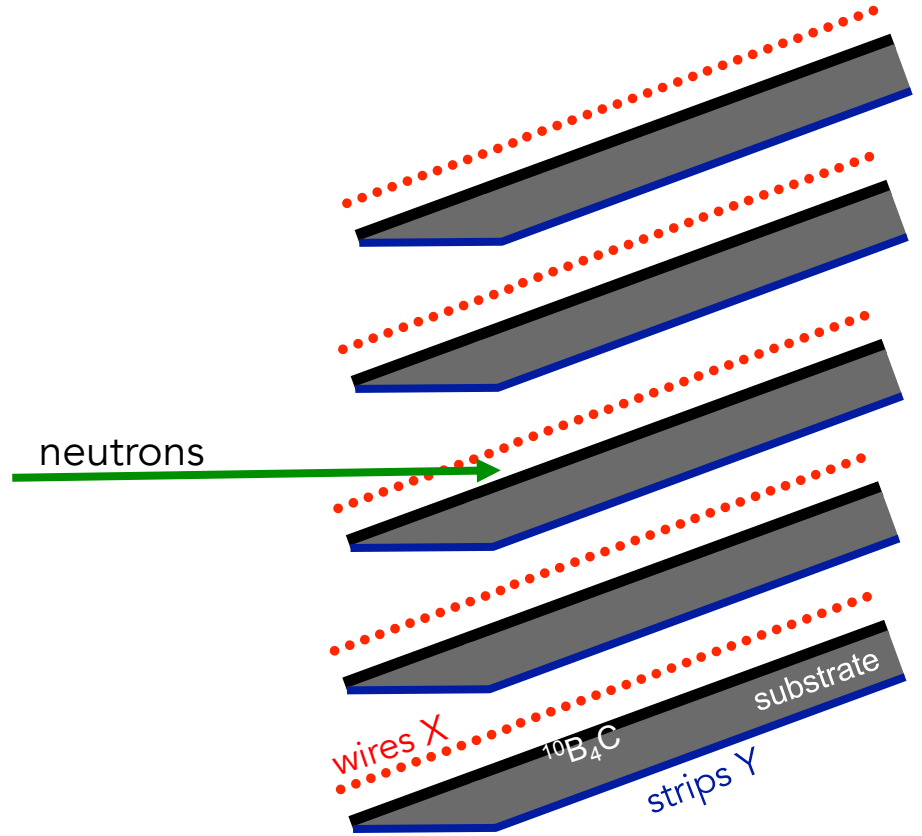
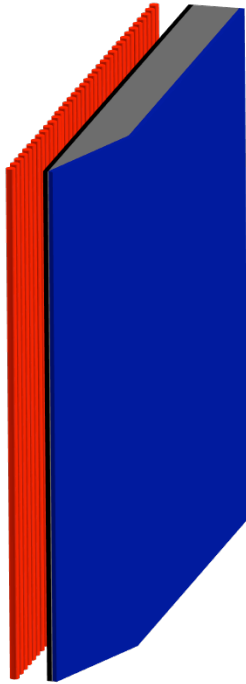
Efficiency 45% at 2.5Å
 A single Boron layer inclined at 5 degrees

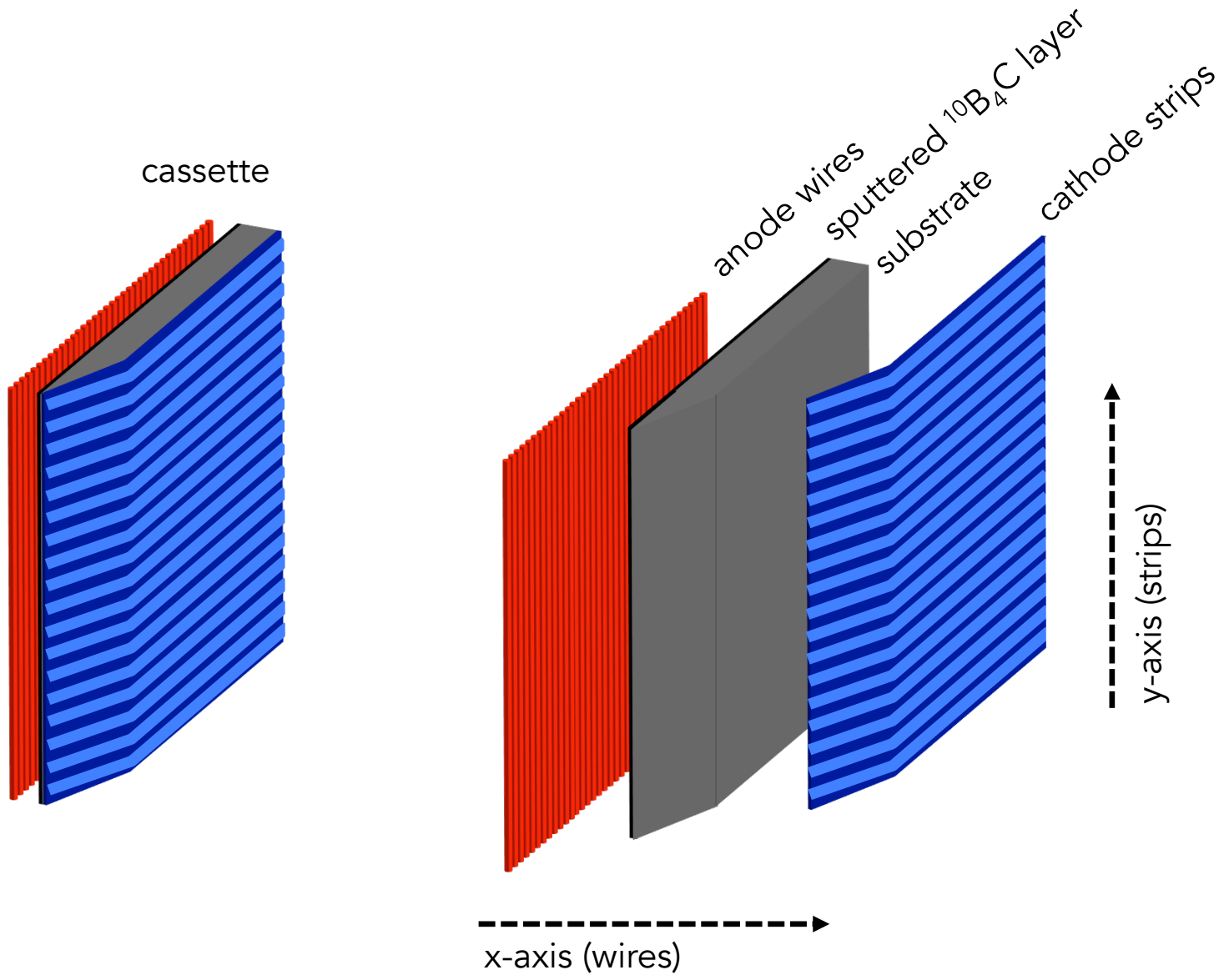
The intensity is spread over a wider surface
 (5 degrees = factor x10)

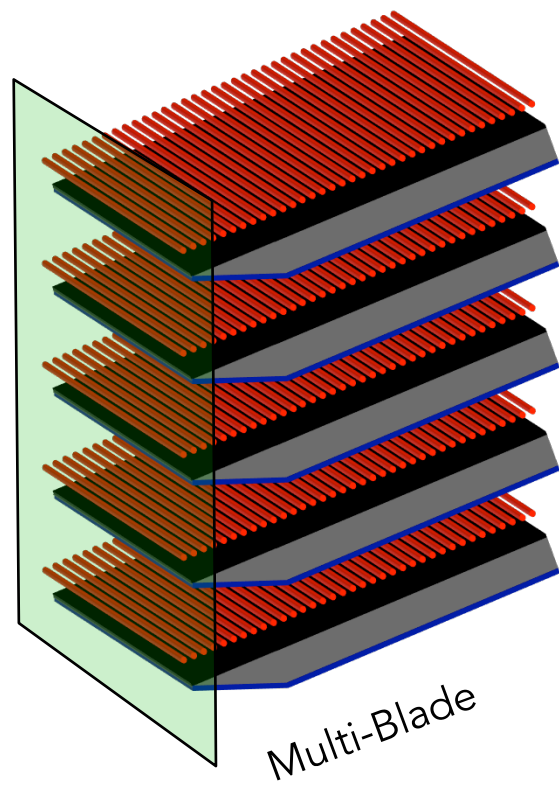
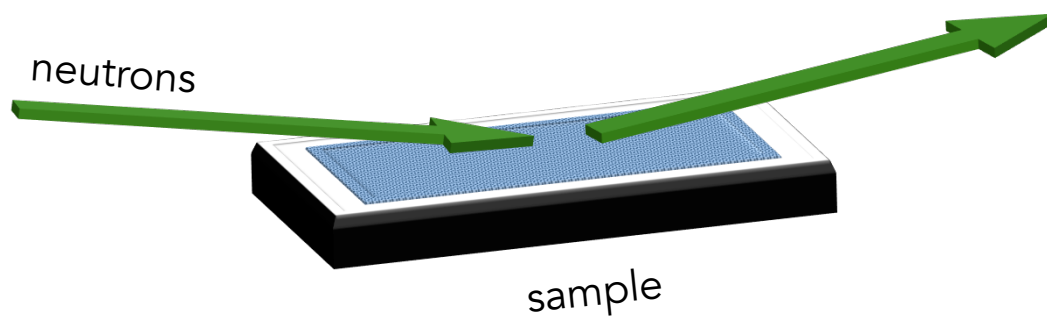
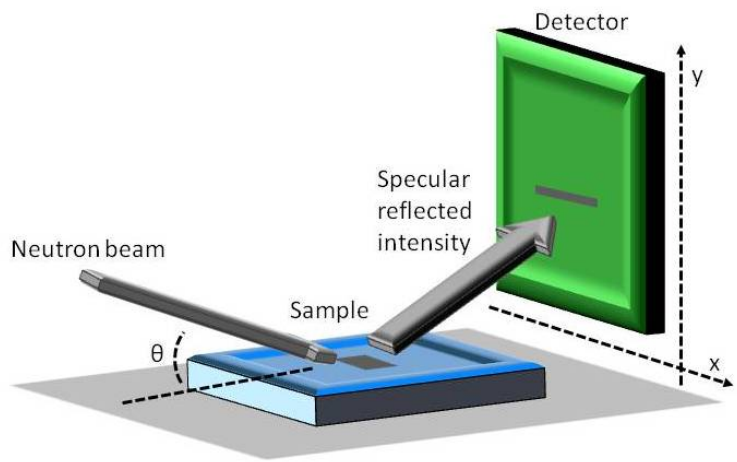




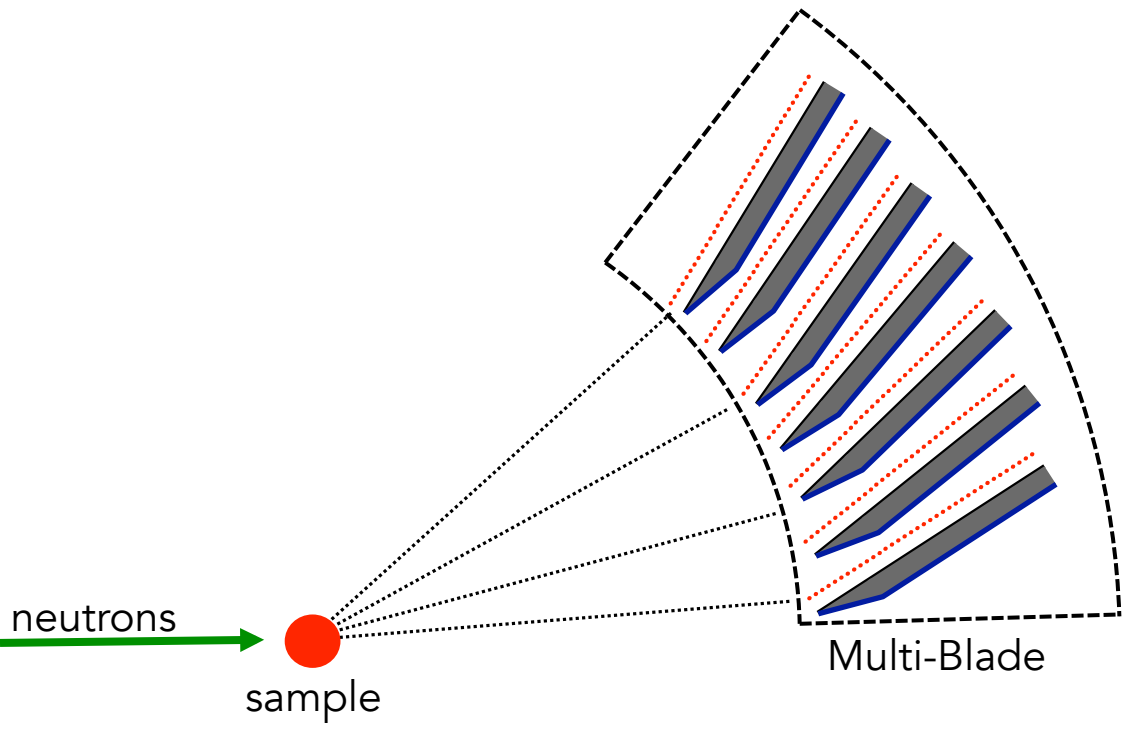
cassette



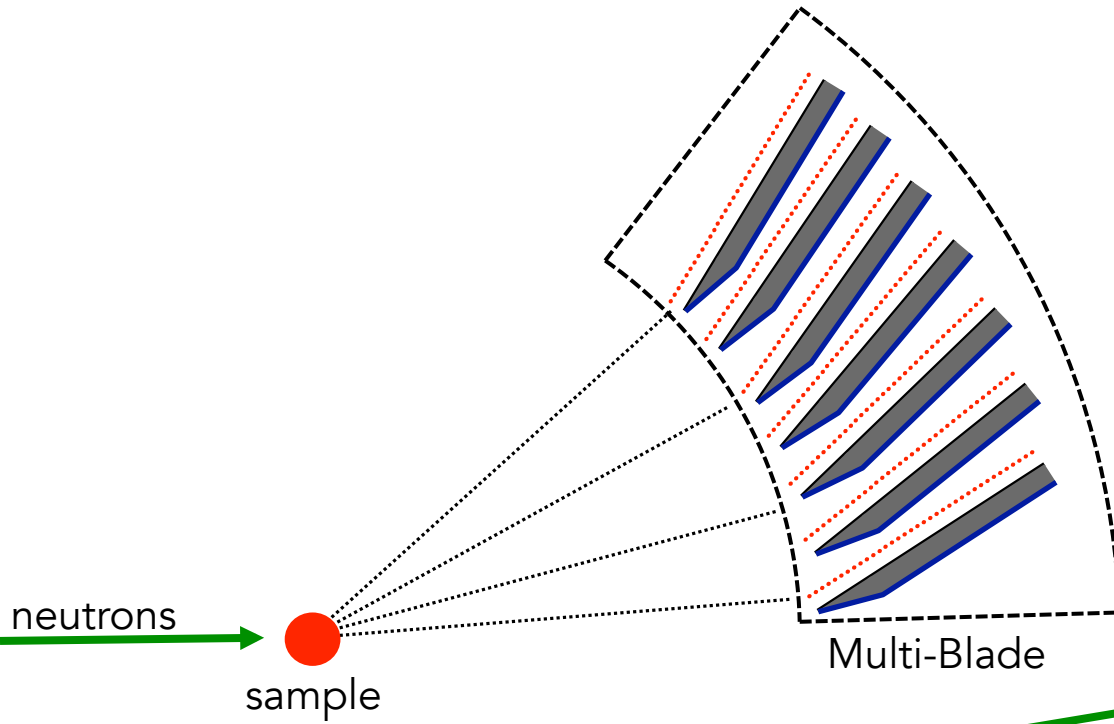




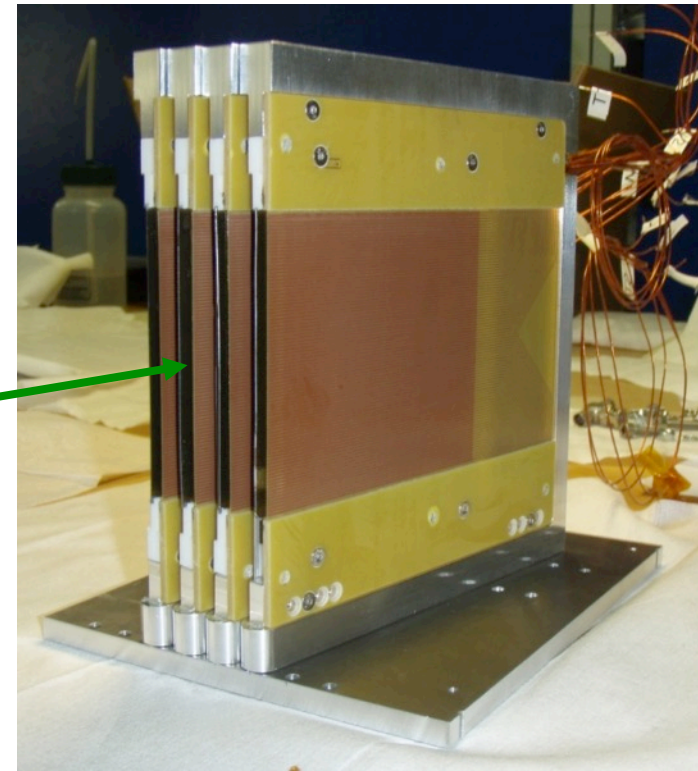
(Not in scale)



4 cassette demonstrator:
proof of concept in 2012



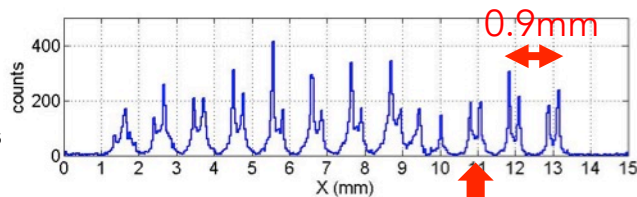
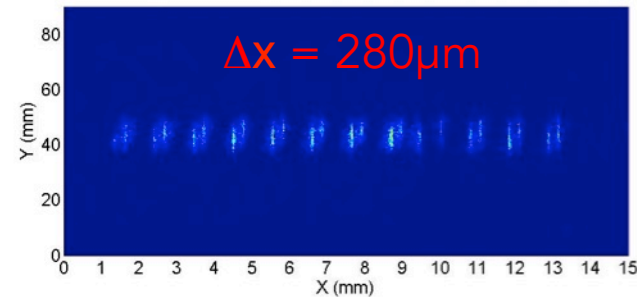
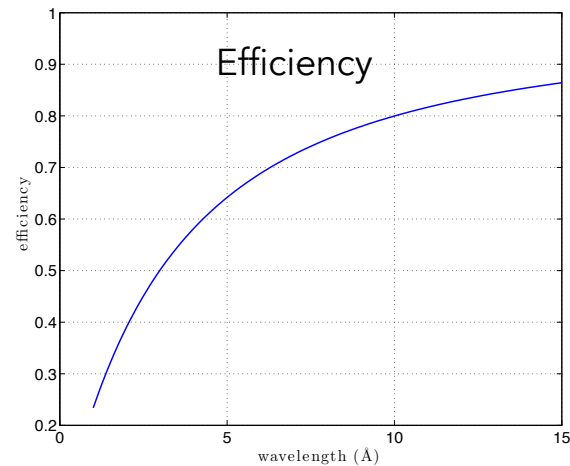
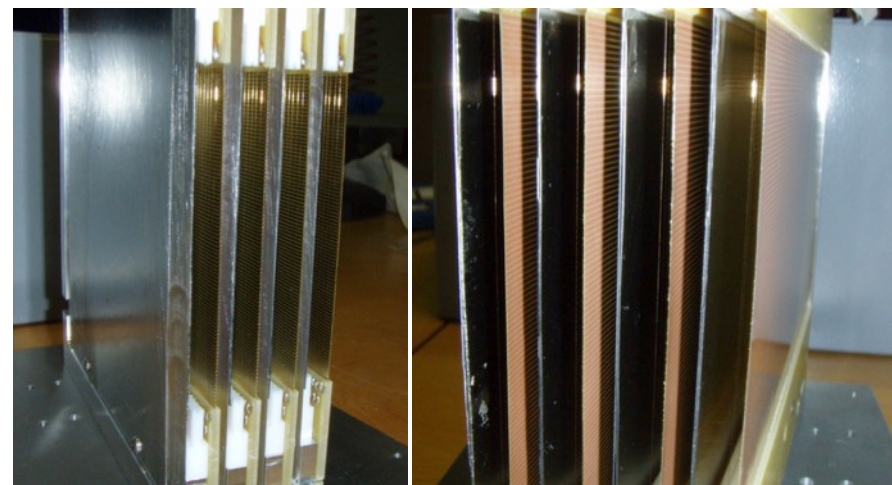
neutrons
hit the layers at 5°



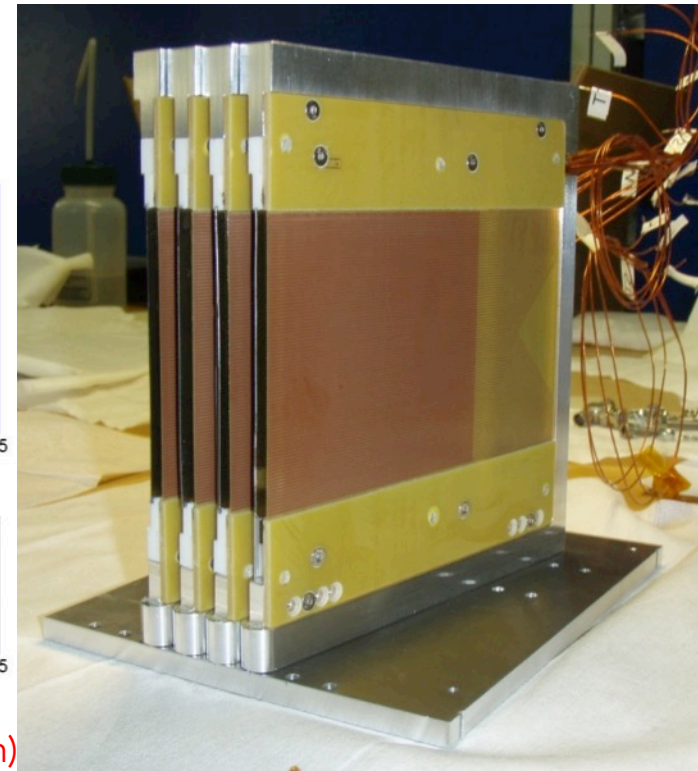
4 cassette demonstrator:

Results:

- Measured Efficiency **45%** at 2.5\AA
- Spatial Resolution **$4\text{mm} \times 280\mu\text{m}$**
- Counting rate capability **$\sim 5000\text{ n/s/mm}^2$** at 2.5\AA
(limited by the electronics)
- Atmospheric pressure operation
(thin vessel window, **low scattering**)
(cost effective materials)



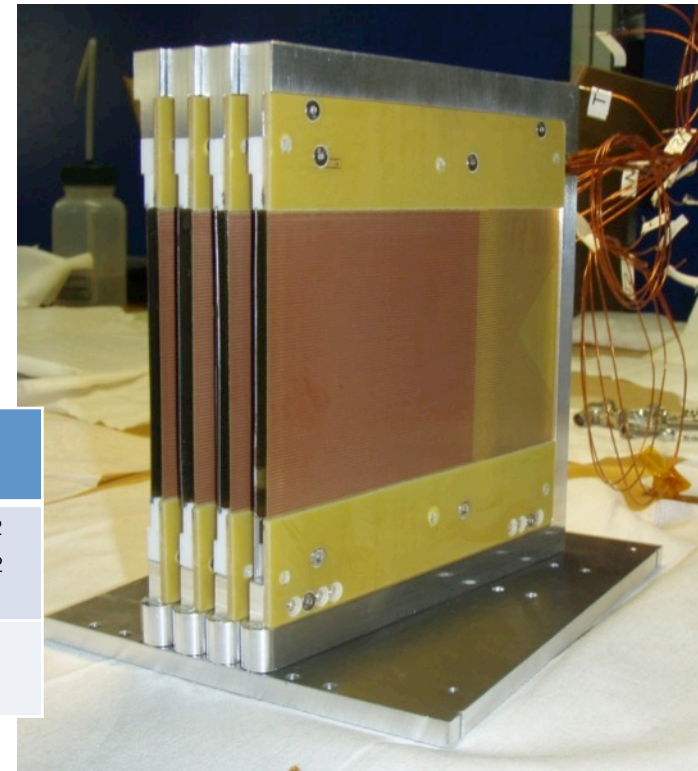
Neutron beam ($\sim 0.2\text{mm}$)



4 cassette demonstrator:

Results:

- Measured Efficiency **45%** at 2.5Å
- Spatial Resolution **4mm x 280µm**
- Counting rate capability **~5000 n/s/mm²** at 2.5Å (limited by the electronics)
- Atmospheric pressure operation (thin vessel window, **low scattering**) (cost effective materials)



The ESS requirements

	FREIA	Estia
Max local rate	10^5 n/s/Å/mm ²	<ul style="list-style-type: none">• Conventional refl. 10^5 n/s/Å/mm²• High intensity mode 10^4 n/s/Å/mm²
Spatial resolution	4mm x 1mm	4mm x 0.5mm

4 cassette demonstrator:

Results:

- Measured Efficiency 45% at 2.5Å
- Spatial Resolution 4mm x 280µm
- Counting rate capability **~5000 n/s/mm²** at 2.5Å
(limited by the electronics)
- Atmospheric pressure operation
(thin vessel window, low scattering)
(cost effective materials)

x10

The state of the art

Instrument	Facility	techn.	area (mm × mm)	spatial res. (mm × mm)	efficiency	global rate (s ⁻¹)	local rate (s ⁻¹ mm ⁻²)
FIGARO [9]	ILL	³ He	512 × 256	~ 2 × 7.5	~ 63% @ 2.5Å ~ 90% @ 10Å ~ 80% @ 30Å	3 · 10 ⁷	230
SuperADAM [11]	ILL	³ He	300 × 300	2.8 × 2.8	76% @ 4.4Å	2 · 10 ⁵	-
REFSANS [12]	FRM2	³ He	500 × 500	~ 2 × 2	58% @ 10Å ≥ 50% ∈ [5, 18]Å	2.2 · 10 ⁵	300
INTER [13]	ISIS	³ He, ⁶ Li	200 × 200	~ 1 × 1	-	-	-
POLREF [14, 15]	ISIS	³ He	200 × 200	≤ 1 × 1	-	-	-
BIOREF [16]	HZB	³ He	300 × 300	2 × 3	~ 60% @ 10Å	2 · 10 ⁵	300
LR	SNS	³ He	200 × 200	1.3 × 1.3	-	-	-
MR	SNS	³ He	210 × 180	1.5 × 1.5	-	-	-
Platypus [17]	OPAL	³ He	500 × 250	1.2 × 1.2	~ 60% @ 10Å	2 · 10 ⁵	300
SOFIA [18, 19]	J-PARC	³ He	128 × 128	2 × 2	-	-	300
		⁶ Li	256 × 256	4 × 4	-	-	300

x20

x300

The ESS requirements

	FREIA	Estia
Max local rate	10 ⁵ n/s/Å/mm ²	<ul style="list-style-type: none"> • Conventional refl. 10⁵ n/s/Å/mm² • High intensity mode 10⁴ n/s/Å/mm²
Spatial resolution	4mm x 1mm	4mm x 0.5mm

4 cassette demonstrator:

Results:

- Measured Efficiency 45% at 2.5Å
- Spatial Resolution **4mm x 280µm**
- Counting rate capability **~5000 n/s/mm²** at 2.5Å
(limited by the electronics)
- Atmospheric pressure operation
(thin vessel window, low scattering)
(cost effective materials)

x10

The state of the art

Instrument	Facility	techn.	area (mm × mm)	spatial res. (mm × mm)	efficiency	global rate (s ⁻¹)	local rate (s ⁻¹ mm ⁻²)
FIGARO [9]	ILL	³ He	512 × 256	~ 2 × 7.5	~ 63% @ 2.5Å ~ 90% @ 10Å ~ 80% @ 30Å	3 · 10 ⁷	230
SuperADAM [11]	ILL	³ He	300 × 300	2.8 × 2.8	76% @ 4.4Å	2 · 10 ⁵	-
REFSANS [12]	FRM2	³ He	500 × 500	~ 2 × 2	58% @ 10Å ≥ 50% ∈ [5, 18]Å	2.2 · 10 ⁵	300
INTER [13]	ISIS	³ He, ⁶ Li	200 × 200	~ 1 × 1	-	-	-
POLREF [14, 15]	ISIS	³ He	200 × 200	≤ 1 × 1	-	-	-
BIOREF [16]	HZB	³ He	300 × 300	2 × 3	~ 60% @ 10Å	2 · 10 ⁵	300
LR	SNS	³ He	200 × 200	1.3 × 1.3	-	-	-
MR	SNS	³ He	210 × 180	1.5 × 1.5	-	-	-
Platypus [17]	OPAL	³ He	500 × 250	1.2 × 1.2	~ 60% @ 10Å	2 · 10 ⁵	300
SOFIA [18, 19]	J-PARC	³ He	128 × 128	2 × 2	-	-	300
		⁶ Li	256 × 256	4 × 4	-	-	300

x20

x300

The ESS requirements

	FREIA	Estia
Max local rate	10 ⁵ n/s/Å/mm ²	<ul style="list-style-type: none"> • Conventional refl. 10⁵ n/s/Å/mm² • High intensity mode 10⁴ n/s/Å/mm²
Spatial resolution	4mm x 1mm	4mm x 0.5mm

4 cassette demonstrator:

Results:

- Measured Efficiency **45%** at 2.5Å
- Spatial Resolution **4mm x 280µm**
- Counting rate capability **~5000 n/s/mm²** at 2.5Å
(limited by the electronics)
- Atmospheric pressure operation
(thin vessel window, **low scattering**)
(cost effective materials)

Next demonstrator:

- Counting rate capability
- Overlap and uniformity

The ESS requirements

	FREIA	Estia
Max local rate	10^5 n/s/Å/mm ²	<ul style="list-style-type: none">• Conventional refl. 10^5 n/s/Å/mm²• High intensity mode 10^4 n/s/Å/mm²
Spatial resolution	4mm x 1mm	4mm x 0.5mm

Next demonstrator (9 cassettes):

- Counting rate capability
- Overlap and uniformity



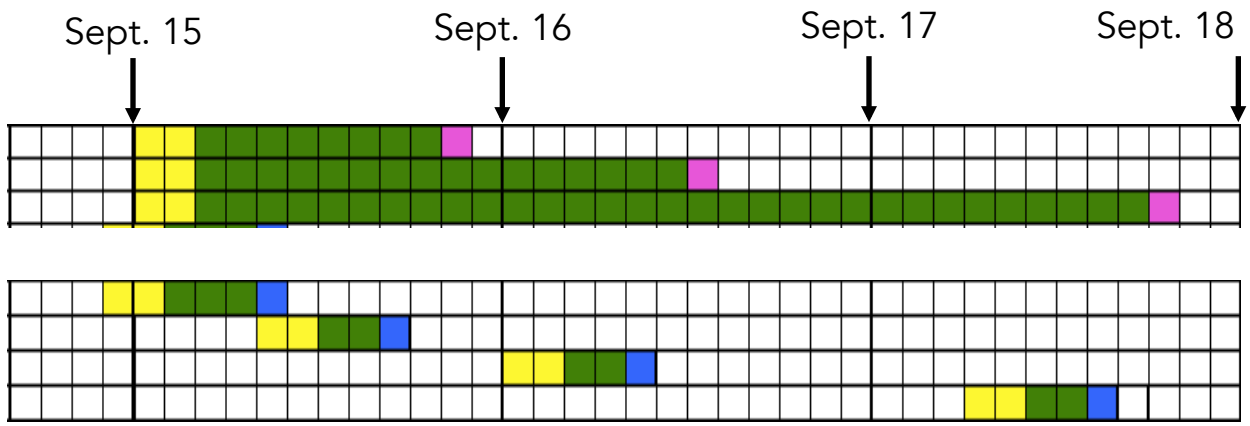
- Build technology prototype
- Tests at both beam line and Reflectometry beam line
- Electric field modeling
- Testing and availability of beam line
- Build technology prototype
- Data analysis
- Detailed GEANT4 on detector performance

All three partners will work together on the final detector for the ESS Reflectometers

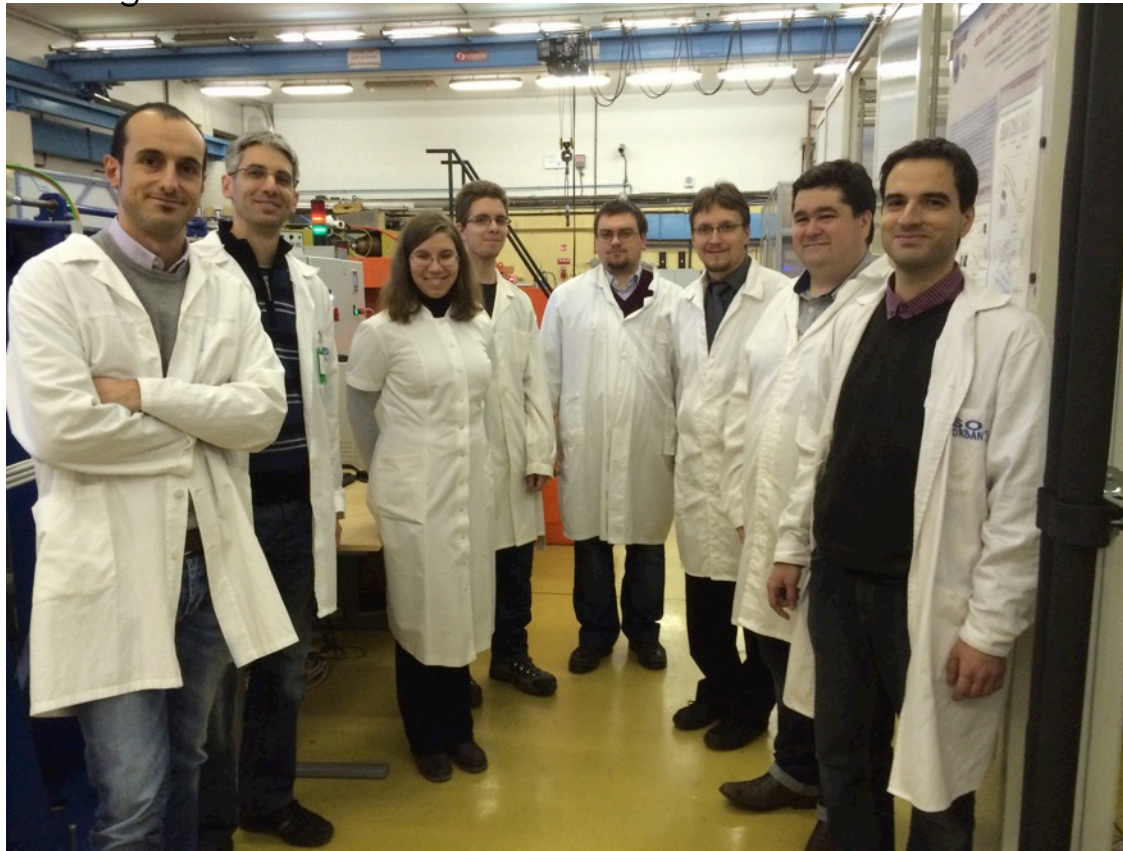
Task 4.2 Neutron Detectors – The Intensity Frontier

D4.2 Counting rate capability
 D4.6 Detector Characterization
 D4.12 Reflectometry detector

MS12 Improvement of the Multi-Blade design
 MS16 Improvement of the counting rate cap.
 MS20 Characterization of the demonstrator
 MS29 1st Detector construction



- Planning
- Implementation
- Deliverable
- Milestone



Francesco Piscitelli

Tibor Zsíros

Eszter Dian

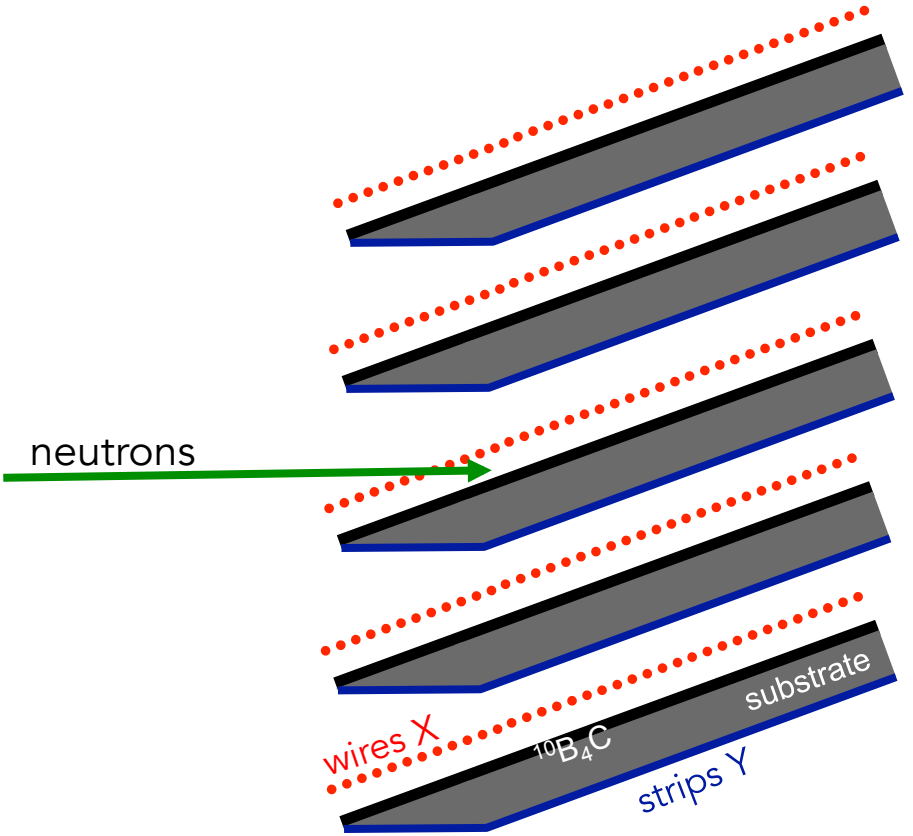
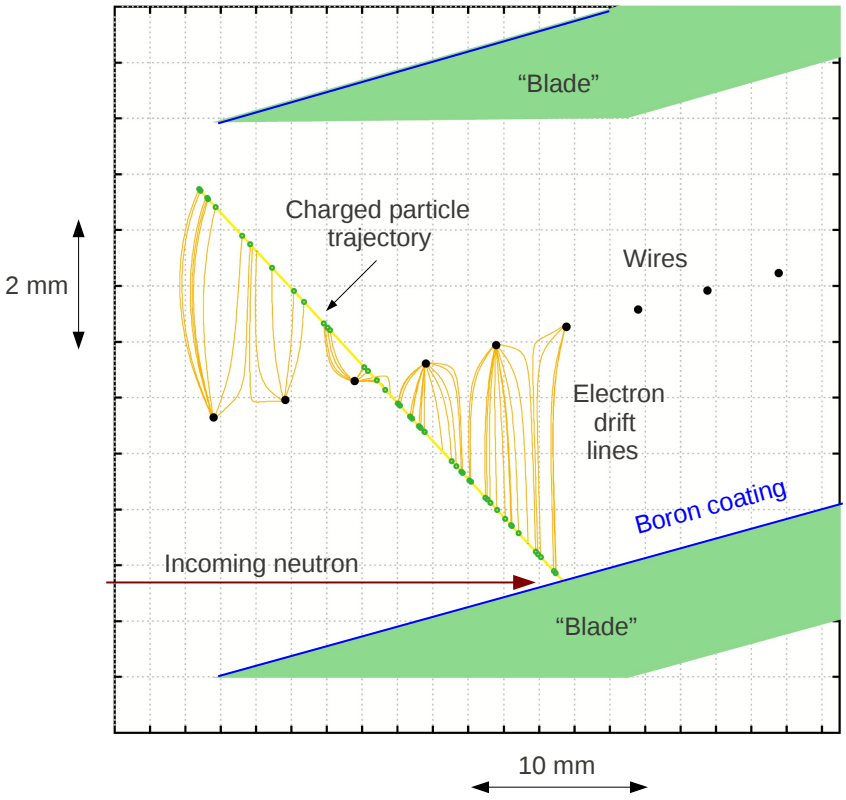
Péter Pázmándi

Gábor Kiss

Dezső Varga

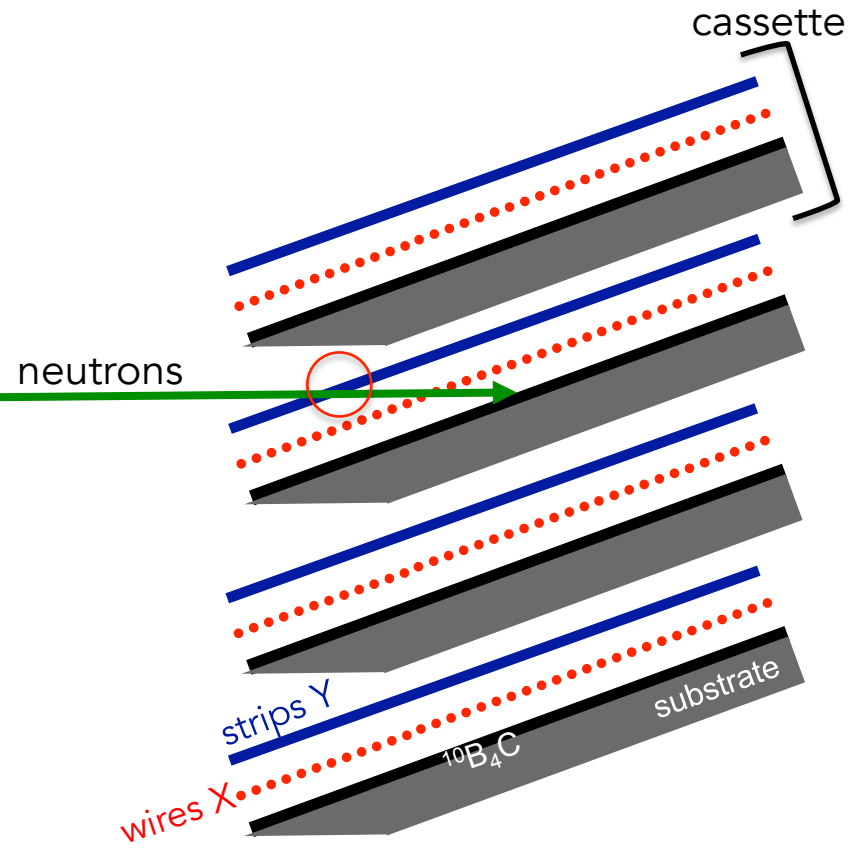
Richard Hall-Wilton

János Orbán

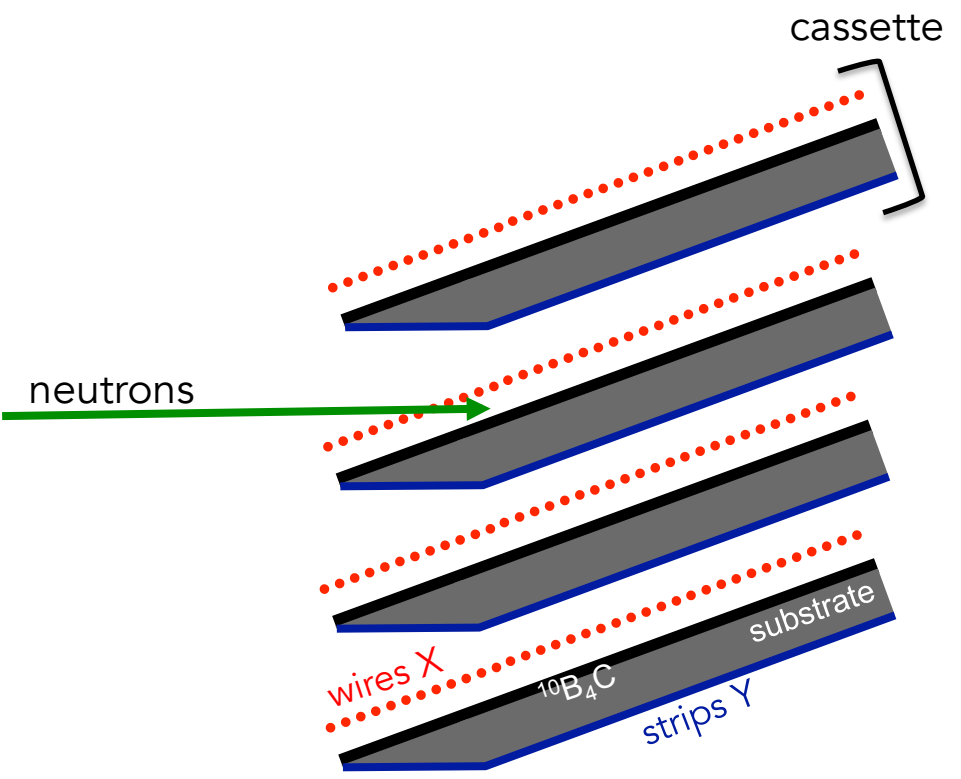


Materials evaluation

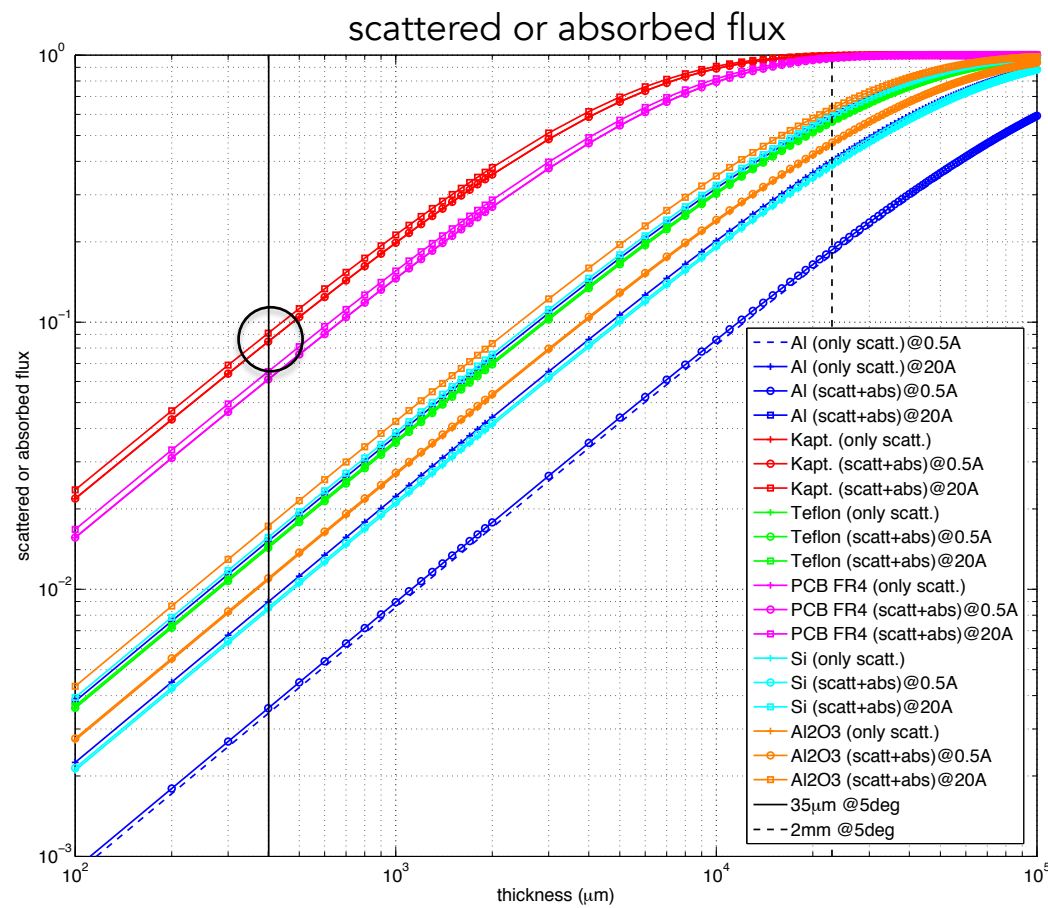
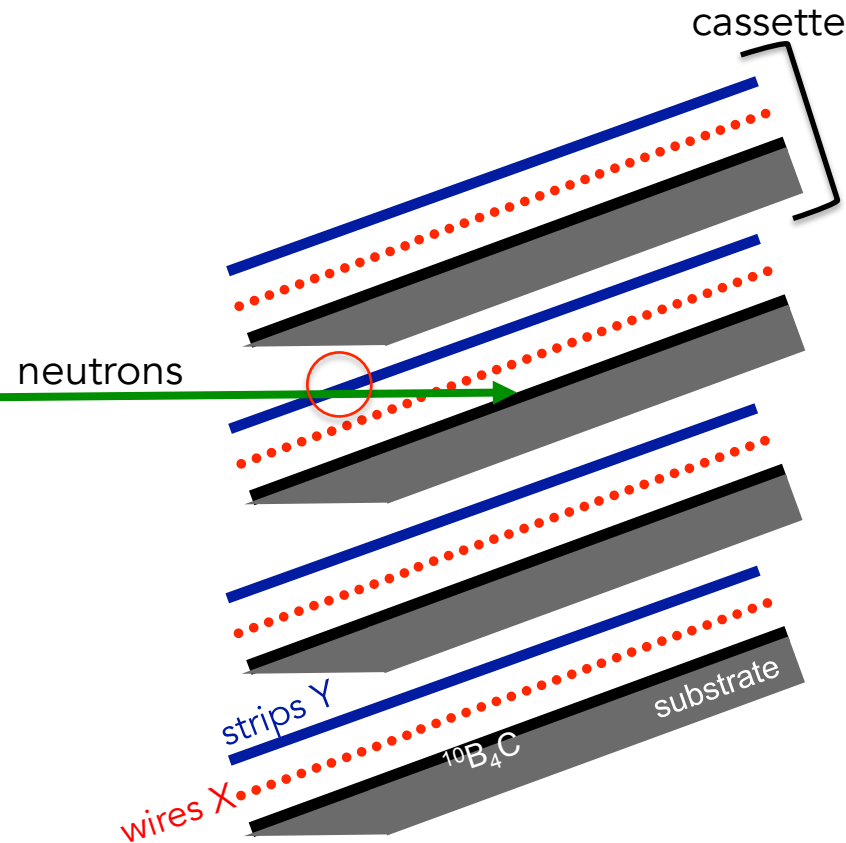
Old Design



New Design

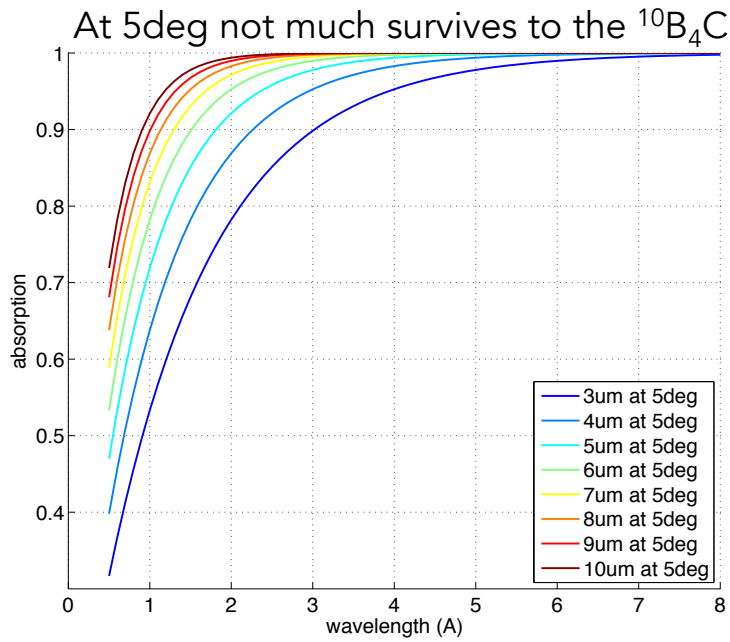
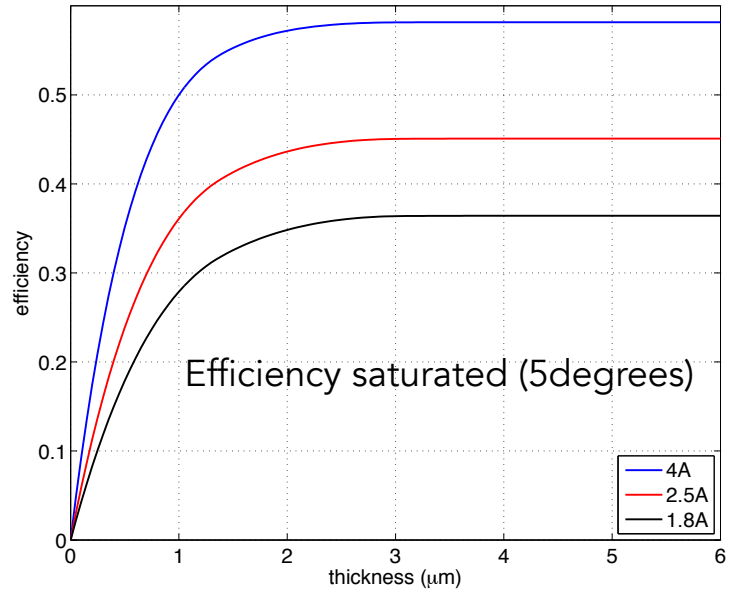


Old Design



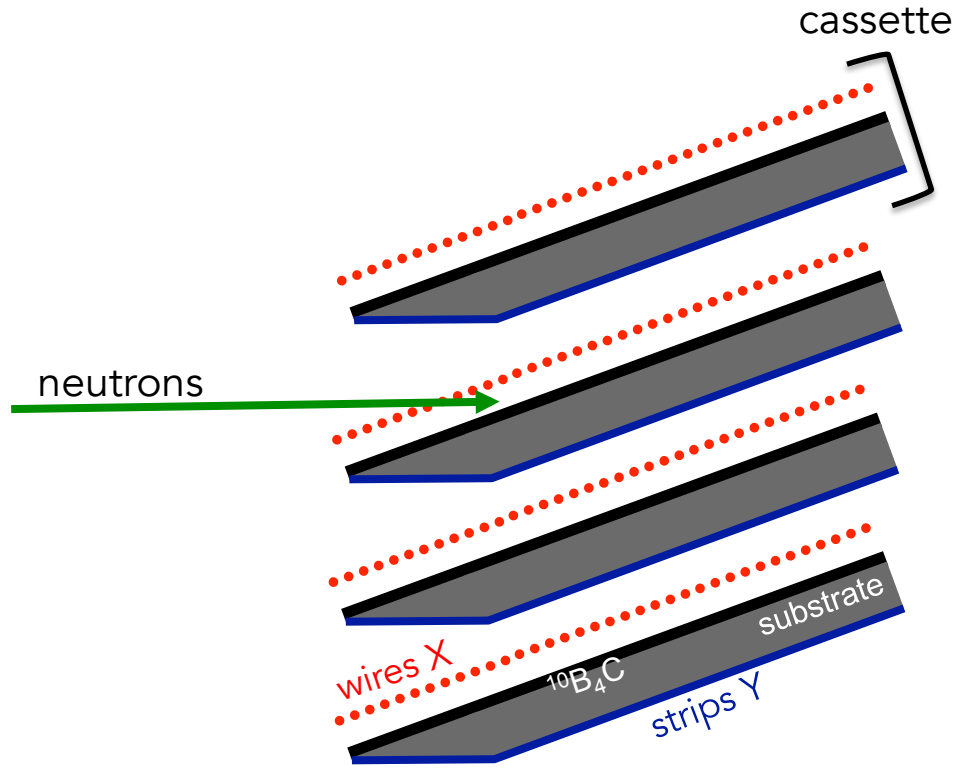
Any material holding the strips at 5deg scatters too much!

Materials evaluation



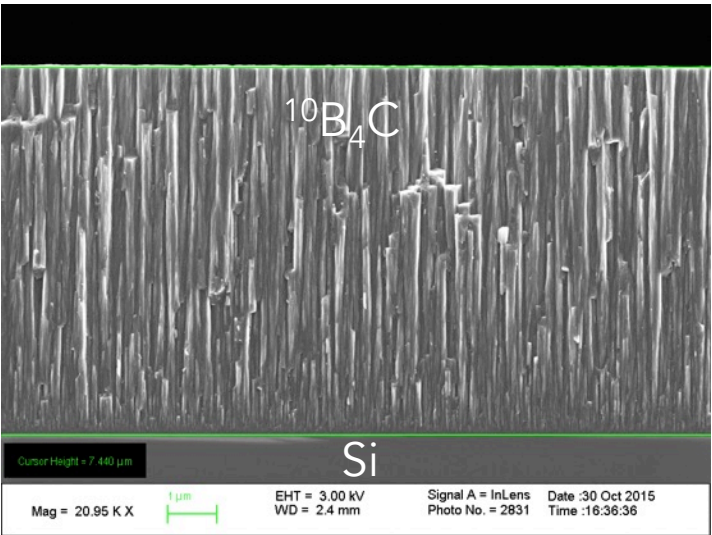
New Design

- Substrate as thick as necessary
- Kapton (strips) shielded by $^{10}\text{B}_4\text{C}$



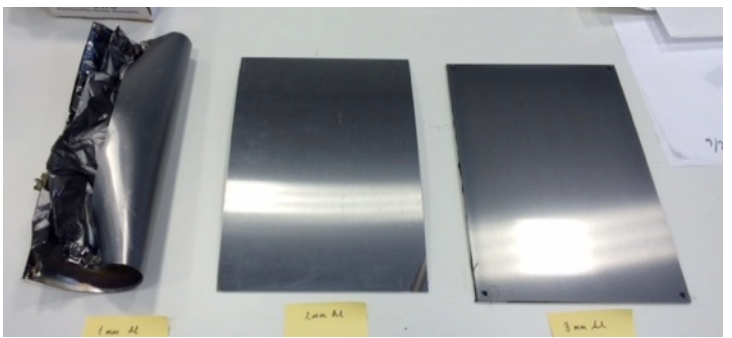
Materials evaluation

Planarity is an issue on large surfaces

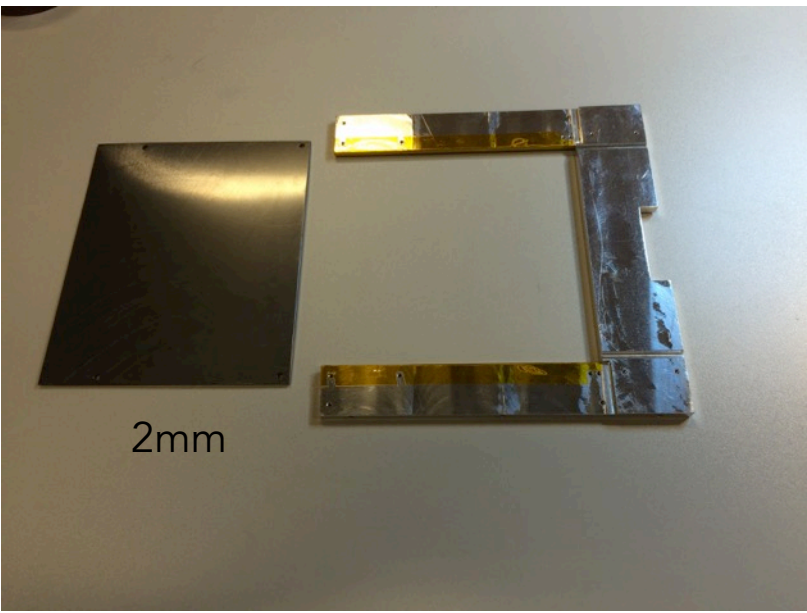


$\sim 7\ \mu\text{m}$ single-side

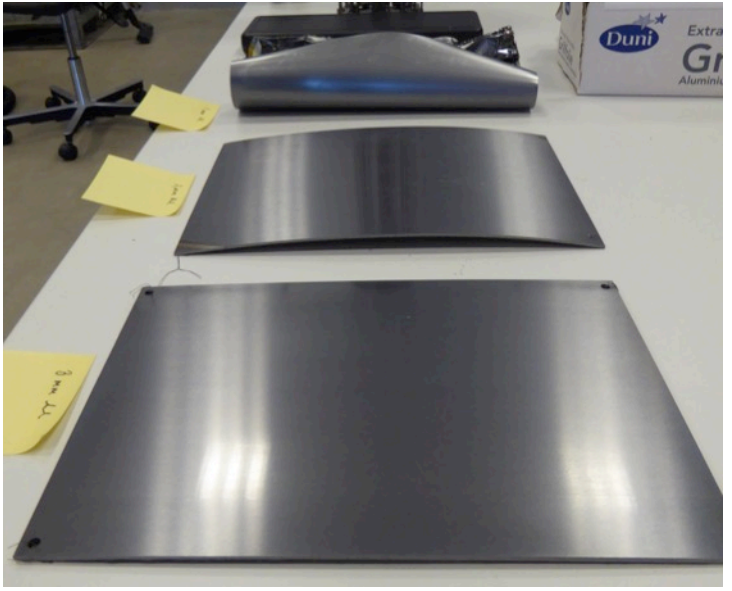
200x300mm² Al-plates single-side coated



1mm 2mm 3mm

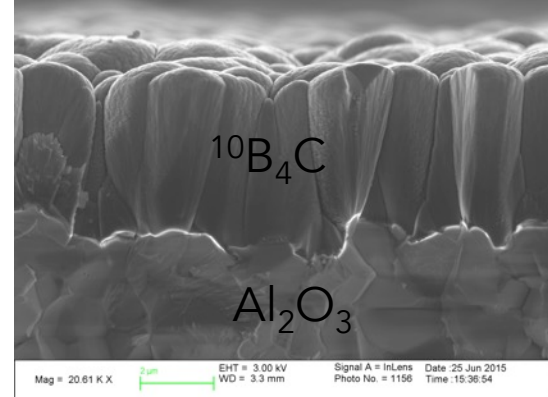
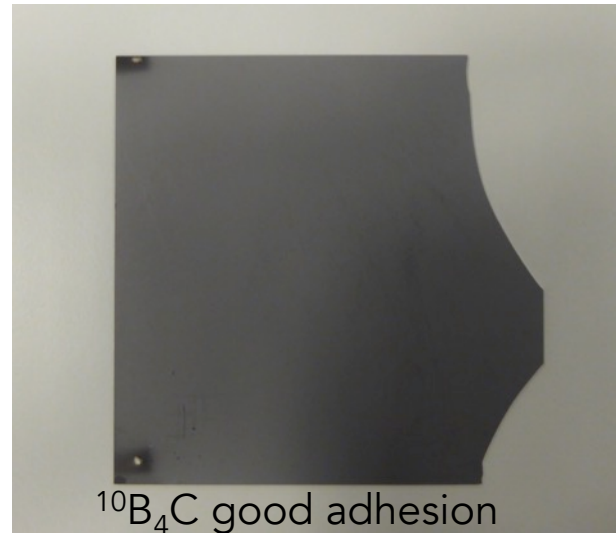
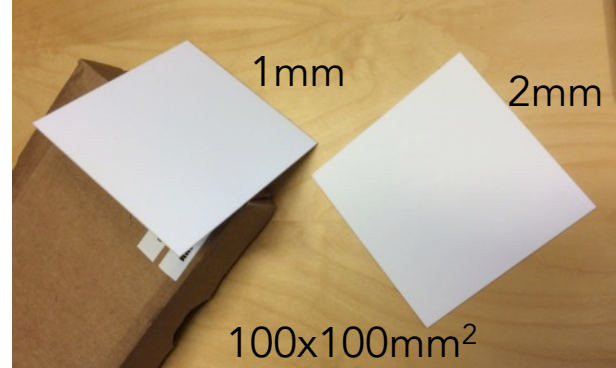
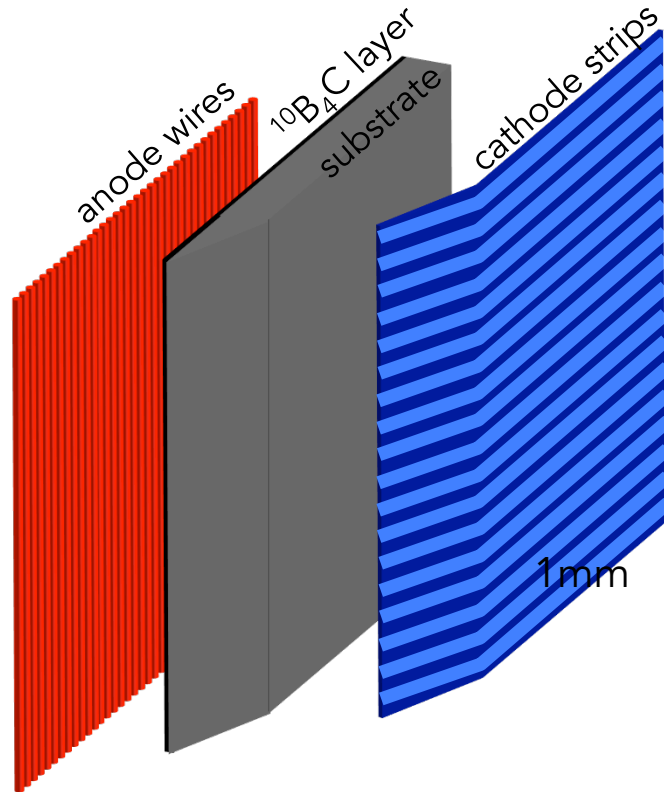
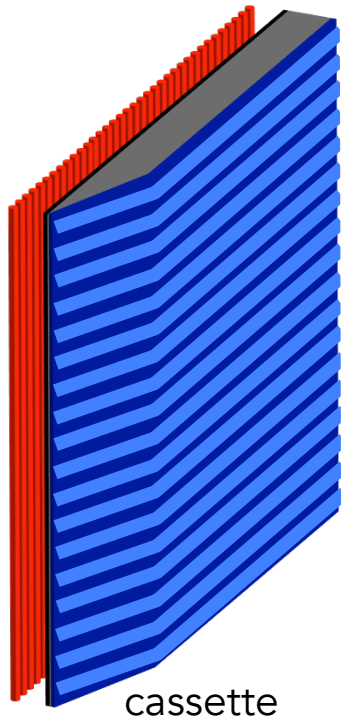


2mm



1mm
2mm
3mm

Al₂O₃ substrate



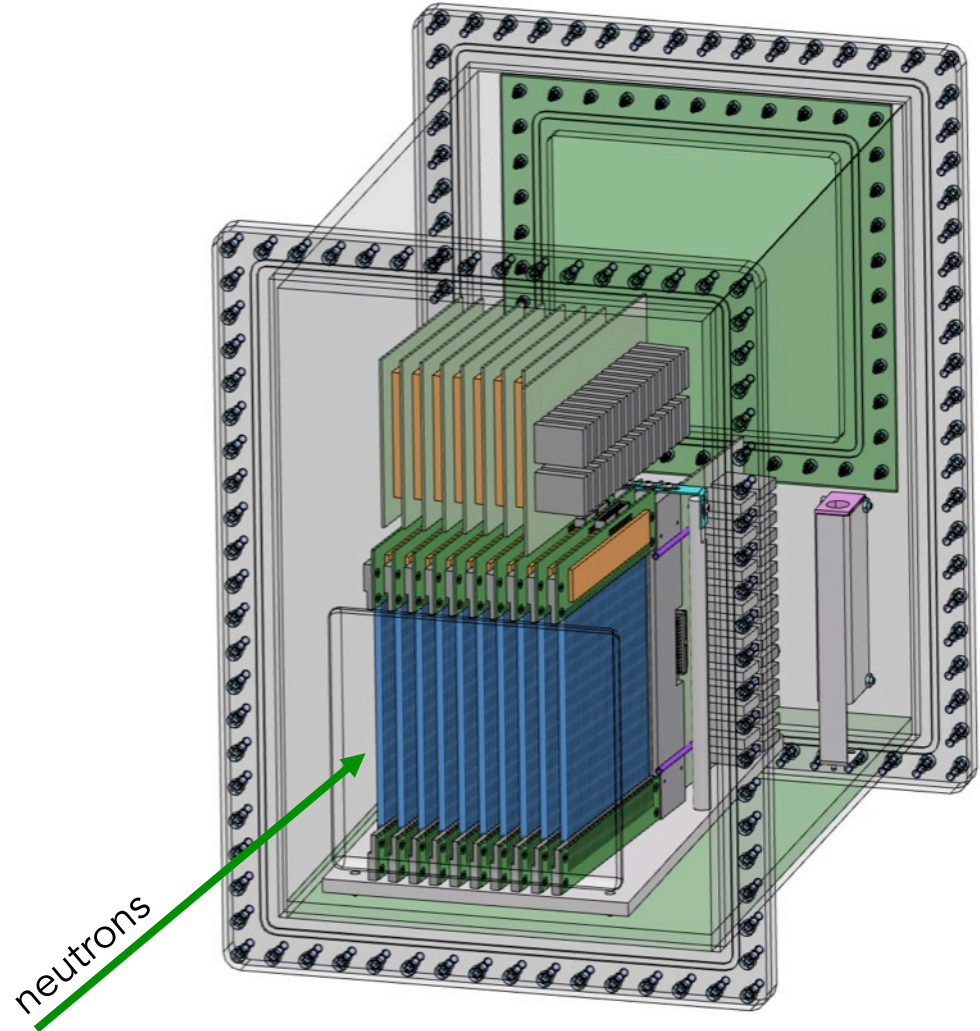
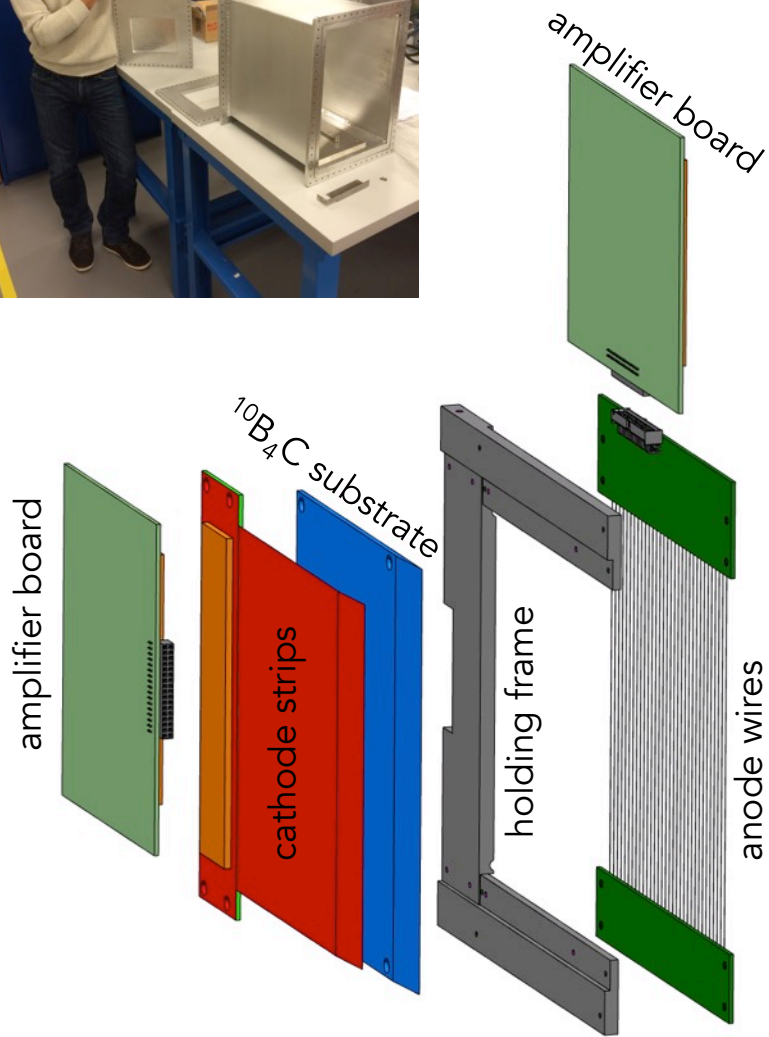
Advantages:
planarity, electrical insulation (strips can be deposited?)

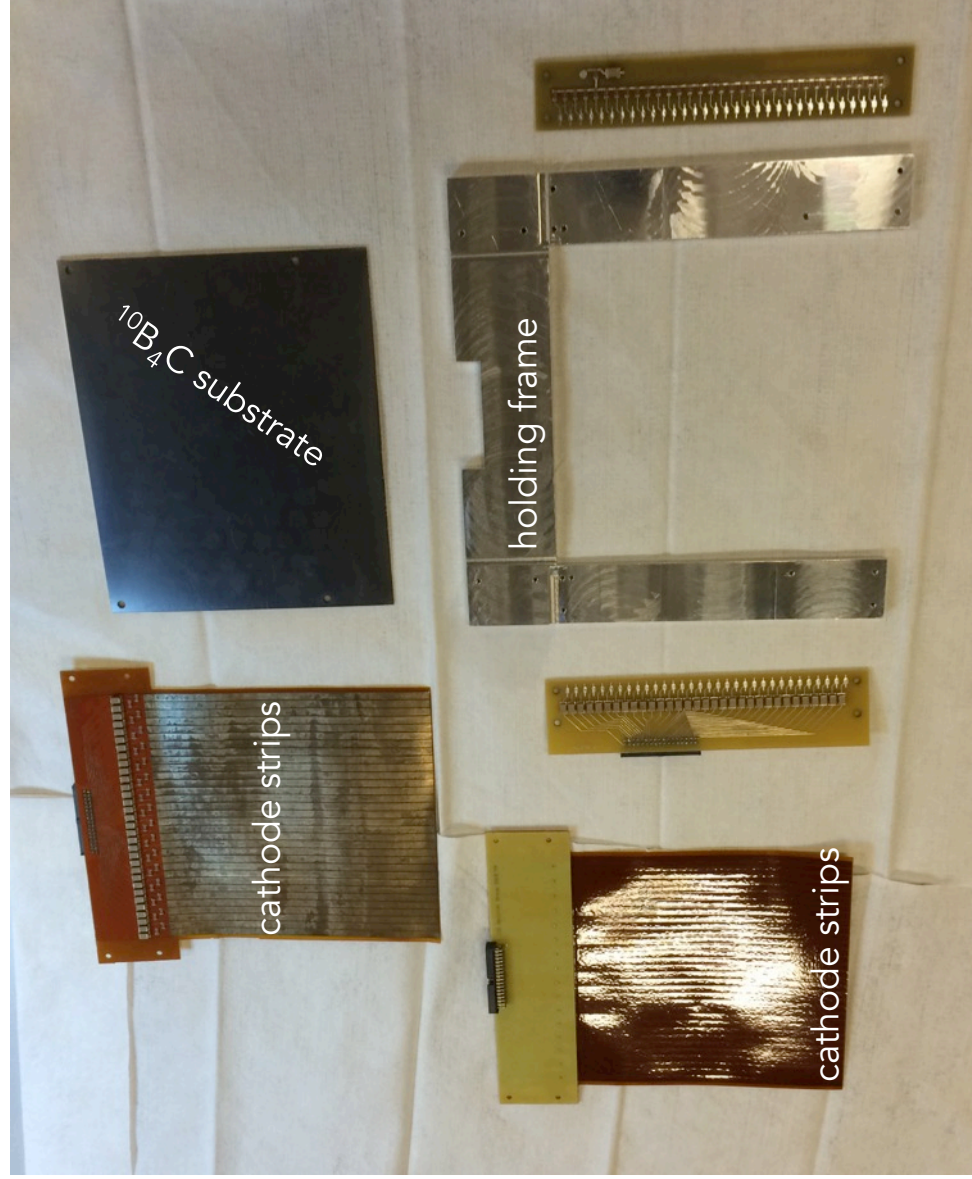
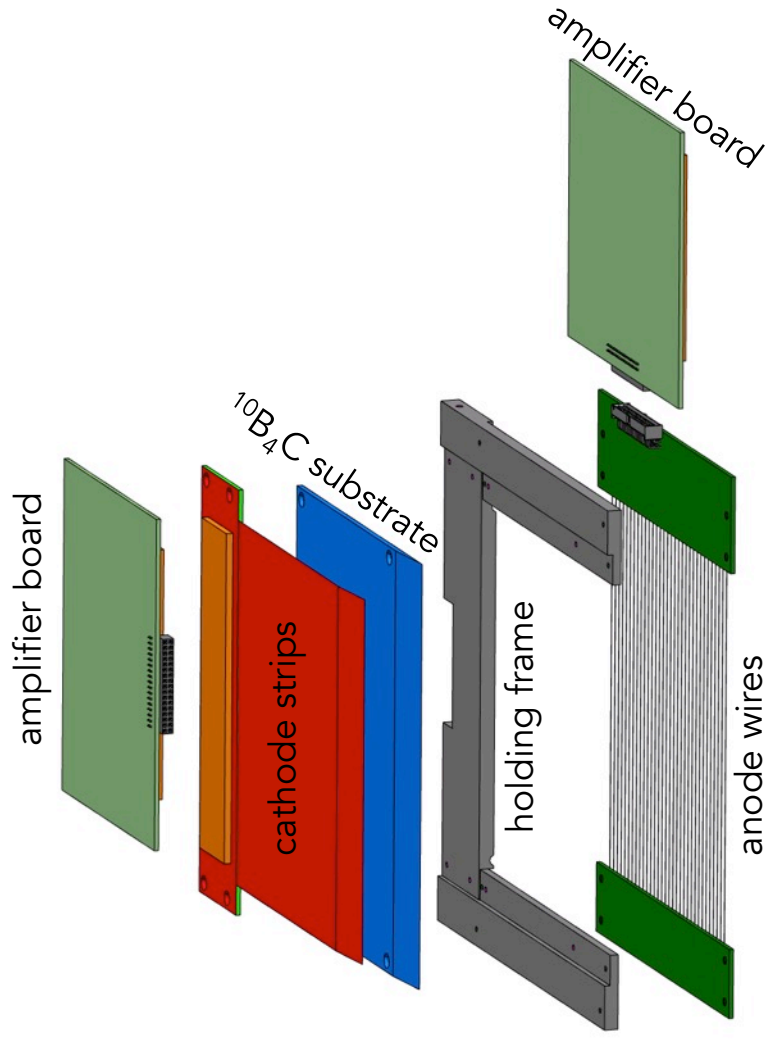
Disadvantages:
Availability in large surfaces?
Brittle!

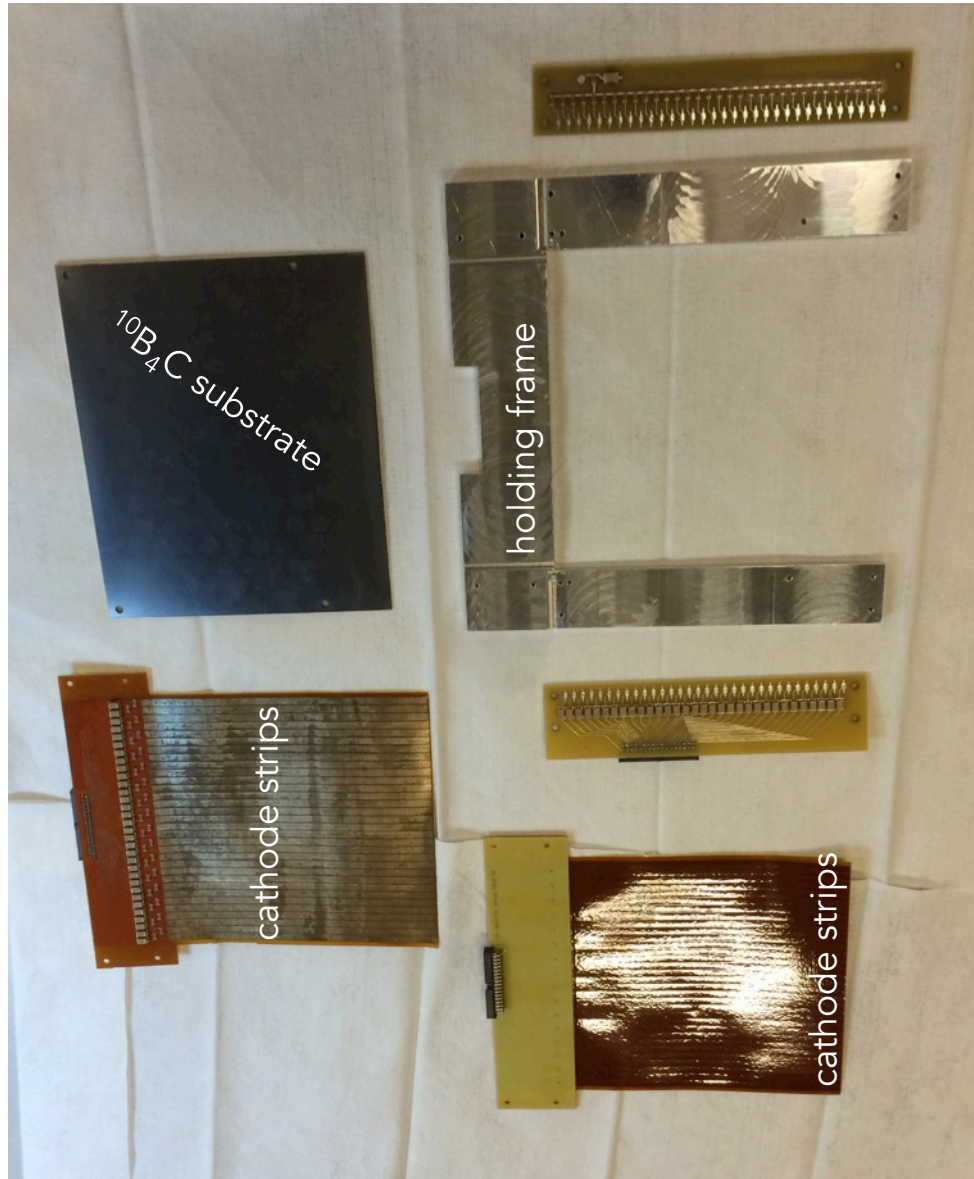
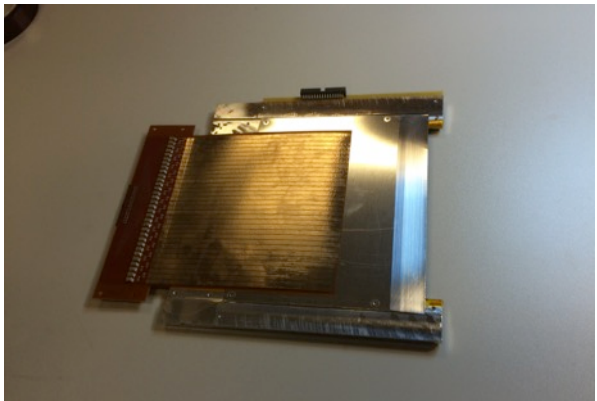
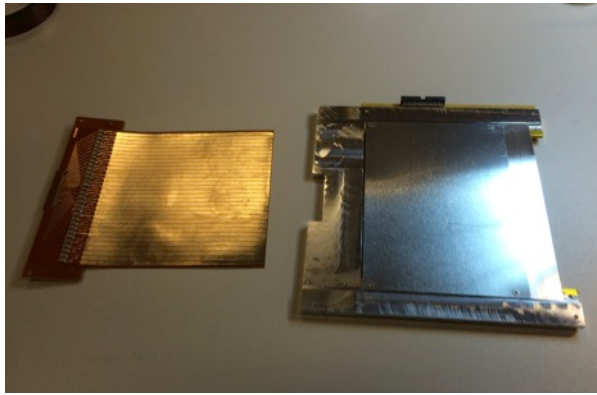
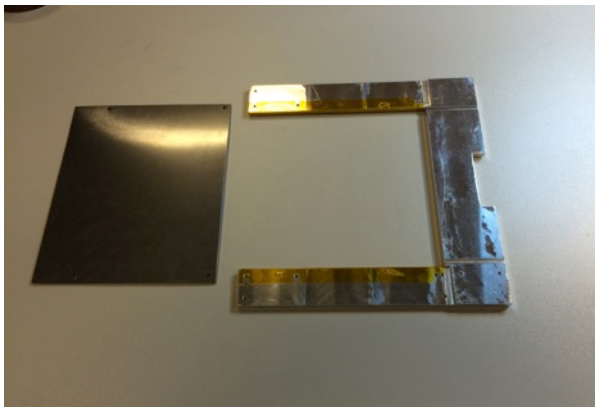
Multi-Blade mechanical design

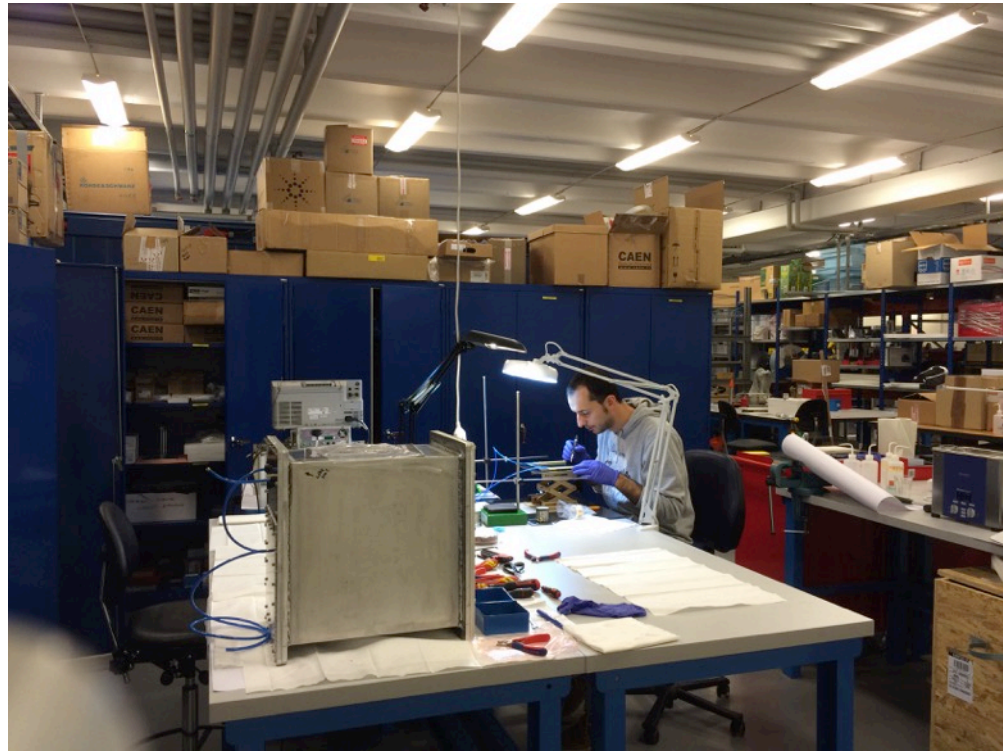


10x10cm² demonstrator



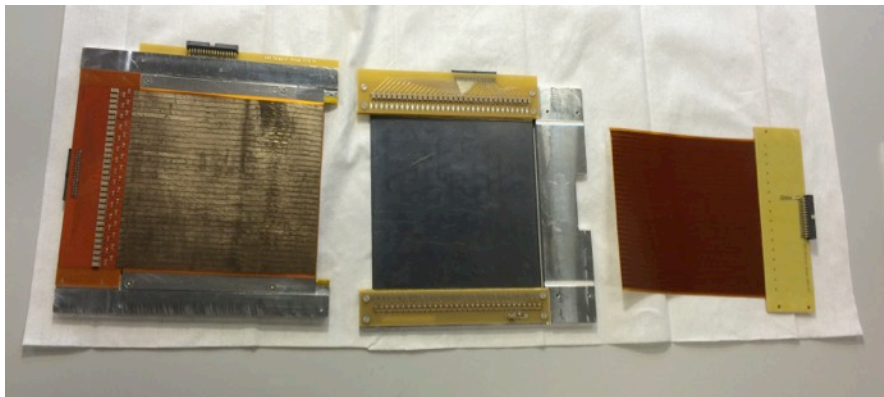
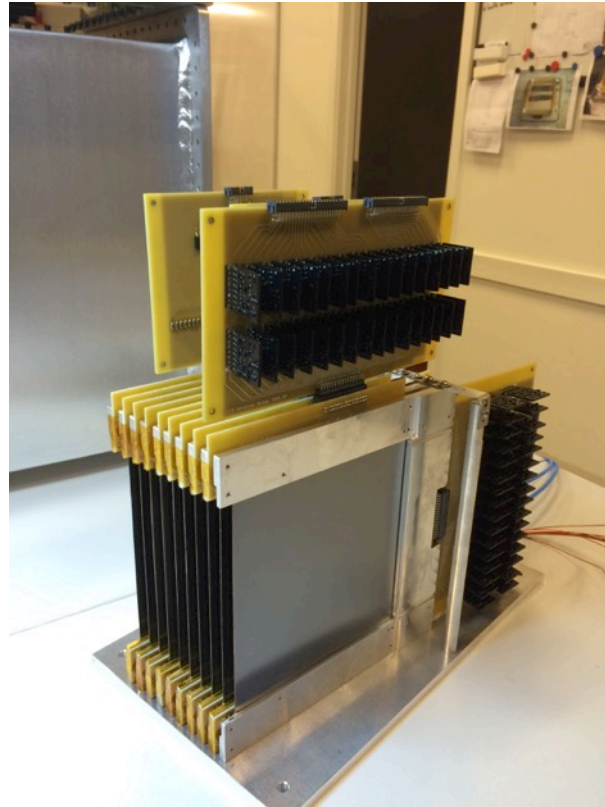
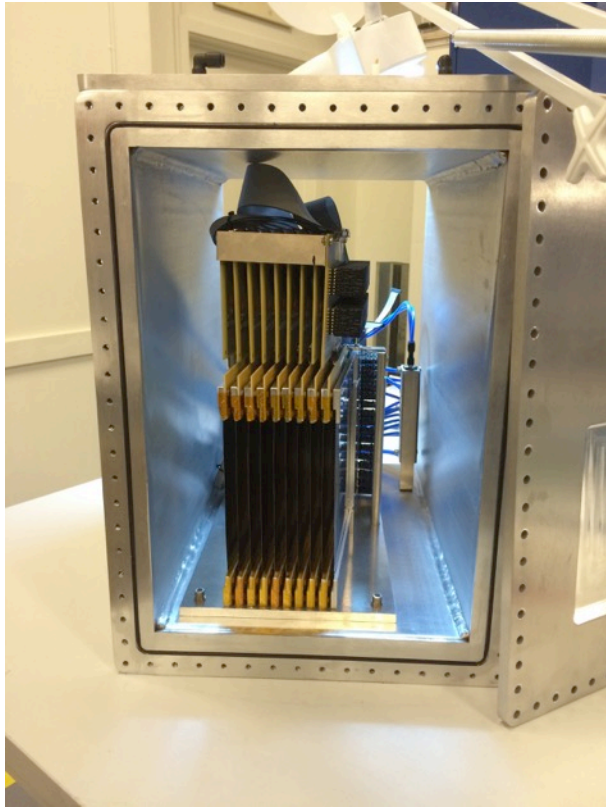






Assembly completed in December 2015



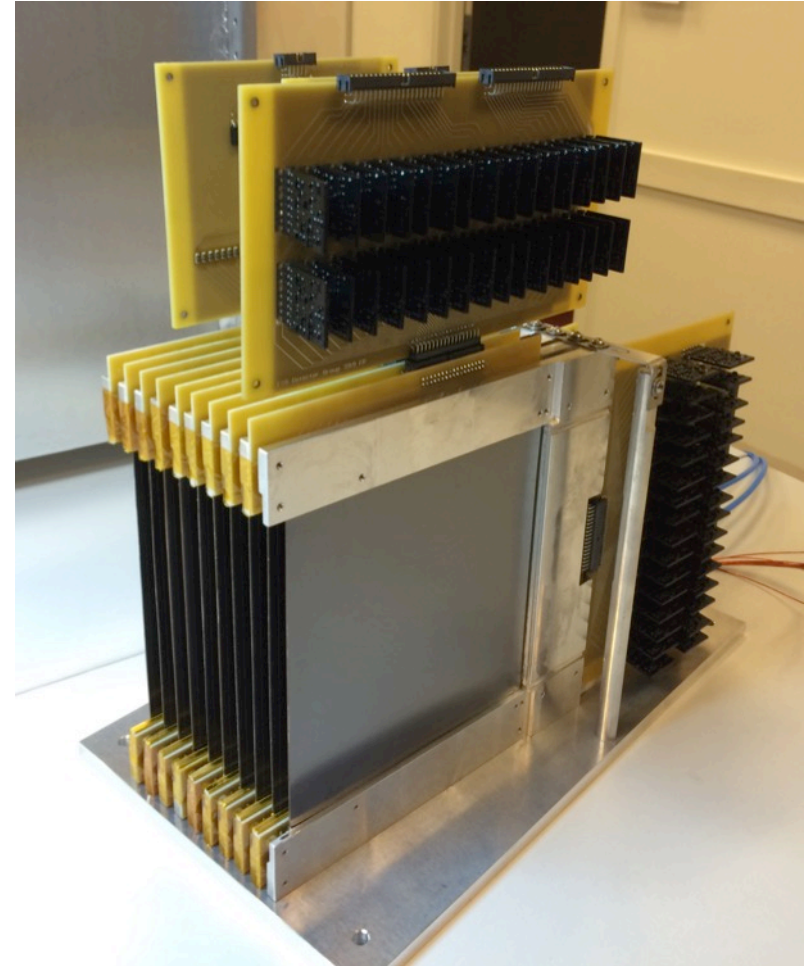
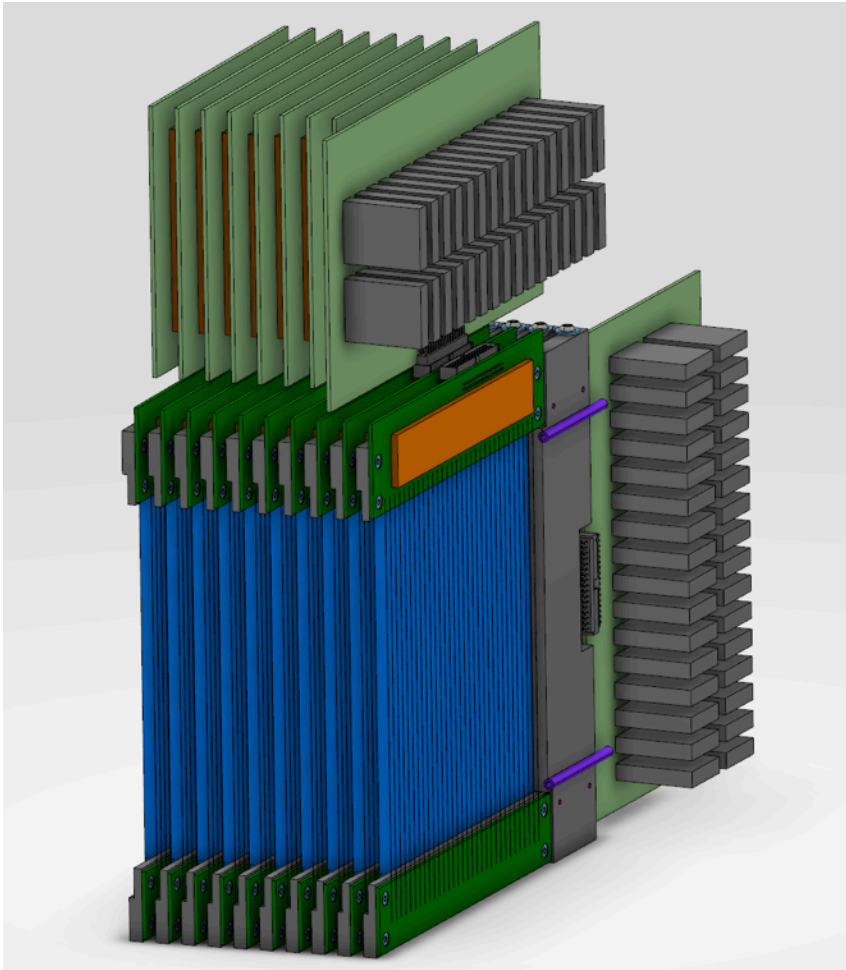


1 blade area: $\sim 120 \times 120 \text{ mm}^2$

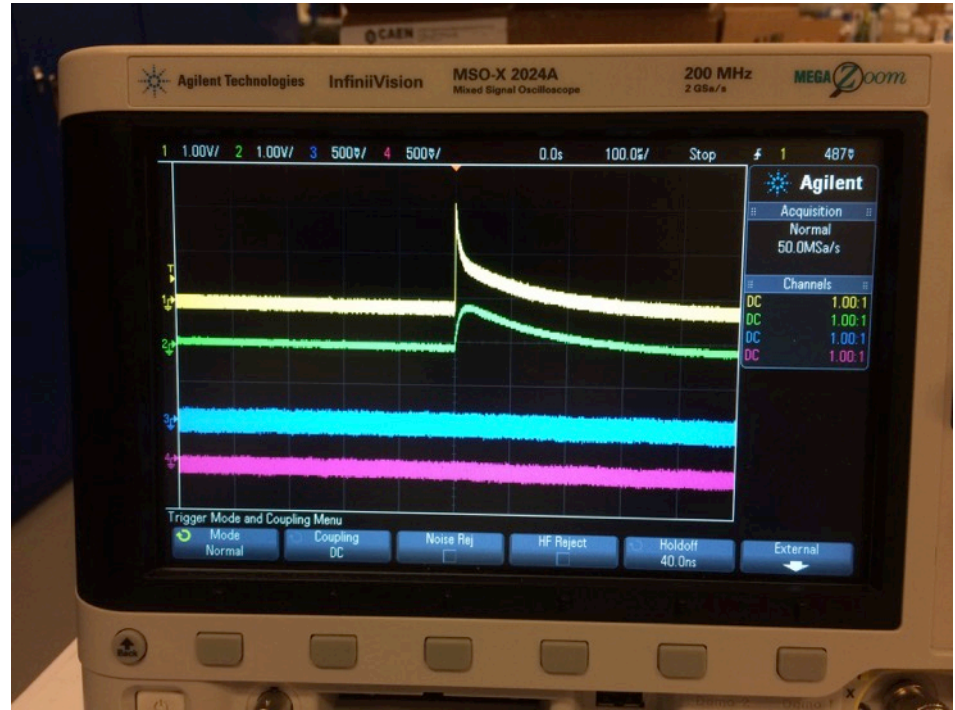
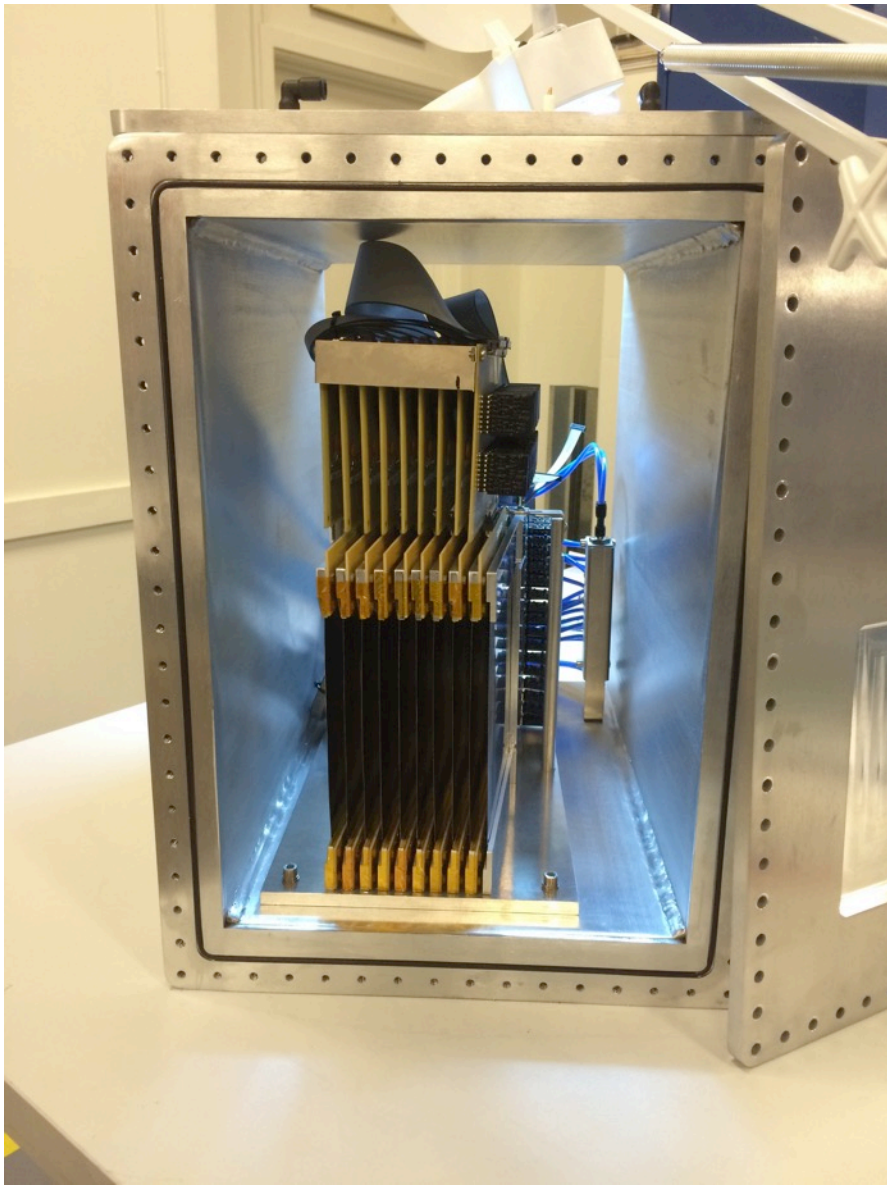
9 cassettes (10 blades)

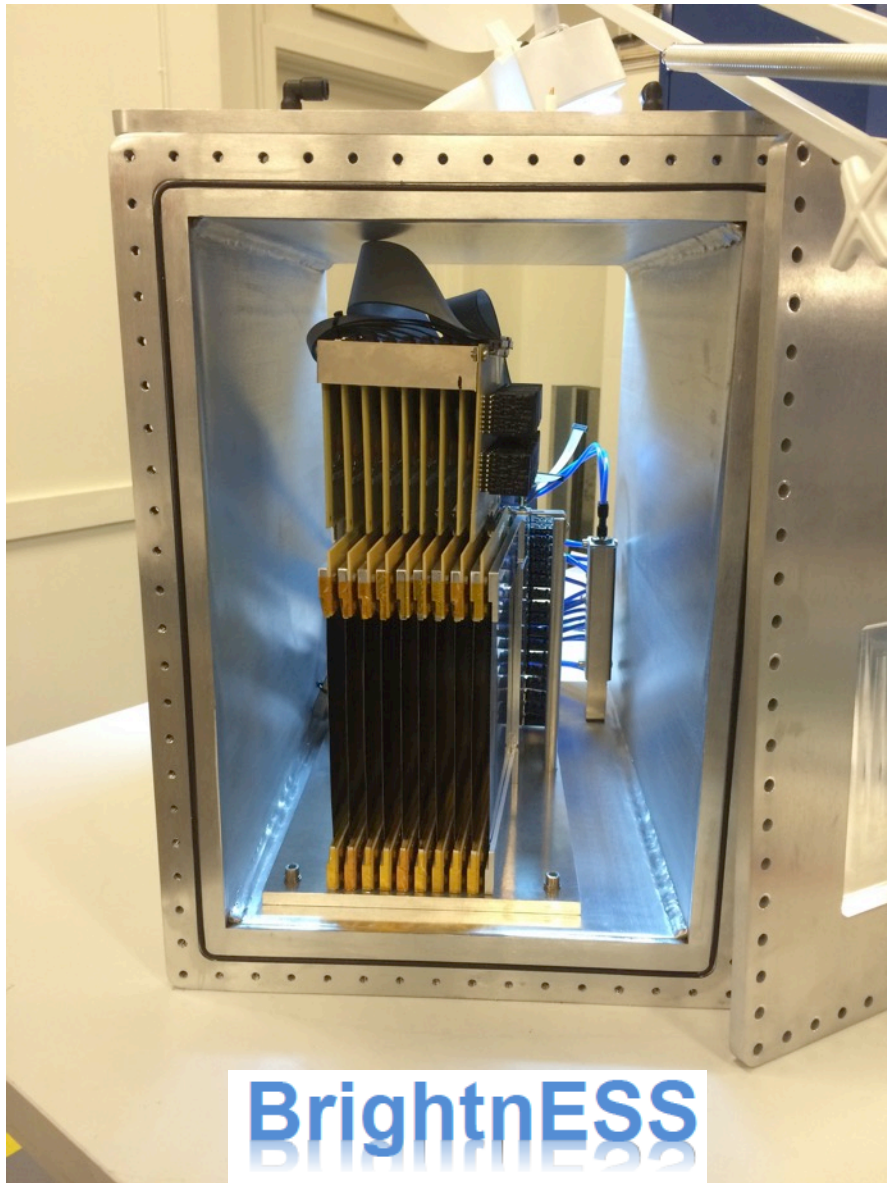
Coating area: $\sim 10 \times 120 \times 120 \text{ mm}^2$ (single side)

Detector active area: $\sim 10 \times 9 \times 120 \text{ mm}^2 = 90 \times 120 \text{ mm}^2$



HV on! (at EMBLA)





Demonstrator ready!

Tests to come:

- SF (Lund University) - Now
- BNC (Budapest) - February
- Real instrument - ...



LUND UNIVERSITY



Thank you.